Foraminiferal Analysis of the Late Miocene-Early Pleistocene Mangaopari Mudstone, South Wairarapa, New Zealand

Shelby Stoneburner

TE WHARE WĀNANGA O TE ŪPOKO O TE IKA A MĀUI
VICTORIA
UNIVERSITY OF WELLINGTON

TABLE OF CONTENTS

List of Figures

List of Tables

Abstract

The foraminiferal content of thirty-two samples from the late Miocene-early Pleistocene Mangaopari Mudstone within the southern Wairarapa region have been examined with the aim of determining the age and depositional environment of the unit. In particular the study addressed whether or not there were glacioeustatic cycles present in the unit. Integrating foraminiferal faunal distributions and sedimentological analysis provided geological, paleoclimactic, and paleoceanographic evidence to aid in the reconstruction of the paleoenvironment. The data was then compared with conclusions from previous studies.

The section was divided into two different parts (upper and lower) based on changes in foraminiferal assemblages and grainsize distributions. The age and depositional environment of the Mudstone is suggested by the presence of several genera and species of foraminifera which is supported by grainsize analysis. The presence of *Martinottiella communis* and *Karreriella cylindrica* between 0-157.1m stratigraphically suggest that accumulation began in bathyal conditions at depths greater than 400m between. This is supported by grainsize analysis which indicates a medium silt with a high percent mud content ranging from 91.5-100%. This demonstrates deposition beginning in the late Miocene-early Pliocene at bathyal depths greater than 400m. The upper part of the mudstone (157.6-216.3) illustrates a regressive sequence with a distinctive shift to a much shallower depositional environment at outermost shelfal depths likely of 150-200m. This is represented with the presence of *Truncorotalia sp. and Zygochlamys delicatula*. Grainsize also support this discovery with a shift to very fine sandy silts with a percent mud content ranging from 83-93%.

Previous findings conclude that this distinctive shift was caused by glacioeustatic cycles yet our data do not correlate with our glacioeustatic findings. Therefore, this shift is believed to be triggered by a tectonic event.

Acknowledgements

A would like to acknowledge first and foremost my supervisors Mike Hannah, Cliff Atkins, and Martin Crundwell, without their constant advice, support, and knowledge this Master's Thesis would seize to exist. To Mike, who provided upmost encouragement and guidance every day, making sure I was always on track, and that I had all the tools necessary for completion. To Cliff, who aided in the grainsize interpretations and provided sedimentological advice. To Martin, who aided in the identification of countless foraminifera, without your patience and teaching skills I could not have achieved this. A special thanks to Dene Carrol who has the insane ability to think in 3D, and provided help with measuring the section. Another thank you to Jane Chewings, who helped with any work achieved in the lab and always faced every task with a big smile. For those of you who helped in the field, a huge thank you for taking the time to join me on my mission. All of your passions for geology have truly inspire me.

To Hannah-Kate Duncan, who I feel I will always have an unpaid debt to. You have been my backbone this year and have never failed to make me smile.

To Tane Morris, who is not only my best friend but is also extremely talented in graphic design and helped me provide foraminiferal plates for this study. Not only have you contributed to this study but you also helped make many memories along the way.

To my family back in Florida, thank you for always supporting me by provided an environment filled with love and encouragement which has shown in my growth and accomplishments. I am blessed to come from such a loving family who has put up with my obsession with geology since a young age.

To my Garage Project family, thank you all for showing me all the magic Wellington has to offer and for all of your support while I completed my thesis. Each and every one of you are such lovely people and it makes me so proud to be part of such a great team.

I would like to dedicate this thesis to my dear friend Chase Hoover, whose legacy I strive to follow every single day and will live by for the rest of my life.

1. Introduction

The late Miocene – early Pliocene sequence of strata in the Mangaopari area of the southern Wairarapa region have long been a focus for palaeontological, sedimentological and stratigraphical studies. The Mangaopari Mudstone is an extensive mudstone that displays marine strata that accumulated during the Plio-Pleistocene that has since been uplifted onto the Wairarapa region. This region is part of the southern Hikurangi Margin, where the Pacific Plate is being obliquely subducted westward underneath the Australian Plate at rates of 41-48mm/yr. along the Hikurangi Trough. (Cole and Lewis, 1981; Beanland et al., 1998; Nicol et al., 2007; Reilly et al., 2015). The Mangaopari mudstone is located within the southern region of the forearc basin, bounded by the fold and thrust zone (Figure 1).

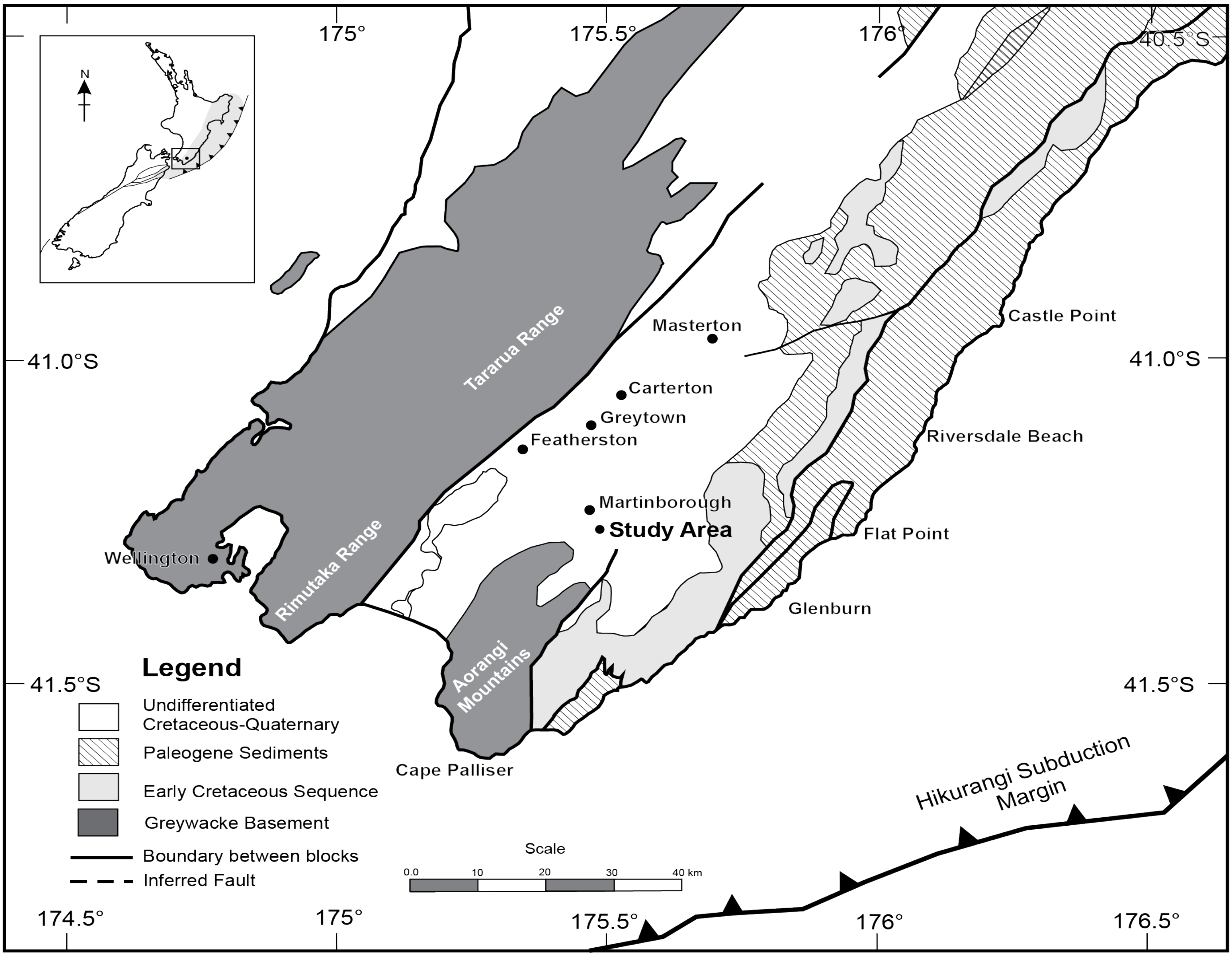

Figure 1. Location of the Mangaopari Mudstone field area adapted from Hines et al (2013).

Vella (1963), recognised that strata in the area recorded stratigraphic cycles. He suggested that eustacy was the primary driver of the cyclic sedimentation and recognised several cyclothems. Given the advances in our understanding of the cyclic nature of sedimentation since these early workers, and the high level of interest in unravelling past climates it is timely to reassess this sequence in detail, making use of previously underutilised microfossil data, specifically foraminiferal data.

Foraminifera are a key indicator in marine sediments because of their varied environmental preferences. Foraminifera are abundant throughout the Mangaopari Mudstone, making it suitable for paleoenvironment reconstruction and possible identification of sedimentary cycles. By counting and identifying different benthic and planktonic foraminiferal taxa, and making zonation association of particular species you can then trace their origin and distribution.

1.1 Focus and Aims

The focus of this study is an almost uninterrupted 216m thick succession of Late Miocene to Pleistocene mudstones named the Mangaopari Mudstone which is exposed along Bells Creek 15km Southeast of Martinborough, South Wairarapa (Figures 1 & 2) This study has three aims:

1. Establish the chronology of the sequence using benthic and planktic foraminiferal datums.
2. To document the benthic and planktic foraminiferal biofacies present in the sequence. Identifying the fossils of foraminiferal faunas can define a number of paleoenvironments of significance to geological, paleoclimatic and paleoceanographic studies.
3. Characterise the sedimentary architecture of the sequence using grain size analysis.

4. Integrate the sedimentological and foraminiferal data to provide comprehensive paleoenvironmental assessments in the Mangaopari Mudstone- and in particular to address the possibility of cyclicity.

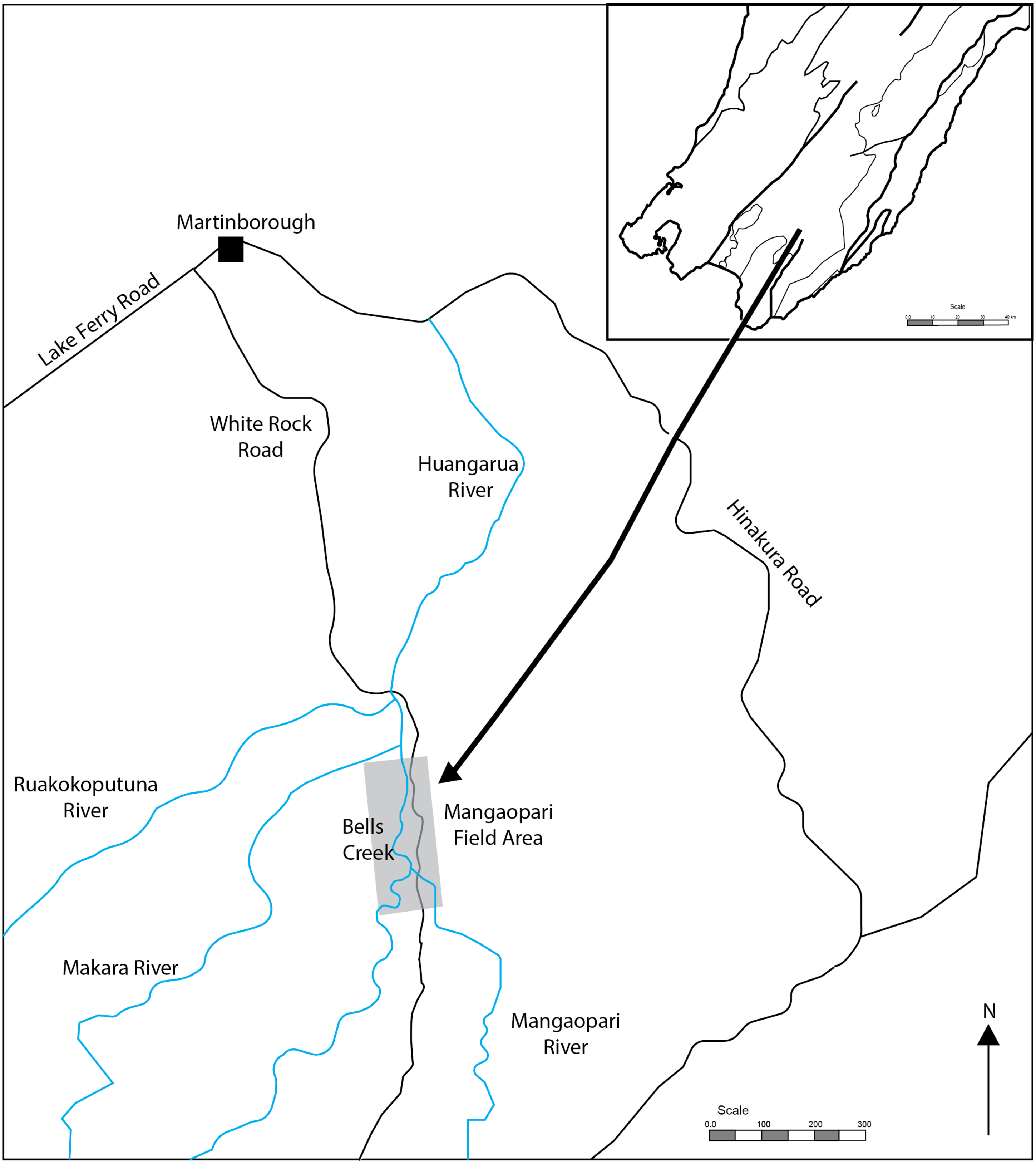

Figure 2. Location of the Mangaopari field area. Adapted from Hines et al (2013).

2. Regional Setting

New Zealand sits in the Southwest Pacific Ocean, covering approximately 24 degrees of latitude from the Kermadec Island to the North and South to Campbell Island (Hayward, 2000).

While the Cooks Strait separates the two main islands of New Zealand, it also connects the Tasman Sea to the South Pacific Ocean making an interesting biogeographical region (Trewick & Bland 2012). Over the last three million years the central New Zealand region has been subjected to various phases of rapid subsidence followed by rapid uplift, resulting in sedimentary basin formation followed by erosion and mountain building. In addition, active arc volcanism has periodically affected extensive areas with the deposition of large ignimbrite sheets and ash falls (Wilson et al. 1995a; Shane et al. 1996b; Naish et al. 1998; Alloway et al. 2005b; Pillans et al. 2005)

By the Early Pliocene much of New Zealand was exposed above sea level, mostly in the northern North Island and the South Island. At about 4.8Ma, subsidence in the southern Wairarapa region led to the formation of the Ruataniwha Strait, a narrow yet laterally extensive inland seaway which flowed from the Hawkes Bay region along the current east coast and eventually emptied into the Tasman Sea (Figure 3, A). The western edge of the Hikurangi margin's accretionary wedge began to uplift at around 3Ma, which created small islands and marine shoals along the easternmost part of Hawkes Bay and northern Wairarapa. At this time, much of the Wanganui Basin was under about 200-400m of water and the Manawatu, Wairarapa, and Hawkes Bay regions were mostly at shelfal water depths of 0-200m (Figure 3, B) (Trewick & Bland 2012).

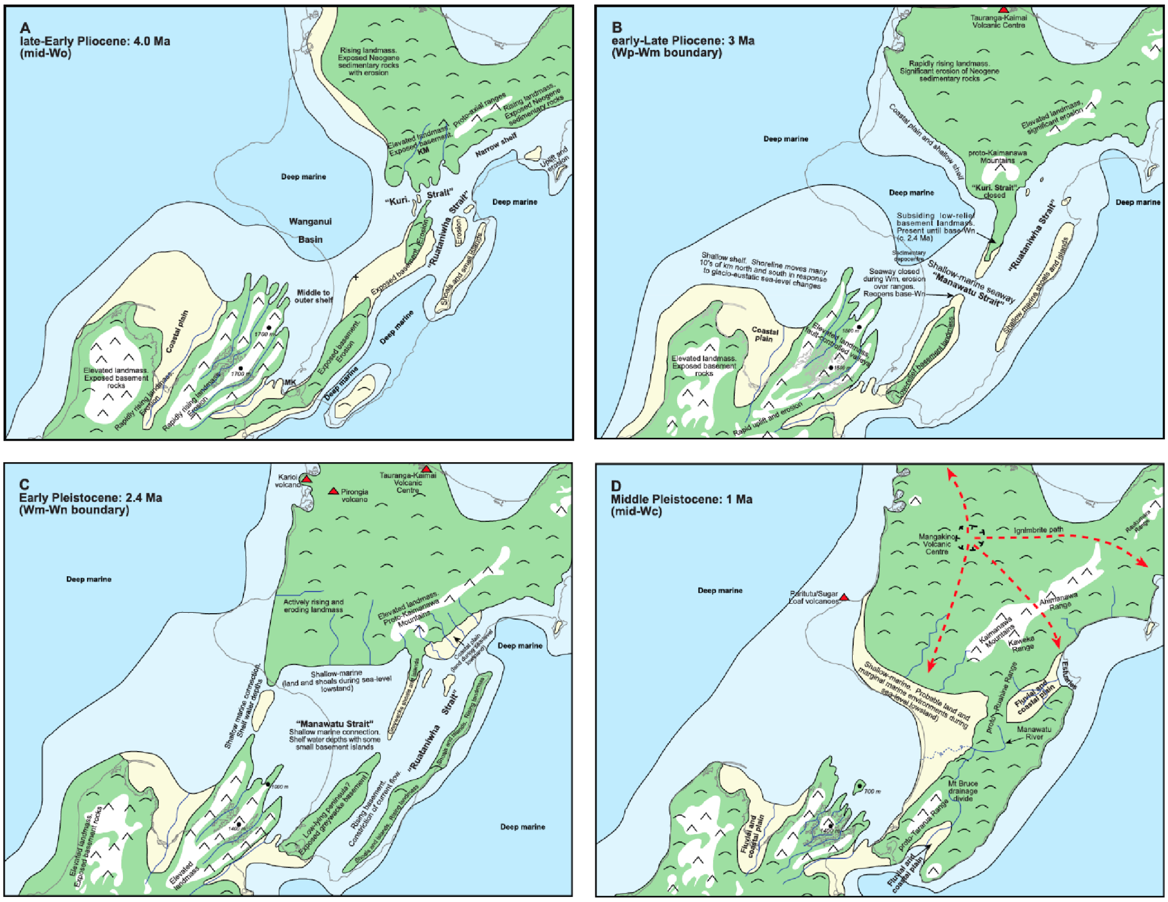

Figure 3. Adopted from Trewick and Bland (2012), visual diagram of the tectonic changes that occurred throughout the Plio-Pleistocene.

Although the southern part of the North Island was dominated by shelfal or deep water environments at this time, the northern parts of the modern North Island were slowly being uplifted. The Manawatu Strait is a paleo seaway that once separated the North and South Island, as it flowed from the eastern Wanganui Basin to the central and southern Hawkes Bay area (Figure 3, C). At around 2.4 million years ago, the Manawatu Strait was at its most prevalent. The Ruataniwha and Manawatu straits gave this region access to a small portion of the Southland Current, which transports cold water typical of species like bivalve *Zygochlamys delicatula* and the foraminifera *Truncotorotalia crassula* northwards along the eastern coast of New Zealand (Vella & Nicol 1970; Crundwell 1987).

At around 1.5 million years, the Ruataniwha Strait was closed off and the Manawatu Strait had developed into two different river systems named the Manawatu River in the north and the Ruamahanga River in the south. This was caused by uplift in central Wairarapa, specifically the Mount Bruce block, which initiated displacement along faults in this area. By about 1 million years ago, continued uplift raised much of Hawke's Bay above sea level and this changed the direction of the Manawatu River to change from east to west, flowing through the modern Manawatu Gorge into the Tasman Sea (Figure 3, D). This also caused the North and South Island to connect via a narrow low-relief land bridge between the Wellington area and the Marlborough for a short period of time. At about 500 thousand years ago, the Cook Strait formed, separating the North and South Island once again, creating the modern North and South Islands of New Zealand. (Trewick & Bland 2012)

Tectonic activity throughout the last four million years caused a combination of continuous subsidence and uplift that has occurred since the activation of the present plate boundary. This tectonic activity led to several changes in the Zealandia land masses which caused a progression from a series of low laying islands to be uplifted into to the modern North and South Islands that make up New Zealand today. In particular, the accumulation of Plio-Pleistocene limestones and marginal marine deposits, which were rapidly uplifted and are represented in the field area in the form of the Makara Greensand, Mangaopari Mudstone Formation, Bridge Sandstone member, and the Pukenui Limestone. The examination of these sedimentary units and in particular the Mangaopari Mudstone from the south Wairarapa clearly illustrates that New Zealand is geologically young, having only acquired most of this landscape in the last half-million years (Figure 4.)(Trewick & Bland 2012).

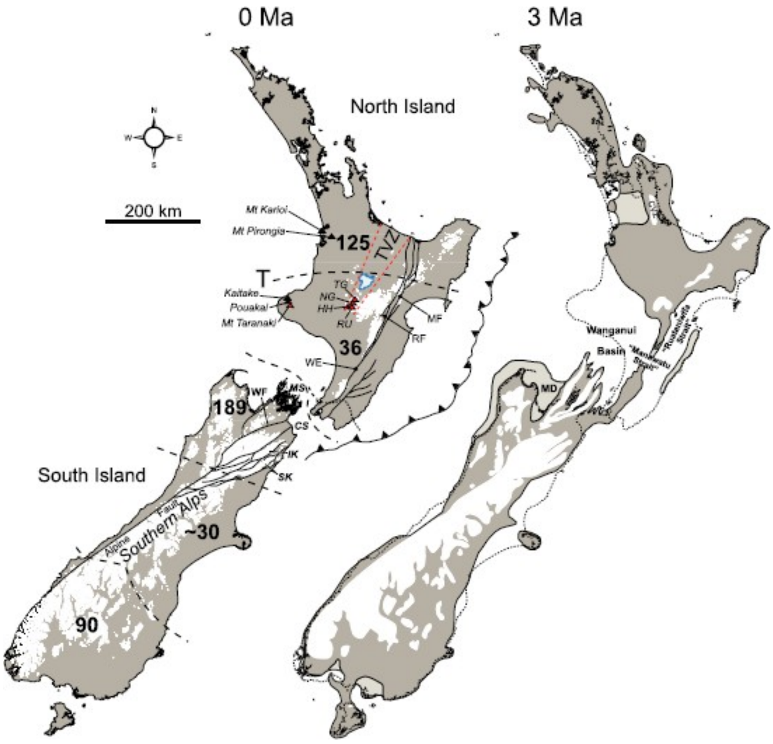

Figure 4. New Zealand at present day (left) and a reconstruction from 3 Ma (right). Adopted from Trewick & Bland (2012)

Today, the North and South Islands of New Zealand are the largest expanse of the Zealandia continent emergent from the ocean in recent geological time (Trewick & Bland 2012). The continental shelf and coastline are impressively extensive compared to its relative size. The coastline covers approximately 11,000km and provides numerous coastal embayments including estuarine, lagoon, and shelfal environments (Hayward, 2000). The coastline is constantly changing due to the influence of major oceanic current systems, tides, and rapid tectonic activity, which in turn effects the biological activity that is recorded in the sediments present today. In the Wairarapa region, this is represented in the paleoenvironment of the late Cenozoic that is displayed in the present day form of extensive uplifted late Miocene to early Pleistocene mudstones, sandstones, and limestones from this region where the Ruataniwha Strait once flowed.

3. Geological Setting

The study area is located in southern Wairarapa region, in the Southern Hikurangi Margin, where the Pacific Plate is being obliquely subducted westward underneath the Australian Plate. (Cole and Lewis, 1981; Beanland et al., 1998; Nicol et al., 2007; Reilly et al., 2015). A subduction trench, the Hikurangi Trough, a 150-kilometre-wide accretionary prism, and the North Island axial ranges formed by a zone of uplifted basement rocks are all components of the forearc region of the Hikurangi Margin (Cole & Lewis, 1981; Beanland et al., 1998; Nicol et al., 2007). The strike-slip motion between the Australian and Pacific Plate causes deformation and uplift along the axial ranges and folding and thrusting that extends from the inner forearc region to the subduction trench (Figure 5) (Cole & Lewis, 1981; Beanland et al., 1998; Nicol et al. 2007).

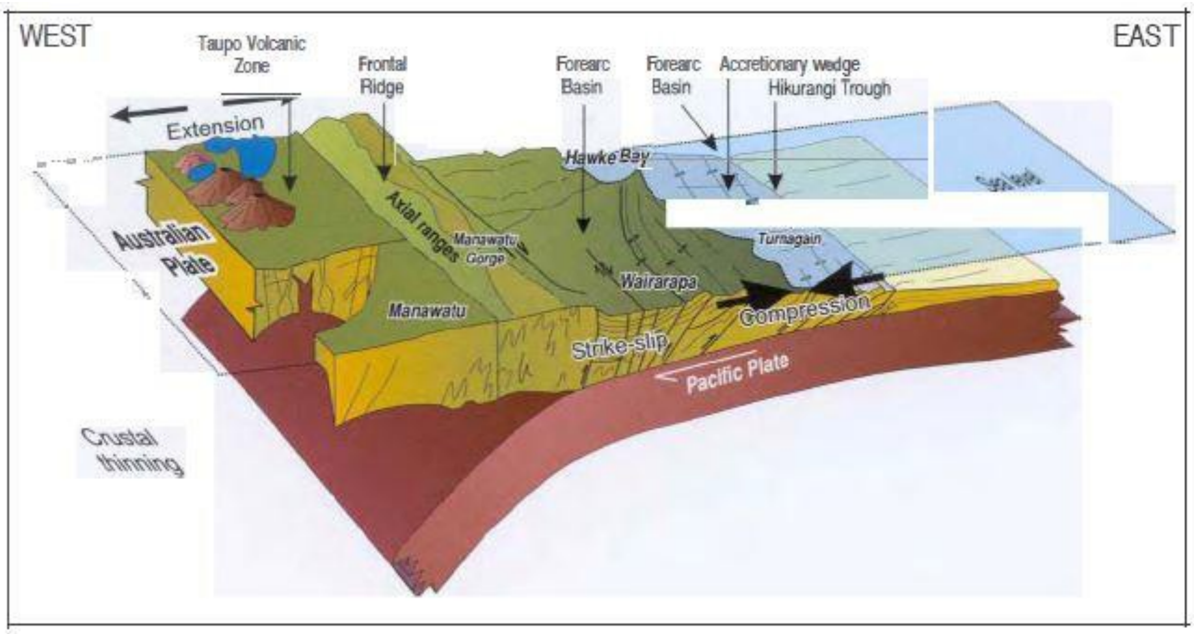

Figure 5. Schematic diagram of the Taupo- Hikurangi Trough that encloses the Wairarapa geological area. Adopted from J.M. Lee & J. G Begg (2002), originally adapted from Lewis (1980).

The Mangaopari mudstone began to accumulate during the late Miocene as a result of the reactivation of the Australian and Pacific plate margin. This reactivation resulted in the Tonga-Kermadec subduction system moving southwards into the New Zealand continental crustal block along the Hikuragi Trough (Crundwell, 1987). During the late Miocene, the transpressional faulting began within the forearc accretionary complex above the Hikurangi subduction zone and created localized subsidence to bathyal depths during the early Pliocene. During this time, there was also extensive glacioeustatic activity occurring that influenced the area dramatically. These glacioeustatic changes are recorded in the sediment which is exposed on land today in the south-eastern Wairarapa in the form of massive marine mudstone, along with marginal marine and terrestrial sediments.

4. Stratigraphy

This chapter provides detailed lithostratigraphic descriptions of the late Miocene- early Pleistocene sedimentary units. These lithographic units were first described by Vella and Briggs (1971) and are illustrated in the stratigraphic column (Figure 6). Stratigraphic units are described here based on their appearance in the field, grainsize analysis, and fossil content with a more detailed focus on the Mangaopari Mudstone. The Mangaopari mudstone for this study was described along Bells Creek, which runs parallel to White Cliff Road- located 15km Southeast of Martinborough, in the southern Wairarapra region (Figure 6).

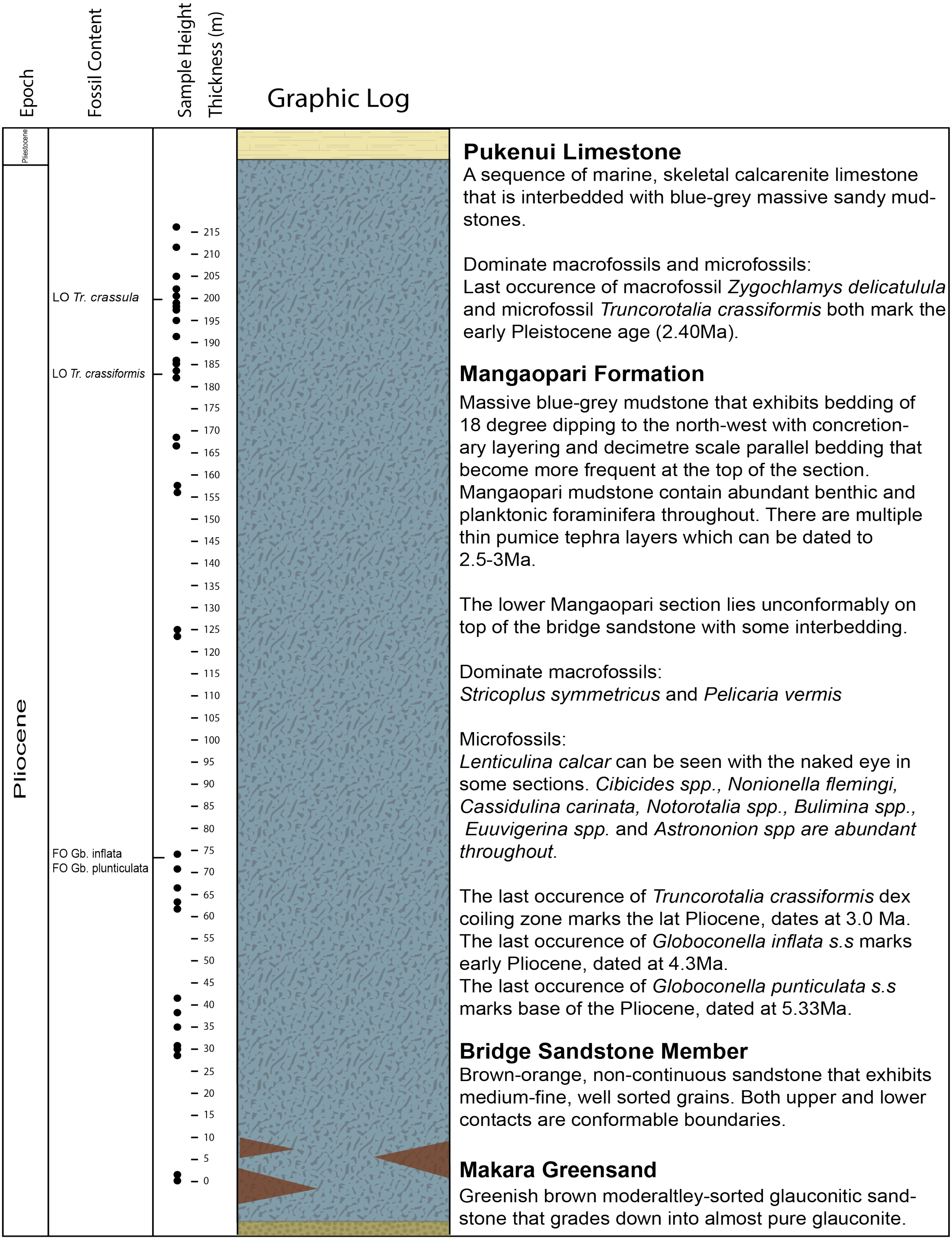

Figure 6. Stratigraphic column showing visual representation of the measured Mangaopari Mudstone and the surrounding sedimentary units.

4.1.1 Makara Greensand

The Makara Greensand is a greenish brown moderately-sorted glauconitic muddy greensand that is poorly consolidated and inclined to slump. It is exposed at the base of the Mangaopari Mudstone along Bells Creek. When the greensand is exposed it is less than a few meters thick and its thickness is unknown at most places. It is believed to be Late Miocene in age and grades down into almost pure glauconite. The glauconite present throughout Makara Greensand is a mineral that forms exclusively in low-oxygen marine settings, particularly on continental shelfs with slow accumulation rates and high organic concentrations. This mineral often forms when bacteria decays organic matter in skeletal marine organisms and replaces it with glauconite. (Vella & Briggs 1971)

4.1.2 Mangaopari Formation

The Late Miocene to early Pleistocene Mangaopari Mudstone Formation is well exposed along Bells' Creek. It was measured by Vella & Briggs (1971) as 600m thick. However, as noted above, this study focuses on the 216m of this section exposed along Bells Creek from the top of the Bridge Sandstone Member to just before the base of the Pukenui Limestone Formation.

The Mangaopari Mudstone is a largely massive blue-grey sandy mudstone that exhibits bedding that is dipping at 18 degrees to the north-west where it makes lower contact with the top of the Bridge Sandstone Member. Concretionary layering and decimetre scale parallel bedding become more frequent at the top of the section. This section is clearly a coarsening upwards sequence that becomes increasingly shell-rich towards the base of the Pukenui Limestone. It also contains abundant benthic and planktonic foraminifera throughout. The benthic foraminifera are visible to the naked eye at some outcrops. There are also multiple thin pumice tephra layers which can be dated to 2.5-3Ma. (Shane 1994) Vella and Briggs (1971) divided this section three separate units; the upper, middle, and lower Mangaopari mudstone. The lower Mangaopari section lies on top of the Bridge Sandstone Member with some distinct interbedding. The top of the Mangaopari slowly grades into the base of the Pukenui Limestone. This upper interval is sometimes referred to as the Greycliffs Formation. The Greycliffs Formation was first described by Vella & Briggs (1971) as a blue-grey sandy mudstone with common macrofossils including *Pelicaria acuminaga* and *Pelicaria rugosa*. Although this is still true today at the base of the Pukenui Limestone, this formation will not be included in this study. Here, I agree with Rodley (1961) in that this unit does not vary enough lithologically from the Mangaopari Mudstone, and is considered Mangaopari Mudstone with grain size that is steadily increasing with stratigraphic height towards the base of the Pukenui Limestone. (Vella & Briggs 1971)

4.2.2. Bridge Sandstone Member

At an outcrop along Bells Creek, towards the base of the Mangaopari Mudstone, the Bridge Sandstone Member appears as a sequence of multiple interbedded brown sandstone layers ranging from 1-6m in thickness within the Mangaopari Mudstone. This non-continuous sandstone exhibits repeated fining upwards sequences with medium-fine, well sorted friable grains that are poorly consolidated. The fining-upward beds suggests that this member is a result of turbidite deposit. Both the upper and lower boundaries are a sharp planar lower contact with the Mangaopari Mudstone. There is a strong sulphurous smell present at some outcrops. (Vella & Briggs 1971)

4.1.3 Pukenui Limestone

Exposed along White Rock Road, opposite Birch Hill Homestead. The Pukenui Limestone is a sequence of marine-skeletal calcarenite limestones that are interbedded with a blue-grey massive, muddy sandstone. This is the youngest section in this study which marks the base of the Pleistocene. The macrofossil *Zygoclamys delicatula* and microfossil *Truncorotalia crassaformis* first appear near the base of the Pukenui Limestone and indicate an age of 2.40 Ma or Early Pleistocene (Raine et al, 2015). The obvious interbedded limestones and sandy mudstones are interpreted as reflections of glacioeustatic sea level fluctuations. (Vella & Briggs 1971)

5. Foraminifera

Foraminifera are Protists, with granulo-reticulose pseudopodia and are agglutinated, secreted calcareous, or organic-walled tests (Hornibrook et al, 1989). They range in age from Cambrian to Recent and exist in all realms of the ocean, from deep sea abyssal depths to shallow marine marshes (Jones, 2006). Their microscopic size and vast abundance in sediments from a wide variety of environments which makes them the ideal fossil group for reconstructing depositional environments and determining the age of New Zealand's Cenozoic sedimentary rocks (Hornibrook et al, 1989).

Foraminifera are key environmental indicator species in the marine realm because different taxa occupy different ecological niches. Temperature, food supply, substrate, turbulence, oxygen concentration, and water depth are all contributors to the distribution and abundance of foraminifera (Hornibrook et al, 1989). Most benthic foraminifera occupy the photic zone, restricting them to shallow marine environments. Living planktonic foraminifera are mainly open-ocean, although wind and ocean currents can bring planktics into quite shallow depths. Marginal, shallow, and deep marine environments can usually be distinguished by the presence or absence of certain benthics or the abundance of specific assemblages (Jones, 2006).

The classification of foraminifera in this study is based purely on morphology, which was studied under a light and/or electron microscope. Foraminifera in this study were identified mostly at a generic level but key species were also identified. The wall structure, chamber arrangement, and aperture were used in the classification at the generic level. The size, shape, coiling direction, and surface ornament was used to identify at species level. Once the foraminifera are identified at species level, they can then be classified into abundant and rare species and further faunal associations can be made. (Jones, 2006)

When needed, a scanning electron microscope can be used for separating closely-related taxa based on their minute surface details. Observing the differences in the morphology, specifically the wall structure led to the classification of foraminifera into the five main suborders shown below (Figure 7). The shape of the assemblages and the wall structure can be correlated to their paleoenvironment and more specifically their environmental preferences, this is shown in (Figure 8), where foraminifers were divided into brackish, inner shelf, mid-outer shelf, bathyal, and abyssal environments based purely on their morphology. (Murray 1991, Boltovsky et al 1991)

The five main suborders based on different wall structures are:

Allogromides

(Proteinaceous or organic-walled forms)

The suborder *Allogromiina* is rarely encountered as a fossil as the tests don't fossilize well and are only found in recent brackish and fresh water environments. There were no *Allogromiina* found in this study.

Textulariina

(Arenaceous or agglutinate forms)

The suborder Textulariina is comprised of benthic foraminifers with agglutinated test and ranges in times from early Cambrian to Recent.

Miliolina

(Porcelaneous calcareous forms)

The suborder *Miliolina*, which range from the Carboniferous to Recent, are benthic foraminifera that lack pores and have multiple chambers. They reside in shallow waters such as estuaries and along coastlines but also include deep-water oceanic forms.

Rotaliina and Lagenina

(Hyaline calcareous)

Primarily include oceanic benthic species but some species are common in estuarine shallow water environments and range in time from Triassic to Recent. These species have a wide variety of shapes but are typically enrolled and multilocular but may be reduces to bi- or uniserial.

Globigerinides

(Hyaline calcareous)

Globigerinides exist as marine plankton from the Middle Jurassic to recent and are typically found at shallow, epipelagic and intermediate, mesopelagic environments. (Jones, 2006) (Armstrong & Brasier, 2004)

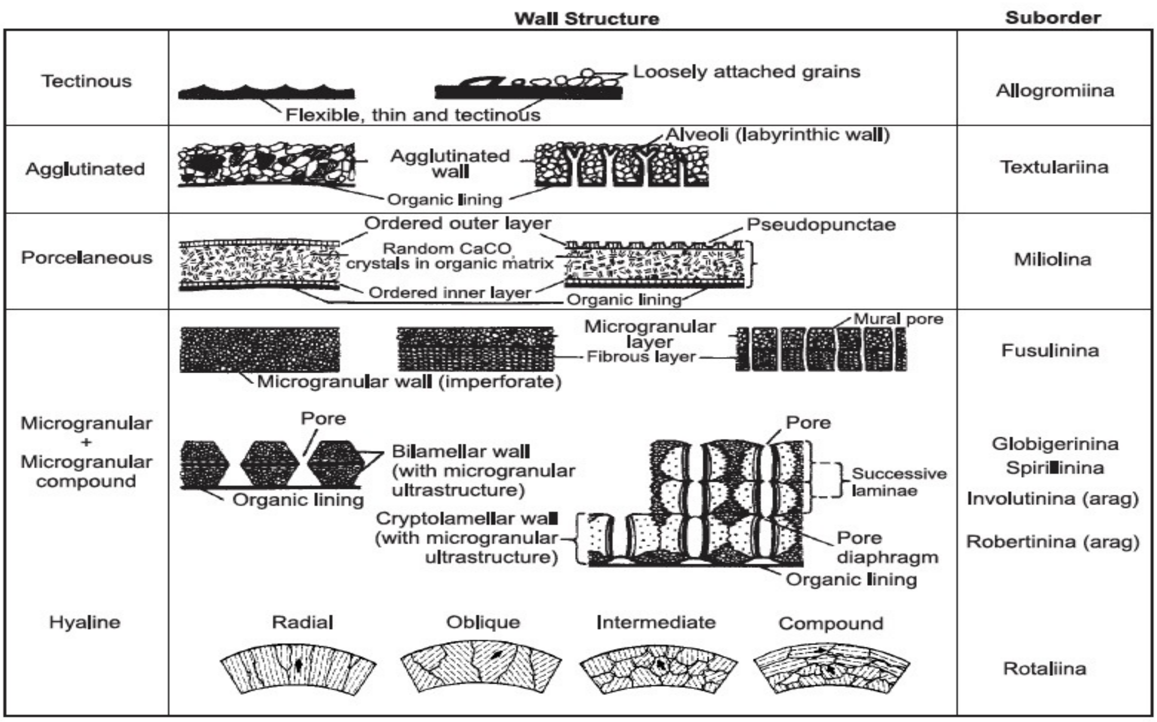

Figure 7. Classification table of the five main suborders of foraminiferal morphology.

In Figure 8, the percentage of Textulariina, Miliolina and Rotaliina plus Lagenina is plotted on a ternary diagram. Faunas dominated by Textulariina (50-100%) are likely to be either from brackish or abyssal water that is below the calcium compensation depth (CCD). Faunas containing greater than 20% Miliolina are typically indicative of a normal marine, inner shelfal environment. Faunas with greater than 75% Rotaliina are usually belonging to slightly brackish, sheltered environments that can occur at any depth down to upper abyssal. Is it rare for Lagenina to occur in high percentages, but when there are (>30%) they are indicative of an outer shelf or upper bathyal environment and are often dominated by *Lenticulina*. (Hayward, 1999)

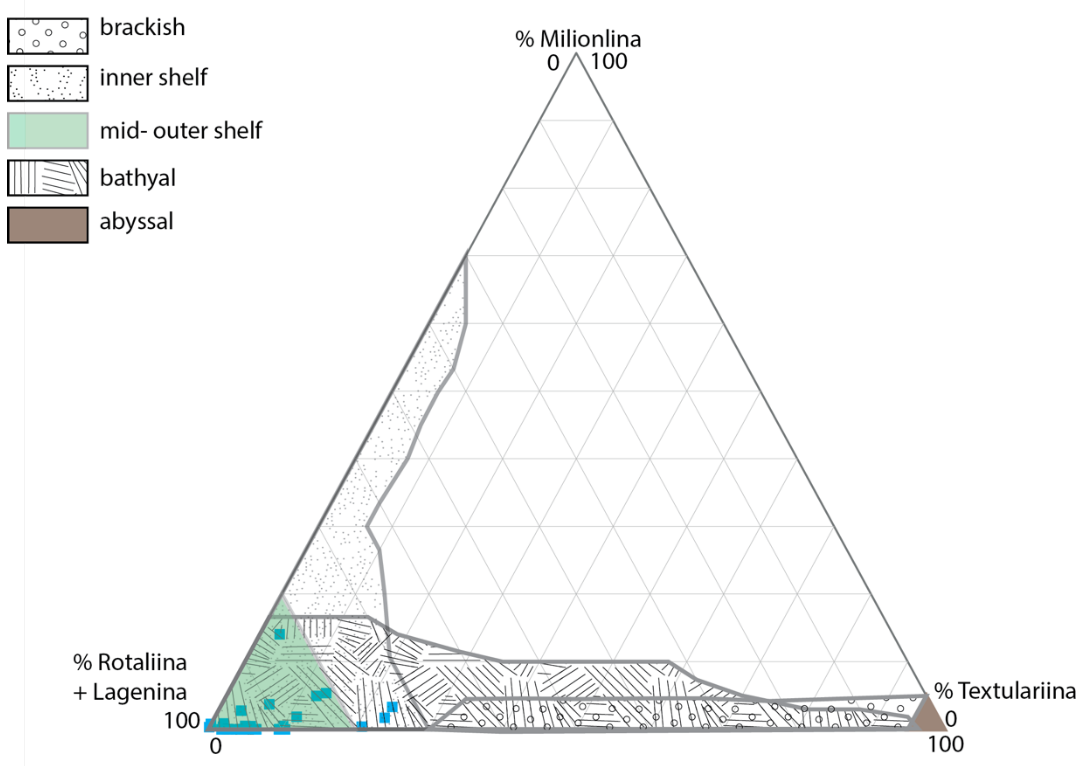

Figure 8. Ternary plot of Miliolina, Textulariina, Rotaliina, and Lagenina. Adapted from B. Hayward (1999).

5.1 Environmental Preferences

Benthic foraminifera often occupy different substrate that can be classified into epifaunal or infaunal environmental preferences. At the genus level, some foraminifera, like *Cibicides* prefer epifaunal harder and coarser-grained substrates such as rocks, sand, sea grasses, and algae that they temporarily or permanently attach themselves to by a flat or concaved umbilical side. Epifaunal species usually develop a thinner test and tend to exhibit more morphological variability than infaunal species (Armstrong & Brasier 2004).

Infaunal species are typically found in the top 10mm of sediment and exhibit tests that are thin-shelled, delicate, poriferous, and are usually elongated (eg. *Bolivinita pliozea)*. This specific morphology favours mid-shelf to bathyal environments. These environments are characterized by silty or muddy substrate, low-energy, and are rich in organic material in which the foraminifers can freely burrow and easily attain food (Armstrong & Brasier 2004).

The amount of nutrients and oxygen also influence the distribution of foraminifera. Rates of nutrient supply from the seafloor to the surface are high in upwelling zones and mid-outer shelfal environments, where there is a high influx of nutrients that tends to discourage photosymbiosis. High rates of primary productivity at the ocean's surface can also lead to anaerobic zones, which are low in oxygen. Species who thrive in upwelling and anaerobic zones are small, thin-shelled, unornamented calcareous buliminaceans such as *Bulimina, Bolivina*, and *Euuvigerina* who favour these conditions and are common in lagoons and the mid-outer shelf (Armstrong & Brasier 2004).

Water masses are another contributing factor for planktonic foraminiferal distribution. There are five water masses around New Zealand; these include Subtropical-Temperate, Sub Antarctic, Antarctic Intermediate Water, Deep-water and Antarctic Bottom Water.

Previous studies, such as Hayward (2000) and Crundwell et al (2007) found that specific planktonic taxa are abundantly found in these water masses. Planktonic taxa that thrive in Subtropical-Temperate waters with high salinity and temperature include *Orbulina universa, Hirsutella hirsuta, Truncorotalia crassaformis*, and *Truncorotalia crassula*. Species that thrive in more temperate waters include *Neogloboquadrina incompta* and *Globoconella inflata.* In Sub Antarctic waters, where the temperature and salinity is low, *Neogloboquadrina pachyderma* is common.

6. Previous Interpretations

Vella & Briggs (1971) and Collen & Vella (1984) established the basic stratigraphic frame work used today and Lamb & Vella (1987) linked the local stratigraphy of the area to regional scale tectonic development of the East Coast margin of the North Island. More recent studies (e.g. Gammon 1995; Clarke 1998) have focused on the younger Plio-Pleistocene strata. Palaeontological studies have focused on the molluscan fauna (Vella 1953; Vella & Briggs 1971; Beu, 1984) with only a few examining the foraminiferal assemblages (Devereux, et al. 1970; Clarke 1998). Most of these palaeontological studies were aimed at improving the biostratigraphy of the area, with little attention given to paleoclimate reconstructions. The exception is the early work on paleomagnetic and oxygen isotope stratigraphy that utilised thick sequences of mudstone and large, well-preserved foraminifera (e.g., Devereux et al., 1970, Kennett et al., 1971, Lienert et al., 1972).

Vella & Briggs (1971) defined each stratigraphic unit present in the northern Aorangi range from upper Miocene to lower Pleistocene in age. They identified twelve different Cenozoic units over small distances of only a few kilometres in the Ruakokoputuna-Makara area and established the stratigraphic framework used today. Collen & Vella (1984) revised work using a new biostratigraphic analysis and additional ages provided by tephra marker beds. Cole & Lewis (1981) later pointed out that the Taupo-Hikurangi subduction zone slowly has evolved due to the rotation of accretionary elements, causing the original NW-trending subduction system north of New Zealand to separate from the NW-trending volcanic arc. During the Pliocene-Pleistocene, oblique subduction and deposition continued and intensified due to the Taupo-Hikurangi margin rotating in line with the NNE-tending Kermadec system. Cole & Lewis (1981) then denote that this caused a marginal basin to develop and create the Taupo Volcanic Zone. Beu & Edwards (1984) used deep-sea cores, fossil datum and oxygen isotopes to correlate widespread New

Zealand sequences with the global sea- level changes. In doing so, Beu (1984) identified eight different glacioeustatic cycles within the Pleistocene and late Pliocene Nukumaruan Stage in southern Wairarapa.

Crundwell (1987) mapped twenty-one lithostratigraphic units of Neogene age from the Wainuioru Valley, which is 30 kilometres east of the field area. Out of the twenty-one units recognized by Crundwell (1987), thirteen of these are described for the first time. Crundwell (1987) found that the sediments contains rich microfaunal assemblages which he categorized into 12 different foraminiferal zones and subzones.

7. Methods

7.1 Measured Sections

A section of the Mangaopari Mudstone was documented and described along Bells Creek, where sediments were also collected and measured to give a detailed report of the sedimentary units. The massive mudstone was measured from the top of the Bridge Sandstone Member, where the lower part of the Mangaopari Mudstone overlies it making a sharp contact at approximately (-41.320287, 175.475627). Measurements stopped towards the base of the Pukenui Limestone, just after the Birch Hill mailbox (-41.317989, 175.47317). The section was measured using a geological compass, a Jacobs's staff, and measuring tape. These coordinates where later added to Google Earth and plotted onto Adobe Illustrator to calculate the true stratigraphic thickness, which is illustrated in the stratigraphic column (Figure 6).

7.2 Sample Collection

1. The field area is a one hour drive from Wellington and accommodation is available nearby. School of Geography, Environment and Earth Sciences provided transport.
2. Section measurements and sample collection started at a sharp contact between the top of the Bridge Sandstone Member underlying the Mangaopari Mudstone Formation. At this location there is an obvious dip of 18 degrees and a dip direction of 327 degrees. Sample collection ended at an outcrop near the Birch Hill mailbox, towards to the base of the Pukenui Limestone. Where possible, samples were collected at approximately 5-10m intervals through the entire sequence, noting their geographical coordinates and height at each location.

3. For each sample, a GPS coordinates was collected to aid in their placement in the measured section.

4. In the lab at VUW, samples were placed in an oven at 40°C for 48 hours to dry completely. Sub-splits were prepared for grain size analysis, microfossil recovery and archived material.

7.3 Foraminifera Collection and Analysis

Detailed palaeoenvironmental analysis was undertaken focusing on the age and depositional environment by examining the presence and/or abundance of certain foraminiferal biofacies. (Hayward et al, 1999)

4. Foraminiferal faunas were recovered using standard washing procedures, by adding Calgon and hot water broke down the larger bulk samples and was washed through a 63 micron seize to remove mud fractions, leaving the coarser sand fraction. Once washed thoroughly and mud was removed the samples were placed back into the oven at 40°C for 48 hours to dry.
5. The samples were then split with a micro splitter into aliquots to ensure that there were 300-500 specimen counted in each sample.
6. The microscope facilities at VUW and Geological Nuclear Sciences were used to recover, count, identify and analyse benthic and planktonic foraminiferal faunas. The scanning electron microscope at GNS was used to further identify and photograph foraminifera that proved difficult to identify using a light microscope.
7. Foraminiferal data was analysed using two different statistical software; R Studio and Tilia along with Microsoft Excel. Plots were created to emphasize the paleo logical patterns. These plots were later edited using Adobe Illustrator.

7.4 Grain Size Analysis

Grainsize distribution of samples was documented at VUW using the Beckman-Coulter Laser particle size facility. The data produced by the Beckman Coulter instrument was analysed to calculate the proportions of clay, silt, and possibly sandstone. This provided a better understanding of the depositional environment in which the sediments were deposited. Before the samples are able to be analysed by the Beckman Coulter Laser they were first digested in hydrogen peroxide (H_2O_2) to remove organic material. Hydrochloric acid (HCl) was then added to remove carbonate material. After both organic and carbonate material was removed the samples were then ready to undergo grain size analysis. The data produced by the Beckman Coulter instrument was then further analysed using Gradistat.

7.4.1 Sample Processing for Grain Size Analysis

1. Upon arrival at Victoria University, samples were placed in an oven at 40°C for 48 hours to ensure complete dehydration.
2. The mudstone proved to be well cemented and was crushed using a hydraulic press. Once disaggregated into smaller pieces, 0.15g of sample was placed into a beaker and carefully disaggregated using a wooden spatula to ensure sediments were broken down without damaging individual grains. Once this was completed samples and duplicates were put into 50mL centrifuge tubes.
3. Samples were covered with 2 millilitres of 27% hydrogen peroxide (H_2O_2) every two hours for six hours and then left overnight to chemically react.
4. The following day, the samples were topped up with deionized water and placed on a hot plate and heated to 70°C to speed up the chemical reaction. Once reactions were complete, samples were transported to 50mL tubes.

5. The 50mL tubes were placed in the centrifuge and spun at 4500 rpm for ten minutes, then drained and topped with deionized water and this process was repeated three times to remove remaining H_2O_2. After the third spin, all of the excess water was drained off.
6. 2 millilitres of 10% hydrochloric acid (HCl) was added to samples and topped with deionized water then allowed to sit until the reaction had finished. The remaining material was centrifuged again at 4500 rpm for ten minutes, then drained and topped with deionized water. This process was repeated three times and then drained to ensure the removal of excess HCl.
7. Samples were placed in the ultra sonicator along with 80ml of 10% calgon to disaggregate.
8. Once the sample was disaggregated they were ready to be analysed on the Beckman Coulter LS-13-320 Laser Diffraction Particle Size Analyser which measured the size distribution ofparticles suspended in liquid by measuring the diffraction or bending of light and calculating the different grain size percentages present in each sample.
9. Each sample and their duplicate was run once on the Beckman Coulter LS-13-320 using the optical module quartz_natural.rf780d, which assumes all material has the same refractive index of quartz.
10. Data from grain size analysis produced summary statistics including percentages of mud, mean grain size, and sorting (μm). Histograms were also produced by the Beckman Coulter which plot volume percentages versus particle size distribution (μm).
11. The data was exported and further manipulated using Gradistat, which produces similar statistics and histograms (Figure 9).

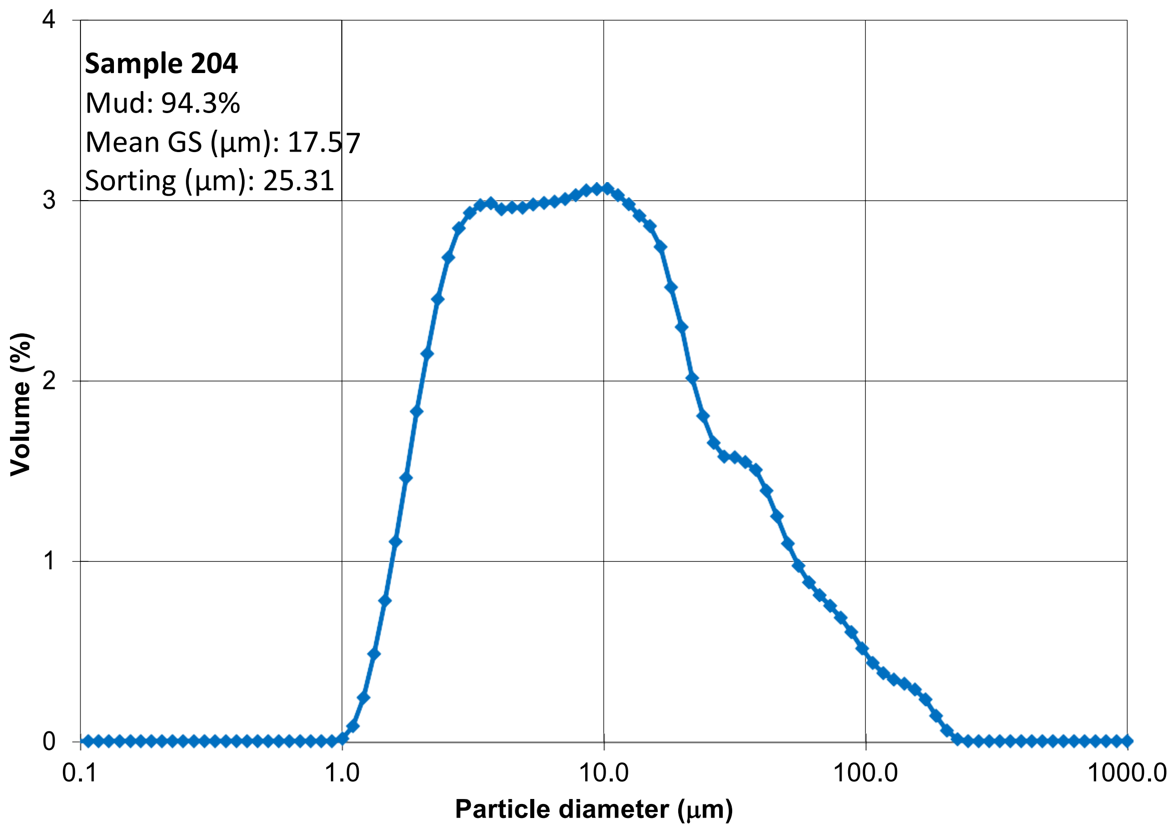

Figure 9. Histogram produced by Gradistat.

8. Results

The section of Mangaopari Mudstone examined in this thesis is 216.3m thick, measured from the top of the Bridge Sandstone Member through towards the base of the Pukenui Limestone Formation. Sampling did not start at the base of the Mangaopari Mudstone as the thin interval of Mangaopari Mudstone between the base of the Bridge Sandstone Member and the Makara Greensand was covered. There are two sample gaps in the middle of the section (from 74.5m-124.3m and from 125-157m) where there are either no outcrops or the existing outcrops are very weathered. Due to lack of outcrops in the area, sample collection stopped towards the top of the Mangaopari Mudstone where it gradually grades into the base of the Pukenui Limestone Formation. In total, there were 32 samples collected (203-235). Benthonic and planktonic foraminiferal assemblages were present and abundant in all samples. Grainsize data was also collected for each of these below. Both display evident changes from the base to the top of the section, with a distinctive shift that is parallel across all datasets.

7.1 Grain Size Analysis

Grainsize analysis was carried out on all 32 samples collected to characterize the sediment and assist in the interpretation of the depositional environment. The graphic log (Figure 10), represents a visual impression of the Mangaopari Mudstone based on observations in the field combined with grain size analysis results. Selected histograms produced by Gradistat were added to the log to pin point the changes occurring throughout the section. The differences in percentages of mud, mean grain size (µm), and particle sorting (µm) are shown to the right. The full list of sample statistics and histogram produced by Gradistat are listed in appendix 11.4.

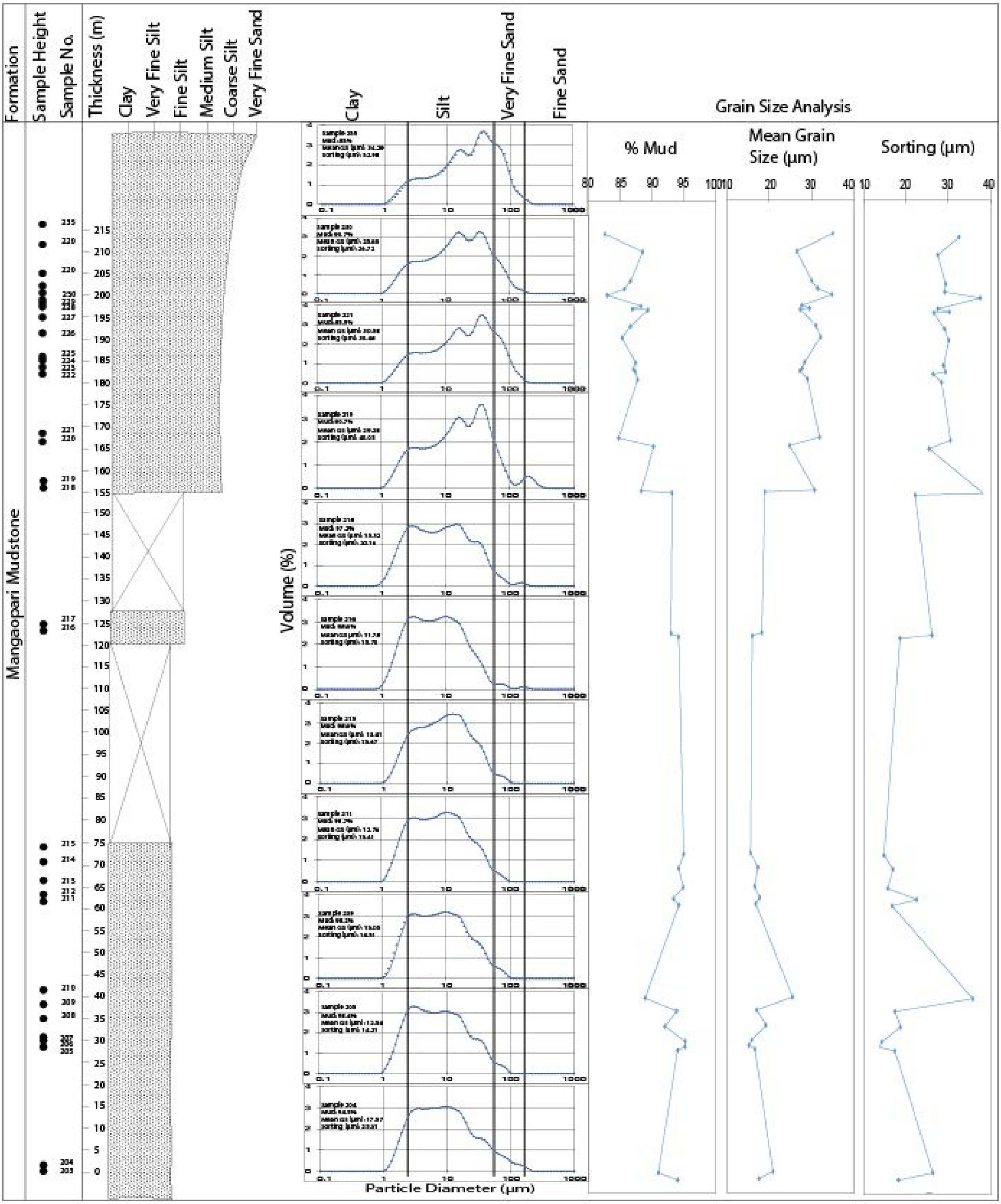

Figure 10. Graphic log and selected grainsize histograms and summary statistics from the 216m section of the Mangaopari Mudstone.

Grain size analysis provides evidence of gradual changes throughout this section from very fine silt at the base to a very fine sand at the top, yet there is a distinctive abrupt shift in grain size at 157.1m from medium silts to very fine sands. Therefore, the section was divided into two parts, the lower part of the section ranging from 0-157.1m and the upper part of the section ranging from 157.6-216.3m.

The lower part of the section below 157.1m includes samples 203-218. These samples are medium silts with a relatively broad, either unimodal or bimodal distributions with a slight coarse skew. The modal peaks occurring in the range from 5-15µm and mean grain size ranges from 10.82- 23.06µm and standard deviation (sorting) values between 9.75-25.31µm. The percent mud is consistently high, with a range from 91.5-100%.

The distinct shift to coarser grainsize distribution occurs above 157.1m. This upper part of the section includes samples 219-235. These samples range from coarse silts to very fine sandy silts with a broad finely skewed slightly bimodal peaks in the 30-40µm range. The mean grain size ranges from 22.26-34.29µm and shows an irregular increase up section, along with an increase in standard deviation which ranges from 24.19-40.05µm. Percentage of mud also displays an irregular but gradual decrease from 93.3-83.0%.

Overall, the grainsize data shows an upward coarsening trend from medium silts to very fine sandy silts with a marked increase in grainsize and decrease in percent mud and sorting between 157.1 to 157.6m.

8.2. Foraminiferal Assemblages

At least 300 foraminifers were counted from each of the 32 samples collected. To achieve this count the samples were carefully split using a micro splitter to reduce the abundance of foraminifera in each sample so that a minimum of 300 specimen were mounted. The full dataset including all genera is shown in appendix 11.3. In the plots shown below (Figures 11-17), generic abundances are expressed as a percentage plotted against stratigraphic height. Minor genera (less than 5%) were grouped into a single category due to their low percentages to adequately show their presence against the other genera, these assemblages are included in Table 1.

Once the minor genera were grouped together, it became clear that there are distinctive changes in dominant taxa throughout the section including a large shift in taxa that occurs near 157.1m (Figure 11), but it is hard to pinpoint this shift precisely due to missing sections. The two barren sections from 74.5m-124.3m and 125-157m are shown in grey. Unfortunately, the major shift in taxa occurs in the upper part of the missing section. The shift in grainsize data from medium silts to very fine sandy silts at 157.1m supports this shift in taxa. The large grainsize and faunal shift at 157.1m lead to the division into the upper and lower parts of the section, with the lower part of the section existing from 0-157.1m and the upper part of the section existing from 157.6-216.3m. Dominant genera belonging to each part of these sections is also displayed in Table 1.

Stratigraphic Height	Sample Number	Assemblages
Lower Part (0-157.1m)	203-218	*Karreriella, Lenticulina, Dentalina, Chrysalogmisas, Globobulimina, Stilostomella, Plectofrondicularia, Trifarina, Siphouvigerina, Gyroidinoides, Gyroidina, Bolivina, Pullenia, Chilostomella,* and *Oridorsalis.*
Throughout the section, including Minor Genera (>5%)	*203-235*	*Anomalinoides, Anomalina, Astrononion, Sphaeroidina, Bolivinita, Bulimina, Truncorotalia, Neogloboquadrina, Zeaglobigerina, Globigerina, Euuvigerina, Notorotalia, Elphidium, Haeuslerella,* and *Globoconella.* **Minor genera:** *Martinottiella, Eggerella, Sigmoilopsis, Pyrgo, Saracenaria, Nodosaria, Chrysalogmisas, Stilostomella, Vagunulina, Gladulina, Amphicoryna, Pseudonodosaria, Lagena, Fissurina, Stainforthua, Sigmoidella, Oolina, Proxifrons, Virgulopsis, Dyocibicides, Discorbinella, Pileolina, Patellinella, Gavenilnopsis, Cancris, Rosalina, Zeafloris, Neoconorbina, Nonionoides, Melonis, Pleurstonella, Globocassidulina, Osangundaria, Hoeglundaria Hirsutella,* and *Orbulina.*
Upper Part (157.6m-216.3m)	219-235	*Siphotextularia, Quinqueloculina, Globigerinita, Turborotalia*, *Evolvocassidulina, Cassidulina,* and *Nonionella*

Table 1. Assemblages that were divided into sections based on faunal distributions

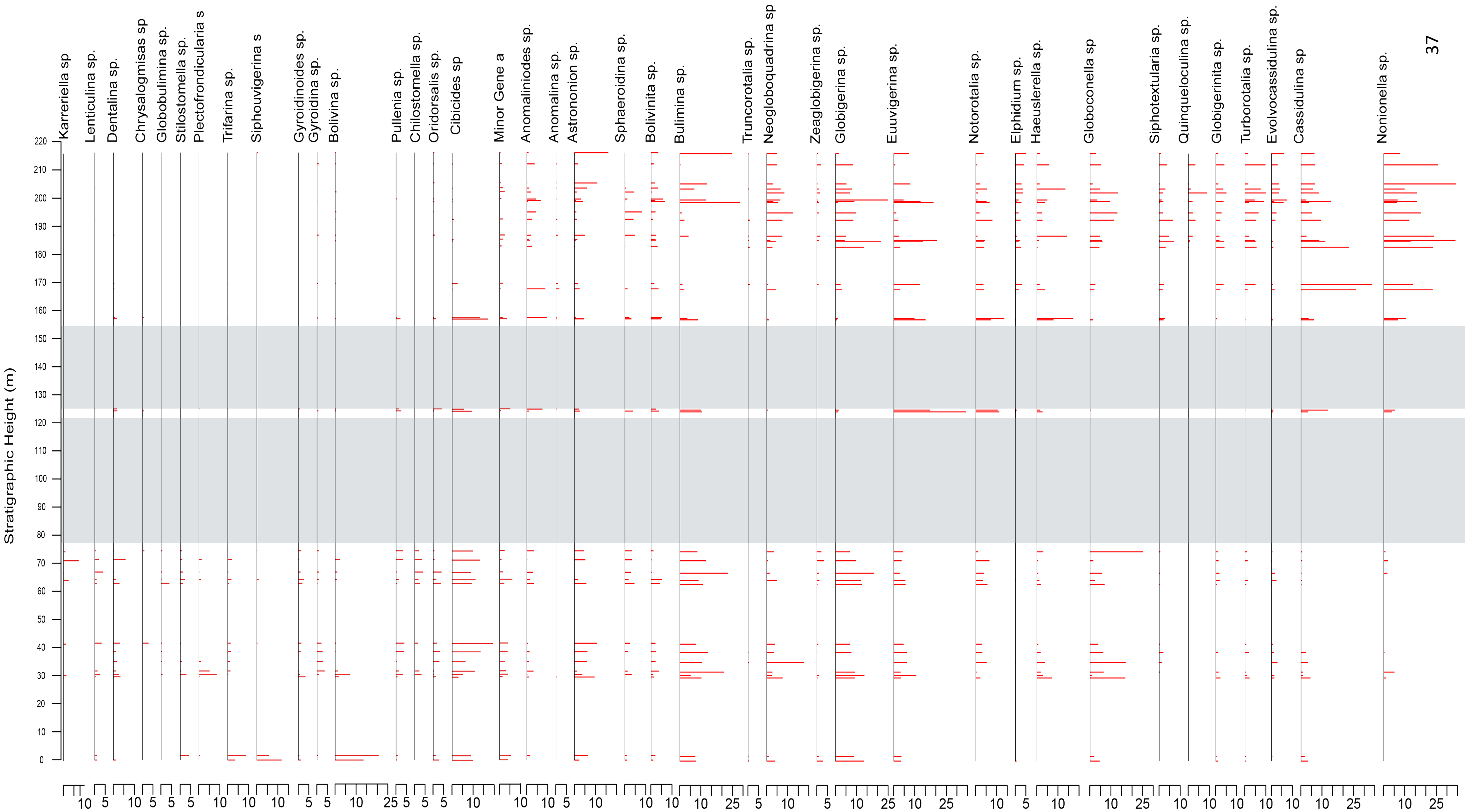

Figure 11. Histogram showing abundant genera (<5%) and minor genera (>5%) grouped together.

Faunal changes are re-presented in (Figure 12), where the more abundant genera from (Figure 11) were selected to outline and emphasize the shifts in taxa dominance. The taxa dominant in the lower part of the section are shown in green, while taxa shown throughout the section are shown in red, and taxa more dominant in the top of the section are shown in blue. *Notorotalia* and *Bulimina* are both present throughout the section, while *Bolivina* and *Leticulina* are more common to the bottom part of the section and are only abundant in the first 74m, with low abundances continuing up through the section. *Cibicides* is abundant up until 157.1m and then slowly decreases. Dominant genera towards the top of the section, becoming abundant at 157.6m are *Nonionnella* and *Elphidium.* Again, the shift in assemblages occurs somewhere within in upper realms of the missing section from 125-157m and it is difficult to pinpoint a precise location.

There is an abundance of faunal data documented from the samples collected in the Mangaopari Mudstone which will allow the reconstruction of the Plio-Pleistocene paleoenvironment. In both Figures 11 and 12, faunal distributions and obvious changes throughout the section are depicted as reflections of either depth ranges, age ranges, environmental preferences, or variations in grain size. These will be debated later in the discussion. (Hayward, 1999)

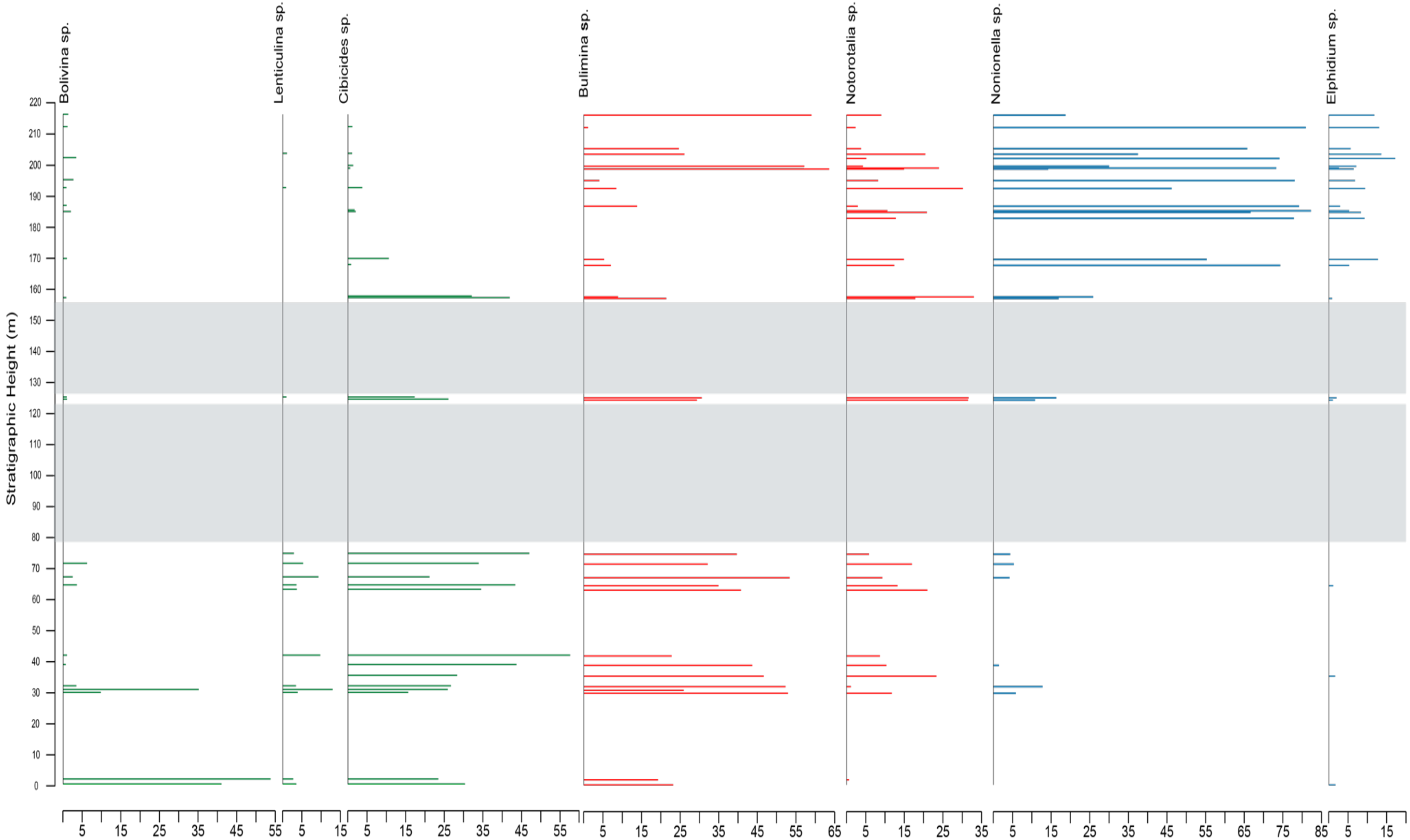

Figure 12. Major shifts in abundant taxa outlined throughout the section, with missing sections outlined in grey.

8.3 Epifaunal and Infaunal Genera

Infaunal and epifaunal taxa were divided here based on their wall structure (Table 2) and then plotted against stratigraphic height to better understand the type of environment in which these species occupied (Figure 14). As discussed in Chapter 4.2.3, benthic assemblages tend to favour different substrates based on their morphology. As shown below, percentages of epifaunal genera in the lower part of the section are low and gradually increasing with stratigraphic height, ranging between 35-55%.

A distinctive shift occurs at 157.6m, where percentages of epifaunal abundance increases dramatically to 75-85% and then continue to fluctuate between 55-80% from 185-216.3m. Very low percentages of epifaunal genera occur at 30m and 199m, which is possibly due to poor preservation or high concentrations of organic matter which cause infaunal species that favour low oxygen conditions to become abundant. Infaunal species mirror this plot, showing the opposite trend. Infaunal species *Bolivinita pliozea* and epifaunal species *Cibicides deliquatus* were compared in Figure 13 to provide a better understanding of the specific morphological differences amongst assemblages and their environmental preferences.

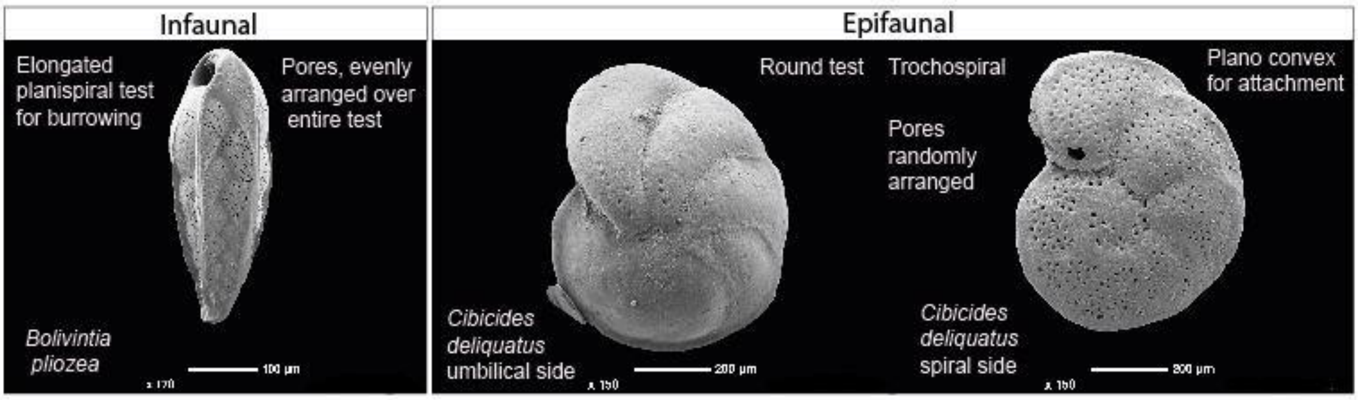

Figure 13. Morphological differences in epifaunal and infaunal assemblages.

Infaunal Assemblages	Epifaunal Assemblages
Karreriella, Haeuslerella, Siphotextularia, Martinottiella, Eggerella, Sigmoilopsis, Quinqueloculina, Pyrgo, Saracenaria, Lenticulina, Nodosaria, Dentalina, Chrysalogmisas, Stilostomella, Vagunulina, Gladulina, Amphicoryna, Pseudonodosaria, Lagena, Fissurina, Stainforthua, Sigmoidella, Oolina, Plectofrondicularia, Proxifrons, Globobulimina, Bulimina, Bolivina, Virgulopsis, Trifarina, Siphouvigerina, Euuvigerina, and *Bolivinita*	*Lenticulina, Dyocibicides, Cibicides, Discorbinella, Pileolina, Patellinella, Gavenlinopsis, Cancris, Rosalina, Zeafloris, Nonionoides, Nonionella, Elphidium, Notorotalia, Gyroidinoides, Gyroidina, Anomalinoides, Anomalina, Astrononion, Sphaeroidina, Pullenia, Laticarinina, Oridorsalis, Cassidulina, Evolvocassidulina, Globocassidulina,* and *Hoeglundaria*

Table 2. Infaunal and Epifaunal fossil assemblages.

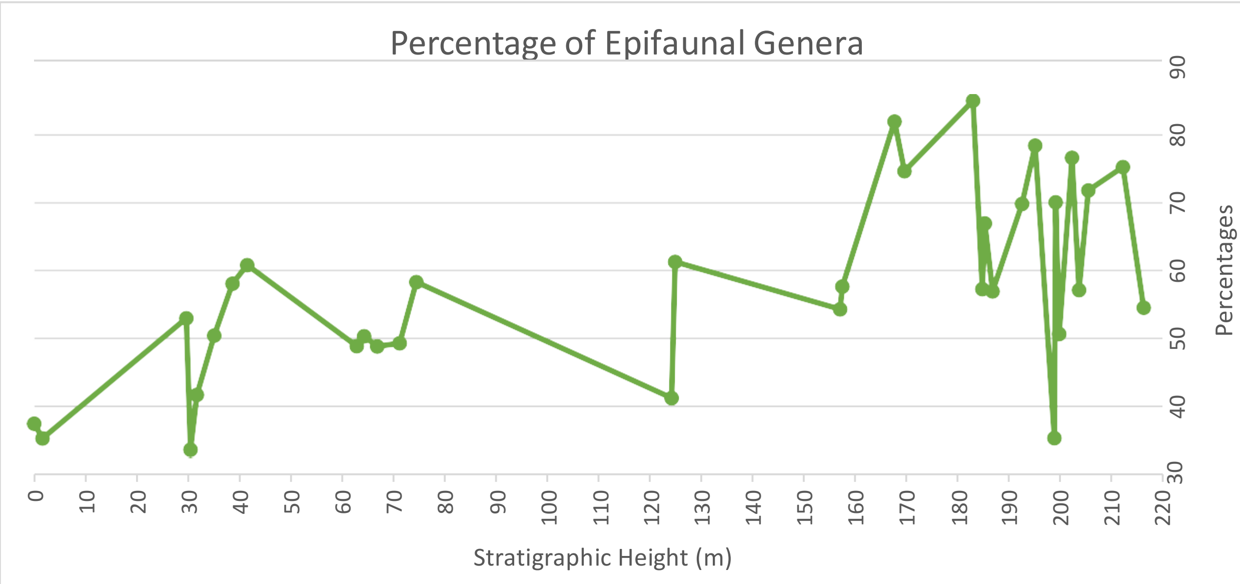

Figure 14. Epifaunal genera percentages plotted against stratigraphic height (m).

8.4 Temperature Indicative Genera

As mentioned in Chapter 4.2.3, water masses are a contributing factor when examining planktonic distribution because assemblages are linked directly with particular water masses. Crundwell et al (2007) provides sea surface temperature models based on planktonic foraminiferal assemblages and makes faunal associations with distinctive water masses. Crundwell et al (2007) then presents these planktic assemblage as water masses that reflect glacioeustatic cyclicity.

During the Plio- Pleistocene, major uplift and subsidence gave rise to several paleo seaways which in turn transported cold water masses to otherwise Subtropical-Temperate areas. Planktonic species were assigned into assemblages representing Subtropical- Temperate, Temperate, Sub Antarctic, and Eutrophic water masses (Table 3). Eutrophic assemblages are included here to display species that dwell in environments that are rich in nutrients and low in oxygen (Table 3). The distributions are illustrated below in Figure 15, with assemblages typical of Sub Antarctic waters plotted in dark blue, Temperate in light blue, Subtropical-Temperate in green, and Eutrophic in grey.

Water Mass	Assemblages
Subtropical- Temperate	*Hirsutella spp., Truncorotalia spp., Truncorotalia crassaformis, Truncorotalia crassula* and *Globigerina*
Temperate	*Globoconella inflata* and *Neogloboquadrina incompta*
Subantarctic	*Neogloboquadrina pachyderma*
Eutrophic	*Globigerinita glutinata* and *Turborotalia quinqueloba*

Table 3. Water masses and fossil assemblage associations based on Crundwell et al (2004 & 2007).

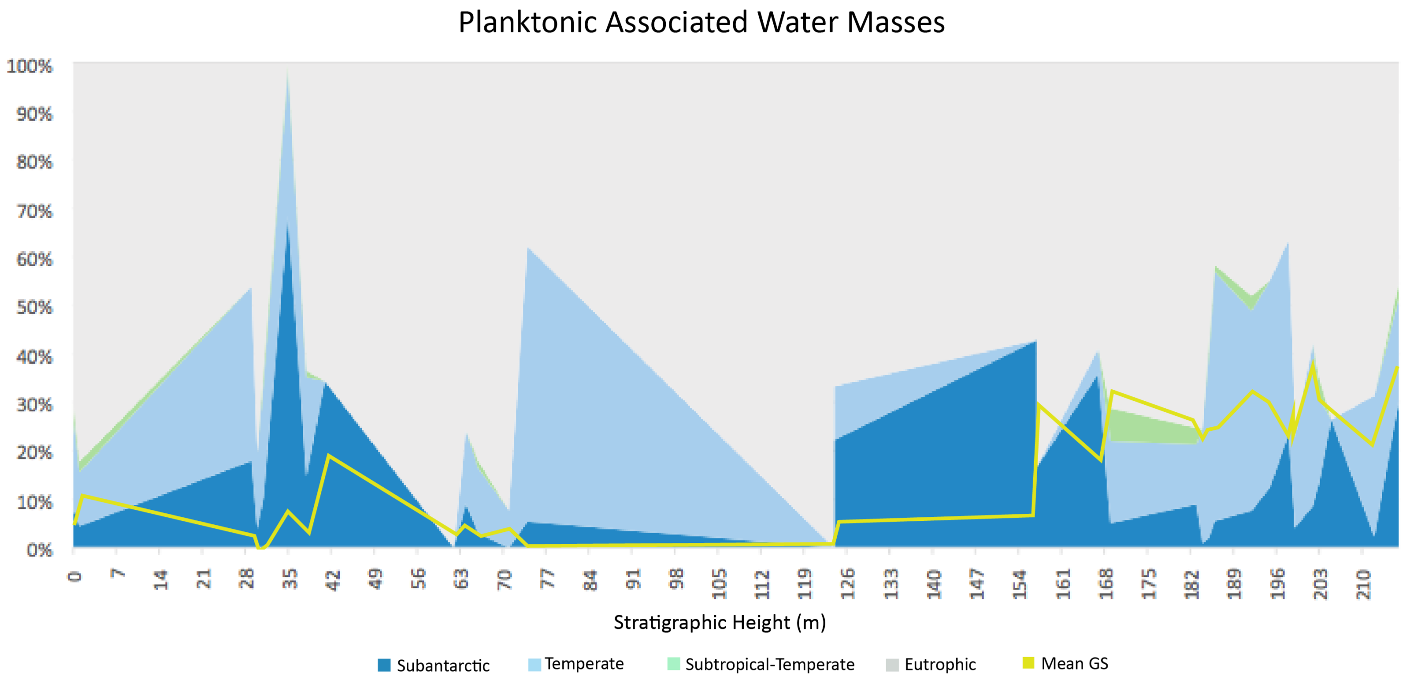

Figure 15. Planktonic assemblages and their typical water mass association based on Crundwell et al (2004 & 2007) along with the mean grain size (um) throughout the section (mean GS not in percentages).

Subtropical-Temperate water assemblages appear in low abundance (>5%) in the first 0-14m and at 168-216m in the section. Sub Antarctic waters assemblages show peaks of <20% at 35m, 42m, 125m, 154m, and 162m. Temperate water assemblages show abundant (<50%) peaks that closely resemble Sub Antarctic peaks. Eutrophic assemblages are present with peaks and troughs fluctuating throughout the section. The mean grain size is shown steadily increasing up section from 5μm-40μm. Again, note the two gaps in this section that are present at 74.5m-124.3m and 125-157m and are easily distinguishable above, where assemblage abundance and mean grain size drops to zero.

8.5 Depth Indicative Genera

Hayward (1999) lists a number of species and their paleodepth zonation based on faunal associations and upper paleodepth limits. The ecological ranges of present-day families, genera, and species are well known around New Zealand and only a few species have drastically changed their preferred environments over time. The modern ranges are used together to deduce a paleoenvironment of the fossil fauna (Hayward, 1999). Crundwell et al (1994), lists paleodepth markers based on their first appearance in a petroleum exploration well along with seismic reflection data, this is displayed in Table 9.

Neogene Paleodepth	Zonation	Species
15-150m	Mid-Outer Shelf	*Nonionella flemingi*
200-400m	Uppermost Bathyal	*Pullenia bulloides* *Cibicides neoperforatus*
150-200m	Outermost Shelf	*Trifarina bradyi* *Hoeglundina elegans*
400-600m	Upper Bathyal	*Martinottiella communis* *Karreriella cylindrica*
>600m	Mid Bathyal	*Eggerella bradyi*

Table 4. Fossil assemblages as paleo bathymetric markers based on Hayward (1999) & Crundwell et al (1994).

The foraminifera faunas in Mangaopari Mudstone were assessed based on total fauna, with a closer look on dominate species plus a few environment-specific indicator species. The Mangaopari Mudstone succession of foraminifera reveal a gradual decrease in paleo depth with the base of the section being deposited at bathyal depth near 600-800m and towards the top deposition of 150-200m. This is clearly illustrated in Figure 16, where paleo depth calibrations of specific taxa from Hayward (1999) and Crundwell et al (1994) were plotted against stratigraphic height.

The deepest paleo depth marker is *Eggerella bradyi,* indicating middle bathyal (>600m) paleo depths found at the base of the section. Upper bathyal (400-600m) paleo depth markers are *Karreriella cylindrica* and *Martinottiella communis* are both present from 30-75m. Both *Trifarina bradyi* and *Hoeglundina elegans* are present in the first 75m. These are believed to be transported down shelf because *Cibicides neoperforatus* and *Pullenia bulloides* are both present up to 125m. *Nonionella flemingi* is present from 125m onward in the section. This shift is taxa clearly displays this shallowing sequence from upper bathyal depths at the base of the Mangaopari Mudstone up to outer shelf depths at the top of the section towards the base of the Pukenui Limestone.

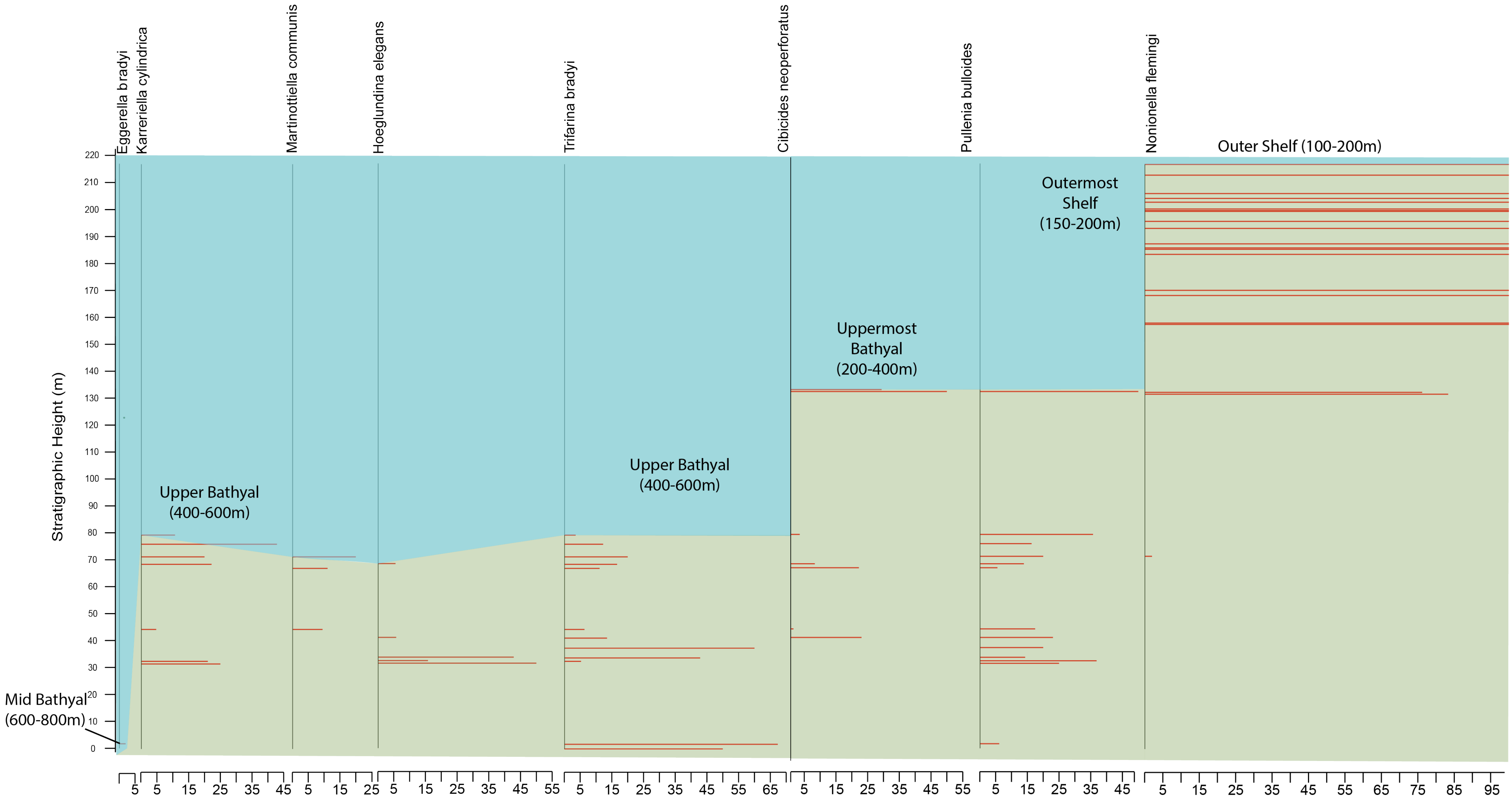

Figure 16. Diagram depicting benthic foraminiferal species and the paleo depths associated. Adapted from Hayward (1999) , Crundwell (1994).

8.6 Age Indicative Genera

The age of the Mangaopari has proved difficult to tie down precisely. Foraminiferal assemblages were also recognized for their age variability based on previous findings. Specific assemblages give clues to stratigraphic age when cross-referenced with the previous findings. Crundwell et al (1994), Vella & Briggs (1971), and Raine et al (2015), divided these planktonic assemblages within the Mangaopari Mudstone into various age zonations based on the foraminiferal distributions, this is further discussed in Chapter 8.5. These assemblages are outlined in table 5 where they are associated with ages. The foraminiferal genera and the age calibrated assemblages are plotted against stratigraphic height (Figure 17).

Duration Ma	**Epoch**	**Lower Boundary Defining Event Lowest Occurrence (LO)**
2.40	Early Pleistocene	LO *Zygochlamys delicatula* (macrofossil) LO *Truncorotalia crassula*
3.00	Late Pliocene	Base upper *Tr. crassaformis* dextral coiling zone
4.30	Early Pliocene	LO *Globoconella inflata*
5.33	Pliocene-Miocene boundary	LO *Globoconella punticulata s.s*

Table 5. Key fossil taxa and their age zonations based on Crundwell (1994) , Vella & Briggs (1971), and Raine et al (2015).

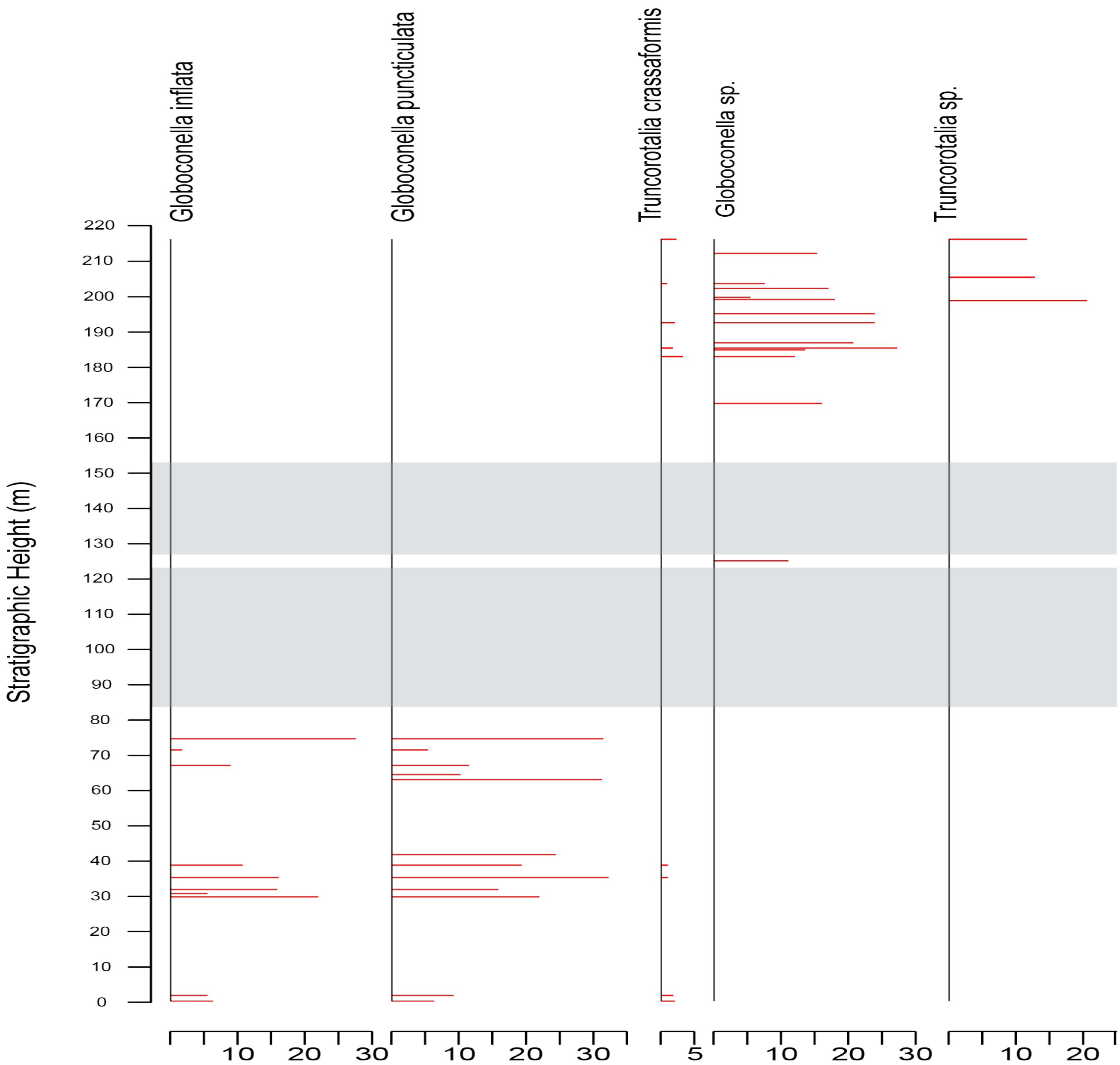

Figure 17. Planktonic species shown as age calibrations.

In Figure 17, assemblages show an obvious trend in age variability that is decreasing in age with stratigraphic height. *Globoconella inflata* and *Globoconella punticulata*, are both only present in the first 74m of the section. *Truncorotalia crassaformis* is shown throughout the section in low abundances. *Globoconella sp.,* first appears at 125m, and becomes abundantly present from 169-216.3m. *Truncorotalia sp.,* is only shown in the top 16.3m of the section. *Zygochlamys delicatula* is not shown above because it is a macrofossil and was only observed in the field, at the base of the Pukenui Limestone.

9. Discussion

9.1 Overall Assemblages

This study provides new foraminiferal assemblage distribution data for the Mangaopari Mudstone Formation, in the southern Wairarapa region. An abundance of benthic and planktic foraminifera were present throughout the section, allowing a reconstruction of the dispositional environments. There are various fluctuations in taxa present from the base to the top of the section, with a distinct shift occurring at 157.1m. In order to explain this shift, additional faunal distributions were then investigated based on environmental preferences, paleo-water temperature indicators, age and depth indicators, and these are linked to the analysis of the grainsize.

9.2 Grain Size Analysis

In previous studies, this coarsening upward shift in grain size was thought to be quite gradual throughout the section. When examining the outcrop, it is clear that this is a regressive sequence that is coarsening upwards and increasing in grainsize towards the base of the Pukenui Limestone. This is supported in general by the grainsize analysis. However, the analysis also reveals that there is a sharp increase in grainsize from medium silts to very fine silty sands at 157.1m. While the coarsening upwards trend is consistent with shallowing in water depth and predominately to terrestrial sediment supply overall, the grain size analysis indicate low energy relatively deep marine pelagic sedimentation of depths indicative of >400m.

None of the samples show grainsize or sorting indicative of high energy (wave or current influence) that would be expected at shore face depths (<50m). Therefore, sedimentation is likely to have occurred in the upper bathyal to the outermost shelf.

9.3 Epifaunal and Infaunal Genera

There is a distinctive increase in epifaunal assemblages with stratigraphic height with a clear shift from infaunal dominance to epifaunal dominance at 157.1m, which directly correlates with grainsize data. The taxa recovered from the base of the section show distinctive infaunal morphology that favour a fairly low energy silty-muddy environment likely of upper bathyal depths of greater than 400m or deeper. The taxa present at the top of the section are mainly epifaunal, and favour coarser grain size, typical of higher energy environments along the outermost shelf in 150-200m water depth. This is supported by grainsize analysis, which depicts a gradual regressive sequence. In the lower part of the section, finer grained sedimentation occurred at bathyal depth where infaunal species are abundant. Then with a distinctive shift at 157.1m to coarser grains, likely of outermost shelfal depths where epifaunal species are more commonly abundant.

The grain size trend documented in Figure 18 compares the percentage of infaunal genera to the percentages of mud. The percent mud is consistently high until 157.1m, with a range from 91.5-100%. Infaunal assemblages are abundant until 157.1m, ranging from 60-40%. Both show an irregular but gradual decrease, with percent mud range from 93.3-83.0% and infaunal assemblages range from 15-65% after 157.6m.

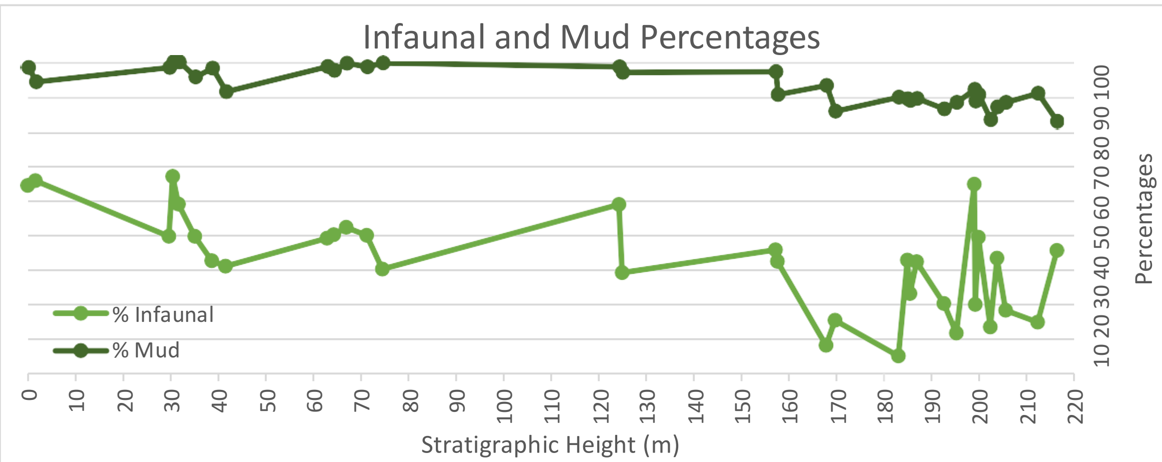

Figure 18. Percentages of Infaunal assemblages and the percentages of mud plotted against stratigraphic height (m).

9.4 AGE

Foraminifera from the Mangaopari Mudstone have been divided into various zones by Crundwell (1994), Vella & Briggs (1971), and Raine et al. (2015) subdivided the following zones based on the foraminiferal paleoecology;

The microfossil *Truncorotalia crassula* is paired with the macrofossil *Zygochlamys delicatula* and their last occurrence together marks *Truncorotalia crassula* zone that starts in the early Pleistocene, dated at 2.40Ma. *Zygochlamys delicatula* was identified in the Pukenui Limestone Formation and was also found grading in the very top of the Mangaopari Mudstone.

Truncorotalia crassaformis zone is a dextral coiling zone of this species that marks the last occurrence of the foraminiferal microfossil *Truncorotalia crassiformis.* This zone marks the Late Pliocene in age and is dated at 3.0Ma.

Globorotalia inflata zone is found to exist with the last occurrence of *Globorotalia inflata* and marks the early Pliocene in age, dating at 4.3Ma.

Globoconella punticulata zone is based on the last occurrence of *Globoconella punticulata*, which marks the Miocene-Pliocene boundary at 5.33Ma. This boundary is believed to correlate with the base of the Makara Greensand.

These zones are displayed in Table 5 and show similar distributions when cross-references with Crundwell (1994), Vella & Briggs (1971), and Raine et al (2015). Therefore, based on faunal depth associations this section can be interpreted to represent an age of >2.93Ma in age (from >5.33Ma at the base of the section to >2.40Ma at the top), stratigraphically ranging from the early Pliocene to Early Pliocene in age.

9.5 Climactic Indicators

Planktonic assemblages that are indicative of paleogeography and different water masses were discussed above in Chapter 7.4 to determine if any changes in water temperature may reflect glacioeustatic sea level changes (Figure 15). Although sample density was not adequate to resolve a full glacioeustatic cycle, the data does show distinguishing parts of these cycles. There are multiple different peaks of each water mass that overall shows sporadic changes throughout the section that are possibly caused by glacioeustatic fluctuations. The abundance of *Neogloboquadrina pachyderma* (sinstral) infers that there are multiple pulses of Subantarctic waters. These pulses are followed by Subtropical and Temperate faunal appearances which suggest the cyclicity is real. These cold water influxes are expected towards the top of the section, where the Mangaopari is coarsening towards the base of the Pukenui but not at the base of the Mangaopari Mudstone. The Ruataniwha and Manawatu Strait are the most plausible causes for the transport of these cold water influxes to this region during 4.8-2.0Ma. Both of these straits aided in transporting cold water typical species like *N.pachyderma* to this region which were deposited in the Mangaopari Mudstone and Pukenui Limestone Formation. Temperate water species that follow a similar trend to the Subantarctic, and were most likely also transported by the Ruataniwha and Manawatu Strait. Although, its most plausible that the Rautaniwha Strait caused most of the influx due its wider opening in the southern region.

Overall, there are two geological processes that lead to regressive sequences, which are either caused by regional tectonic uplift or by glacioeustatic sea-level fluctuations. However, in this study the glacioeustatic fluctuations do not adequately correlate with the surrounding data. Therefore, the regressive sequence presented in the foraminiferal and sedimentological data collected from the Mangaopari Mudstone is interpreted to be triggered by the tectonic uplift that occurred in the late Miocene- Pleistocene.

10. Conclusion

This Masters by Thesis project was undertaken to master the techniques of micropaleontology with the intentions to reconstruct the late Miocene-early Pliocene paleoenvironment in which the Mangaopari Mudstone accumulated. To accomplish this, foraminiferal identification and analysis along with grainsize distribution were investigated with a 216m section of the Mangaopari Mudstone. A better understanding of the late Miocene-early Pliocene paleoenvironmental history within the Mangaopari Mudstone now exists and is documented above. The age of the mudstone proved difficult to ascertain but based on foraminiferal assemblages a broad range from >5.33Ma to >2.40Ma was obtained.

The data presented above and combined in Figure 19 illustrates the deposition of the Mangaopari mudstone began during the late Miocene-early Pleistocene. The presence of several genera and species including *Martinottiella communis* and *Karreriella cylindrica* between 0-157.1m stratigraphically suggest that accumulation began in bathyal conditions at depths greater than 400m between. This is supported by grainsize analysis which indicates a medium silt with a high percent mud content ranging from 91.5-100%.

The upper part of the section (157.6-216.3m) accumulated during the early Pleistocene. The age is suggested with the presence of *Truncorotalia sp. and Zygochlamys delicatula*. Foraminiferal assemblages including *Nonionella flemingi* recovered indicate that by the time of deposition the upper part of the section had shallowed significantly to outermost shelfal depths of 150-200m. Grainsize also support this discovery with a shift to very fine sandy silts with a percent mud content ranging from 83-93%.

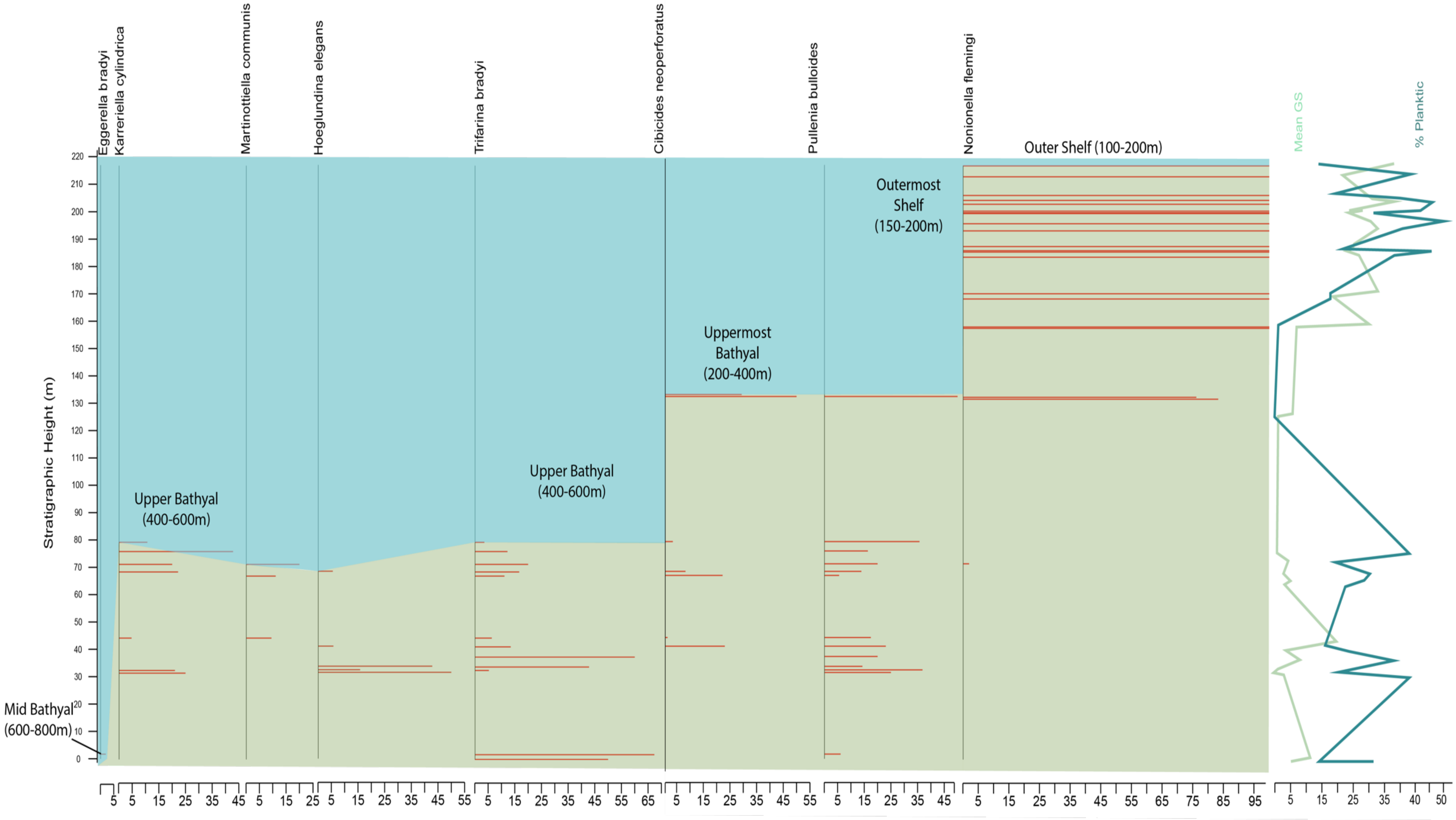

Figure 19 . Combination of paleodepth marker, grain size, and percent planktics.

Together the grainsize analysis and foraminiferal assemblages documents a gradual regressive sequence with a major shift to shallowing conditions occurring at 157.1m. As stated above, regressive sequences are caused by either geological processes or glacioeustatic seal level fluctuations. However, the sudden shift within this regressive sequence does not correlate with the glacioeustatic findings and therefore is believed to be triggered by a tectonic event that was caused by the reactivation of the present Australian and Pacific plate boundary.

Further study suggestions:

a. The samples collected for this project were not of a high enough stratigraphic resolution to confirm the presence of glacioeustatic cycles within the overall shallowing trend documented above. However, the foraminiferal water mass data with the alternations of high and low sub counts of Antarctic species suggest that they are present, The collection and analysis of a high resolution sample collection should be able to confirm this.
b. The use of X-ray fluorescence to determine the chemistry shifts in mineral composition within the mudstone also offers the opportunity to document high frequency cycles.
c. Recent discovery of several tephra layers within the Mangaopari Mudstone (Atkins pers comn 2017) offer the opportunity to refine the very broad age range deduced using foraminifera.

11. References

Armstrong, H., Brazier, M., 2004. Microfossils (Second Edition). Blackwell Publishing, Oxford. 142-188.

Beanland, S., Melhuish A., Nicol, A. & Ravens, J. 1998. Structure and deformational history of the inner forearc region, Hikurangi subduction margin, New Zealand. *New Zealand Journal of Geology and Geophysics*, 41, 325-342.

Beu, A. G. & Edwards, A. R. 1984. New Zealand Pleistocene and late Pliocene glacio-eustatic cycles. *Palaeogeography, Palaeoclimatology, Palaeoecology,* 46, 119-142.

Boggs, Sam Jr. 2006. *Principles of Sedimentology and Stratigraphy*. Fourth Edition. University of Oregon, Oregon, USA, 406-413.

Boltovskoy, E., Scott, D., & Medioli, F., 1991. Morphological Variations of Benthic Foraminifera Tests in Response to Chance in Ecological Parameters: A Review. Journal of Palaeontology. 65(2). 175-185.

Clarke, D. 1998. *A biostratigraphic investigation of the Pukenui Limestone formation, South Wairarapa, New Zealand*. Unpublished MSc thesis, Victoria University of Wellington.

Cole, J. W. & Lewis, K. B. 1981. Evolution of the Taupo-Hikurangi subduction system. *Tectonophysics,* 72**,** 1-21.

Collen, J.D. & Vella, P. 1984. Hautotara, Te Muna and Ahiaruhe Formations, middle to late Pleistocene, Wairarapa, New Zealand. *Journal of the Royal Society of New Zealand*, 14, 297-317.

Crundwell, M. P. 1987. *Neogene Stratigraphy and Geological History of the Wainuioru Valley, Eastern Wairarapa, New Zealand*. Unpublished MSc thesis, Victoria University of Wellington.

Crundwell, M.P., Scott, G.H., Thrashers, G.P., 1994. *Calibrationa of Paleobathymetry indicators by intergrated seismic and paleontological analysis of freset sequences, Taranaki Basin, New Zealand.* Lower Hutt, New Zealand: Institute of Geological & Nuclear Sciences.

Crundwell, M. P., Scott, G., Naish, T., Carter, L., 2007. *Glacial-interglacial ocean climate variability from planktonic foraminigera during the Mid-Pleistocene transition into the temperate Southwest Pacific, ODP Site 1123*. Geological and Nuclear Sciences. Lower Hutt, New Zealand: Institute of Geological & Nuclear Sciences.

Devereux, I., Hendy, C.H. & Vella, P. 1970. Pliocene and early Pleistocene sea temperature fluctuations, Mangaopari Stream, New Zealand. *Earth and Planetary Science Letters,* 8, 163-168.

Gammon, P.R. 1995. Hautotara Formation, Mangaopari Basin, New Zealand; a record of a cyclothemic Pliocene-Pleistocene marine to non-marine transition. *New Zealand Journal of Geology & Geophysics,* 38, 471-481.

Hayward, B.W., Grenfell, H.R, Reid, C.M, & Hayward, K.A. 1999. *Recent New Zealand shallow water benthic foraminifera: Taxonomy, ecology, and use in paleoenvironmental assessment*. Institute of Geological & Nuclear Sciences monograph 21, 264 p. Lower Hutt, New Zealand: Institute of Geological & Nuclear Sciences, 1-11.

Hines, B. R., Kulhanek, D. K., Hollis, C. J., Atkins, C. B., & Morgans, H. E. G. 2013. Paleocene– Eocene stratigraphy and paleoenvironment at Tora, Southeast Wairarapa, New Zealand. *New Zealand Journal of Geology and Geophysics*, *56*(4), 243-262.

Hornibrook, N.D.B., Strong, C. P & Brazier, R. C., 1989, *Manual of New Zealand Permain to Pleistocene foraminiferal biostratigraphy*.

Howard, H. A. & Brasier, M.D., 2004. *Microfossils*, Second Edition. Blackwell Publishing, Maden, Massachusetts, USA, 16-23.

Jones, R., 2006. Applied Paleontology. Cambridge University. Cambridge, UK. 48-67.

Kennett, J.P., Watkins, N.D. & Vella, P., 1971. Paleomagnetic chronology of Pliocene-Early Pleistocene climates and the Plio-Pleistocene Boundary in New Zealand. Science, 171, 276-279.

Lamb, S.H. & Vella, P., 1987. The last million years of deformation in part of the New Zealand plate-boundary zone. *Journal of Structural Geology*, 9, 877-891.

Lee, J.M. & Begg, J.G. (compilers) 2002. *Geology of the Wairarapa Area*. Lower Hutt, New Zealand. Institute of Geological & Nuclear Sciences. 1-5.

Lewis, K.B., 1980. Quaternary sedimentation in the Hikurangi oblique subduction and transform margin, New Zealand. In: Balance, P.F.; Reading, H. G ed. Sedimentation in oblique slip mobile zones. *International Association of Sedimentologists special publication 4.*

Lienert, B.R., Christoffel, D.A. & Vella, P. 1972. Geomagnetic dates on a New Zealand upper Miocene-Pliocene section. Earth and Planetary Science Letters, 16, 195-199.

Murray, J. W., 2006. *Ecology and Applications of Benthic Foraminifera*. Cambridge University Press. Cambridge, UK.

Murray, J. W., 1991. *Ecology and Paleoecology of Benthic Foraminifera.* Longman Scientific and Technical; New York: Wiley, Harlow, Essex, England.

Naish TR, Abbott SS, Alloway BV, Beu AG, CarterRM, EdwardsAR, Journeaux TJ, Kamp PJJ, PillansB, Saul G, Woolfe KJ 1998. Astronomical calibration of a southern hemisphere Plio- Pleistocene reference section, Wanganui Basin, New Zealand. Quaternary Science Reviews17: 695_710.

Nicol, A., et al., 2007. Tectonic evolution of the active Hikurangi subduction margin, New Zealand, since the Oligocene. *Tectonics*, 26, TC4002.

Pillans B., Alloway B.V., Naish T., Westgate J.A., Abbot S., Palmer A.S. 2005. *Silicic tephrasin Pleistocene shallow marine sediments of Wanganui Basin, New Zealand.* Journal of the Royal Society of New Zealand 35: 43_90.

Raine, J.I., Beu, A.G., Boyes, A.F., Campbell, H.J., Cooper, R.A., Crampton, J.S., Crundwell, M.P., Hollis, C.J., Morgans, H.E.G. 2015. Revised calibration of the New Zealand Geological Timescale: NZGT2015/1. *GNS Science Report* 2012/39. 53 p.

Reilly, C., Nicol, A., Walsh, J., Seebeck, H. 2015. Evolution of faulting and plate boundary deformation in the Southern Taranaki Basin, New Zealand. *Tectonophysics*, 651–652, 1-18.

Rodley, D. R. 1961. *The Geology and Paleoecology of Nukumaruan Strata near the Junction of Ruakokopatuna and Makara Rivers.* Unpublished MSc Thesis, Victoria University of Wellington, 107.

Shane, P., 1994. *A Widespread, early Pleistocene tephra (Potaka tephra 1Ma) in New Zealand: Character, Distribution, and Implications*. New Zealand Journal of Geology and Geophysics; 37:1, 25-35.

Shane, P., Frogatt, P., Black, T. & Westgate, J. 1995. *Chronology of Pliocene and Quaternary bioevents and climatic events from fission-track ages on tephra beds, Wairarapa, New Zealand.* Earth and Planetary Science Letters, 130, 141-154.

Shane P., Alloway B., Black T., Westgate J 1996a. *Isothermal plateau fission-track ages if tephra beds in early-middle Pleistocene marine and terrestrial sequence, Cape Kidnappers, New Zealand.* Quaternary International 34-36: 49-55.

Shane P., Black T.M., Alloway B.V., Westgate J.A. 1996b. *Early to middle Pleistocene tephrochronology of North Island, New Zealand: implications for volcanism, tectonism and paleoenvironments.* Geological Society of America Bulletin 108: 915-925.

Trewick, S.A. & Bland K.J., 2012. Fire and slice: palaeogeography for biogeography at New Zealand's North Island/South Island juncture. *Journal of the Royal Society of New Zealand*, 42:3, 153-183.

Vella, P., 1953. The Genus Pelicaria in the tertiary of East Wairarapa. *Transactions of the Royal*

Society of New Zealand, 81(1), 35-48.
Vella, P. 1963. Upper Pleistocene succession in the inland part of Wairarapa Valley, New Zealand. *Journal of the Royal Society of New Zealand*, 2, 63-78.
Vella, P. & Briggs, W.M., 1971. Lithostratigraphic names, upper Miocene to lower Pleistocene, northern Aorangi Range, Wairarapa. *New Zealand Journal of Geology & Geophysics*, 14, 253-274.
Vella, P. P. & Nicol, E. R., 1970. Chlamys delicatula and the Hautawan Stage. *New Zealand Journal of Geology and Geophysics.* 13(3), 873-876.
Wilson, C.J.N., et al., 1995. Volcanic and Structural Evolution of the Taupo Volcanic Zone, New Zealand; a review. *Journal of Volcanology and Geothermal Research.* 68(1-3), 1-28.

12. Appendix

12.1 Foraminiferal Counts

Elevation (m)	Stratigraphic Height (m)	Sample Number	Benthic count	Planktic count	Total Count	% Benthic	% Planktic	Genus Number	Karreriella cylindrica	Haeuslerella sp.	Haeuslerella parri	Haeusterella cylindrica	Haeusterella finlayi	Siphotextularia sp.	Siphotextularia wairoana	Siphonaperta sp.	Textularia sp.	Martinottiella sp.	Martinottiella cummunis	Eggerella sp.
108.64	216.3	235	296	45	341	84	13	25		5					3					
107.28	212.3	228	173	91	264	61	29	31			15				10					
105.33	205.5	234	266	39	305	86	13	25		4					1					
104.67	203.7	227	221	108	329	53	30	29			45				10					
104.61	202.3	225	149	123	272	61	38	24							5					
103.81	199.8	230	190	128	318	56	38	28			16				4					
104.7	199.2	226	223	122	346	68	29	25					1		7					
103.64	198.9	233	311	34	345	86	10	23		13					2	1				
107.47	195.2	232	175	146	321	61	35	24		8					6					
107.69	192.6	231	253	143	396	63	28	30		11					26					
108.01	186.9	229	257	77	334	63	18	33			48				16					
102.08	185.4	224	217	55	272	84	15	25		3					1					
101.74	184.9	223	147	103	250	57	36	21							18					
100.71	183.0	222	192	91	283	68	28	21					1		9					
99.63	169.7	221	306	62	368	82	14	25					5		9					
98.74	167.8	220	314	47	361	81	13	24					14		7					
98.38	157.6	219	266	6	272	78	2	26		33	14				8					
98.27	157.1	218	264	11	275	86	4	30		21	1				6					
97.66	125.0	217	273	9	282	95	3	28		5										
102.74	124.3	216	253	4	257	96	2	25		7										
103.24	74.5	214	181	127	308	54	41	42	3	10					2					
102.93	71.3	215	234	56	290	73	19	36	21	2										
116.53	66.9	213	195	80	275	69	29	38	1	2					1				1	
105.55	64.3	212	233	79	312	71	25	43	8				4							
121.83	62.9	211	234	64	298	76	21	36					6		1				2	
134.25	41.6	210	229	45	274	79	16	41	3	2					1				6	
107.65	38.6	209	336	93	429	74	22	43		8					9					
108.43	35.1	208	171	93	264	59	35	34					10		4					
99.59	31.7	207	169	45	214	77	21	35		4					1					
100.24	30.5	206	212	54	266	75	20	40	4				8							
96.79	29.6	205	162	101	263	54	38	36	1				19							
96.08	1.6	204	316	54	370	85	15	37												
95.3	0.0	203	118	47	165	71	28	34												

Lagena sp.	1				1		1			1	1	2						2	3		2	1	1	1			4		1	1	1	1	1
Pseudonodosaria																							1		1								
Amphicoryna sp.																			2	8	1	1		1	11	6	2	1	3	8			
Glandulina sp.																								2									
Marginulina sp.																																	
Vagunulina sp.																								1		1							
Stilostomella sp.																					3	3	4	7	4	1	1	2	1	8		16	
Chrysalogmisas sp.																	2			2	3					8							
Dentalina sp.											2				2	2	2	5	5	5	1	17	1	4	9	9	6	5	3	7	9		2
Nodosaria sp.																		1						2	1				4				
Lenticulina peregina																							1		1	1				2			
Lenticulina calcar																						2	6	3		8			3	5	2	3	2
Lenticulina australis				1						1												4	4		2								
Lenticulina sp.																			1		2										1	1	
Saracenaria ampla																											1						
Pyrgo sp.		1			2				1	1	2		1				1																
Quinqueloculina lamarkiana		8	1	4	24	1	7		7	13	7	2	2																				
Quinqueloculina sp.		1								1				1																			
Sigmoilopsis schlumbergeri																																	
Sigmoilopsis sp.																										1				1			1
Eggerella bradyi																																1	

Fissurina sp.		1	1	2	1	4	1			2				1		2	2	1	2			1	1										
Stainforthua sp.																2																	
Sigmoidella sp.																		1															
Oolina hexagona				1																										1			
Plectofrondicularia																																	
Plectofrondicularia pellucida		2	1	23	11	3	1			3	1	4			1																		
Proxifrons sp.				2			1																										
Globobulimina sp.							2	1			1		1																				
Globobulimina pacifica				2		1			12	1			1																				
Bulimina sp.																																	
Bulimina striata	5	7	19	2	11	23	47	6	19	5	18	4	6	3																			
Bulimina aculeata	8	21	8	11	34	5	12	15	14	23	45	32	21	24	30	24	10	8	5				14	9	3	98		40		23	39	1	85
Bulimina elongata				1						1																							
Bulimina marginata																																	
Bulimina bulloides																																	
Bolivina cacozeta																1																	
Bolivina sp.		2																	1														
Bolivina cacozeta																																	2
Bolivina affiliata	23	74	5	19	2					1		7		1							1												
Bolivina aculeata																																	
Bolivina albatrossi										1	2																						

Bolivia minuta	Bolivina watti	Virgulopsis sp.	Trifarina sp.	Trifarina angulosa	Trifarina bradyi	Siphouvigerina sp.	Siphouvigerina canaricasis	Euuvigerina sp.	Bolivinita sp.	Bolivinita pliozea	Bolivinita plioboqua	Bolivinita pohana	Dyocibicides sp.	Cibicides sp.	Cibicides deliquatus	Cibicides neoperforatus	Cibicides molestus	Discorbininella sp.	Pileolina sp.	Patellinella inconspicua
							2	25		12										
1								2		4			1	1						
								24		6										
								1		11				1						
2										1			1							
								15		18			1	1						
								44		7										
								65		23				1						
2								4		7										
1								9		4					4					
1								9		8										
		1						56		6				2						
								35		6				1						
								9		9										
		1	1					46		6				5	5					
								11		13				1						
								27		9	5		1	21	15					1
				1				42		9	4			29	18					
1				1				51		5	2			4	8	5				
								88		10				23		1				
					1		1	14			2	2		9	3	1	9			
					6			11				1		17	8		13			
	1				1			8			1				24		1			
	1				6		3	18			17			25	3	3	5	3		
					2			17		13				14	3	4	7			
	1				4		1	13		6				11	3	1	38			1
1					7			28		11				16	17	12	14	2		
		1			3			17		6				10	6		1			
	1				3			7		8				19	4					
					1			29		1		2		10	3		1			
								9		4				7	1					
	2				33		22	14		4		4		19	4		11	6		
					6	20		6		2				7	6		4	2		

Gavenlinopsis sp.	Cancris sp.	Rosalina sp.	Zeafloris sp.	Zeaflorilus parri	Neoconorbina sp.	Nonioniodes magnalinqua	Nonionella sp.	Nonionella flemingi	Nonionella turgida	Nonionella manlingus	Elphidium sp.	Elphidium charlottensis	Notorotalia sp.	Notorotalia hurpiensis	Notorotalia cathrata	Notoritalia taranakia	Gyroidinoides sp.	Gyroidina sp.	Melonis barleenum	Anomalinoides sp.
								27			17		2	11				1		
1								68			7	4		2				3		
						2		104			9			6						
								33			4	8	10	8						
		3						43			6	4		3						
2								21			2	3	3							
								55			1	1		18						
								22				10		23				1		
								57			1	4		6						
								49			3	7		32						
1					2	1		80			1	2	1	2				3		
								93			1	5		12						
								32			2	2		8	2					
								67			2	6		11						
								52			2	10	14					2		
								84				6	13		1					
								29						35	2			1		
								19				1		15	5			1		
								16				2				31	2			
								10			1					29		2		
	1									3				4			4	3		
								1	1	4				19			1			
										5				11			3	3		
											1			4	7		9	3		
	1															17	6	1		
	1					1										8	4	6		
2	1								1	1						14	5	12		
	1										1		14					8		
										11			1				1	8		
1																	2	3		
	1			1						3						6	9			
5													1				2	2	1	
											1						2			

Cassidulina laevigata																																	
Cassidulina carinata	22	18	20	19	23	8	49	13	17	38	9	24	29	65	125	94	10	17	38	9	2	2	1	2	1		11	9	2	3	12	7	6
Cassidulina sp.																																	
Pleurstomella sp.			1																														
Alabamina sp.																																	
Oridorsalis tenera	2	1	2			1		2	1		3						1	4	12	1		2	11	5	11	5	14	6	1	1	4	5	5
Oridorsalis sp.																					2						1	2					
Chilostomella ovoidea																					7	10	11	6	8	5	1		5	9			
Laticarinina pauperata																					1			1								4	
Pullenia bulloides																				1	10	8	1	5	1	11	12	1	1	7	1	3	
Pullenia sp.						1											1	6	4	5	1	2			1		5		2	2	1	1	1
Sphaeroidina bulloides			1	2	12	4	1	1	26		16			1		5	6				11	10		6	14	7	7		3	9	1	4	2
Sphaeroidina sp.										17								9		10			8										
Astrononion novozealandica				5		1												6								8				5		1	
Astrononion parki	54	5	32	15	3	9	3	14	3	5	17	3	2	1	5	9	2	7	6	5	4	2			13	7	18	10			25		
Astrononion reefi																				2	11	13		6	4	14	9	5		5		23	4
Astrononion sp.	1		1									1			1													1	3				
Anomalina spherica		1		1		1				3	3				4	6	1	1	1												1		
Anomalina sp.			1																														
Anomalinoides subnonioniodes																								1									
Anomaliniodes parvumbilius	3	10	1	4	6	14	23	2	14	10	7	3	4	7		32	26		22	3	11	1	8	4	10	2	6	3	7	1	3	6	

	2	4	4		8	6	2	1	8	5	1	2	2	3	2	1	6	3	3	2	1		8	8	20	5	24	10	14	11	8	21	**Evolvocassidulina orientalis**
2	1		3			4		2	7		1	4		12	3														1				**Globocassidulina subglobosa**
																																	Osangularia sp.
									2	2	2	2																					**Hoeglundaria sp.**
		2	3	3		3			2																								**Hoeglundaria elegaus**
														1				10	11	14	15	16	34	35		22	7	21	8		14		**Globoconella sp.**
																	5		1						1	1	4			3		9	**Globoconella triangula**
2								1			3	6			4		3		1	1	1		12	7		10		15	8	1		1	**Globoconella puncticuloides**
3	3	22	3	7	15	10				7	1	35																					**Globoconella inflata**
3	5	22		7	30	18	11	20	8	9	3	40																					**Globoconella puncticulata**
																		4				1											**Truncorotalia sp.**
1	1				1	1													3		1		3						1			1	**Truncorotalia crassaformis**
																							1										**Truncorotalia crassula**
									1																								**Globigerinoides sp.**
																																	Spharoidinellopsis sp.
3	2	14	2	4	43	11	11		6	2		4		2	3	1	14	3	8	1	1	4	10	17	7	7	5	9	13	9	2	10	**Neogloboquadrina pachyderma (sinstral)**
4	2	6	5	2	4	5			10	2	2	7					2			10	4	21	20	23	12	4	16	14	9		11	7	**Neogloboquadrina imcompta(dextral)**
5	4	1	3			1	2	1	4	3	10	7						3			3	5		3	3	2	1	4	3	1	5		**Zeaglobigerina sp.**
																																2	**Zeaglobigerina woodi**
																													3				**Hirsutella sp.**
23	33	24	37	20		33	19	38	39	50	28	22	3	5	2	3	11	9	39	54	12	17	34	31	4	31	79	19	26	16	22	6	**Globigerina sp.**

Orbulina sp.																						1						1				
Turborotalia quiqueloba		26		25	27	15	32		21	21	7	13	13	16	19	5		1	1		3	4		5	2	2	9		1	3	6	2	1
Turborotalia sp.	5		5					7																									
Globigerinita glutinata	4	11	4	12	14	1	13		9	8	6	5	10	12	14	7	2	1			3	4	5	6	2		5		3	1	5	2	2
Globigerinita sp.																															1		
Globigerinopsis sp.																				1		1	1										

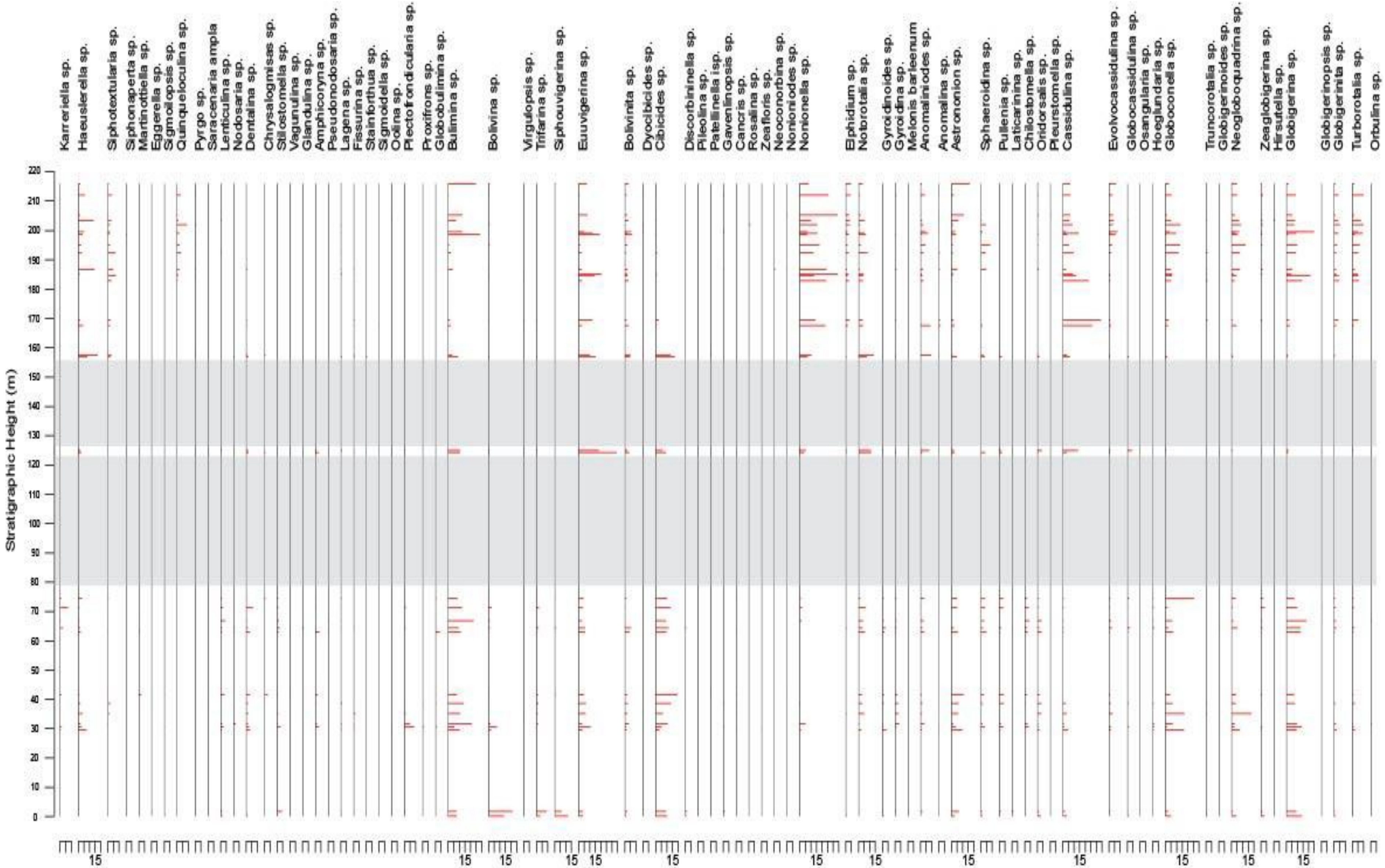

12.2 Complete Foraminiferal Assemblage Diagram

12.3 Grain Size Analysis Data

Strat Thickness	Sample #	Mean GS(µm)	Sorting (µm)	Skewness (µm)	% Mud
216.3	235	34.29	32.98	1.65	83
212.3	228	24.22	26.74	2.19	91
205.5	234	28.38	29.04	1.92	88.4
203.7	227	30.03	28.79	1.64	87.1
202.3	225	34.05	39.14	2.38	83.5
199.8	230	25.60	26.72	2.08	90.7
199.2	226	27.81	30.20	2.30	88.8
198.9	233	25.17	25.59	2.28	92.1
195.2	232	29.61	28.76	1.96	88.4
192.6	231	30.85	29.95	1.81	86.6
186.9	229	26.43	28.45	2.07	89.5
185.4	224	25.72	28.98	2.07	89
184.9	223	25.08	25.34	1.39	89.4
183.0	222	27.20	27.89	2.12	89.9
169.7	221	30.58	30.48	1.63	85.9
167.8	220	22.26	24.19	2.26	93.3
157.6	219	29.28	40.05	3.70	90.7
157.1	218	15.32	20.16	3.85	97.2
125.0	217	14.43	25.05	5.10	97
124.3	216	11.78	15.69	5.30	98.6
74.5	214	11.30	11.03	1.94	99.7
71.3	215	13.41	13.67	2.28	98.6
66.9	213	12.48	12.09	1.81	99.6
64.3	212	13.83	20.60	5.08	97.5
62.9	211	12.76	13.41	2.24	98.7
41.6	210	23.06	37.01	3.48	91.5
38.6	209	13.05	14.31	2.35	98.2
35.1	208	15.61	15.85	1.82	95.7
31.7	207	11.62	10.41	1.45	100
30.5	206	10.82	9.75	1.56	100
29.6	205	12.54	14.21	2.42	98.4
1.6	204	17.57	25.31	3.32	94.3
0.0	203	13.65	15.25	1.86	98.4

12.4 Gradistat Sample Statistics

SAMPLE STATISTICS

SAMPLE IDENTITY: **MM203A** ANALYST & DATE: ,

SAMPLE TYPE: Bimodal, Poorly Sorted TEXTURAL GROUP: Mud

SEDIMENT NAME: Fine Silt

	µm	φ
MODE 1:	3.691	8.084
MODE 2:	50.28	4.315
MODE 3:		
D_{10}:	2.282	4.768
MEDIAN or D_{50}:	7.194	7.119
D_{90}:	36.71	8.776
(D_{90} / D_{10}):	16.09	1.841
$(D_{90} - D_{10})$:	34.42	4.008
(D_{75} / D_{25}):	4.961	1.396
$(D_{75} - D_{25})$:	14.04	2.311

GRAIN SIZE DISTRIBUTION

GRAVEL:	0.0%	COARSE SAND:	0.0%
SAND:	1.6%	MEDIUM SAND:	0.0%
MUD:	98.4%	FINE SAND:	0.0%
		V FINE SAND:	1.6%
V COARSE GRAVEL:	0.0%	V COARSE SILT:	10.8%
COARSE GRAVEL:	0.0%	COARSE SILT:	15.8%
MEDIUM GRAVEL:	0.0%	MEDIUM SILT:	19.4%
FINE GRAVEL:	0.0%	FINE SILT:	23.4%
V FINE GRAVEL:	0.0%	V FINE SILT:	22.1%
V COARSE SAND:	0.0%	CLAY:	6.9%

	METHOD OF MOMENTS			FOLK & WARD METHOD		
	Arithmetic µm	Geometric µm	Logarithmic φ	Geometric µm	Logarithmic φ	Description
MEAN ($\bar{x}$):	13.65	7.914	6.981	8.017	6.963	Medium Silt
SORTING (σ):	15.25	2.890	1.531	2.903	1.538	Poorly Sorted
SKEWNESS (Sk):	1.862	0.083	-0.083	0.147	-0.147	Coarse Skewed
KURTOSIS (K):	6.052	2.436	2.436	0.866	0.866	Platykurtic

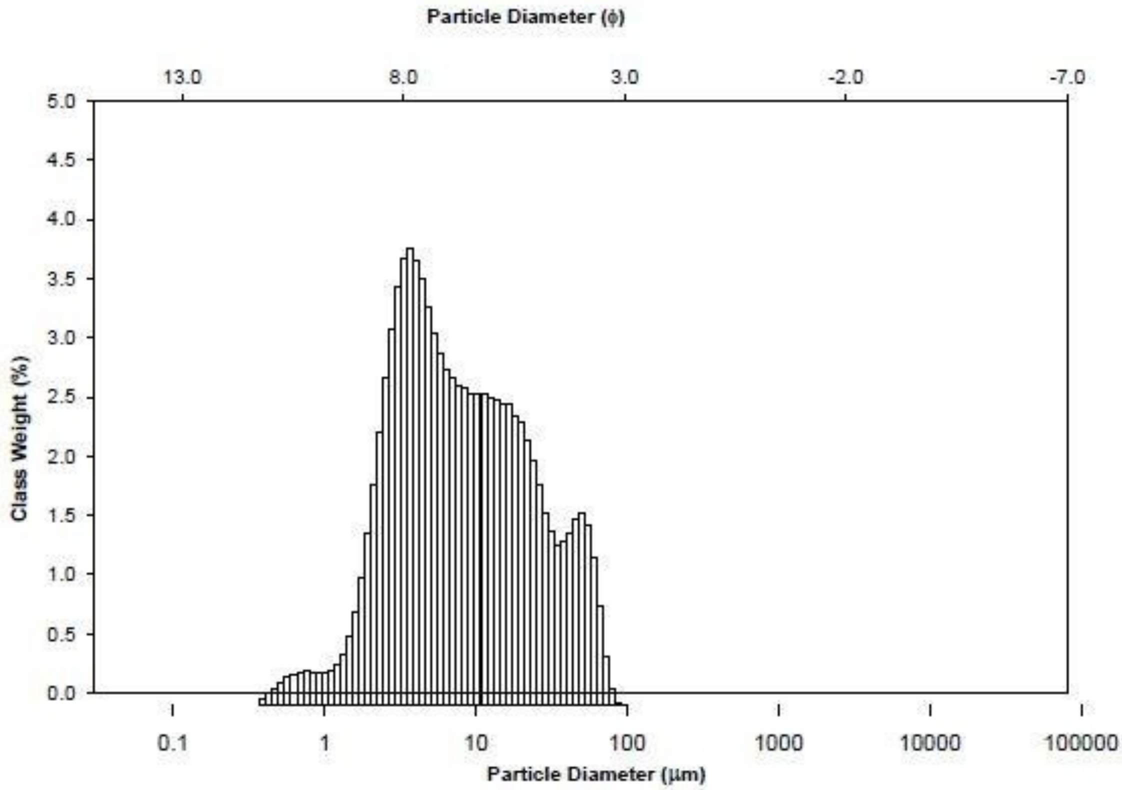

SAMPLE STATISTICS

SAMPLE IDENTITY: **MM204A** ANALYST & DATE: ,

SAMPLE TYPE: Trimodal, Poorly Sorted TEXTURAL GROUP: Mud

SEDIMENT NAME: Medium Silt

	μm	φ
MODE 1:	10.30	6.603
MODE 2:	3.691	8.084
MODE 3:	4.449	7.814
D_{10}:	2.370	4.541
MEDIAN or D_{50}:	8.461	6.885
D_{90}:	42.94	8.721
(D_{90} / D_{10}):	18.12	1.920
$(D_{90} - D_{10})$:	40.57	4.179
(D_{75} / D_{25}):	4.893	1.400
$(D_{75} - D_{25})$:	15.06	2.291

GRAIN SIZE DISTRIBUTION

GRAVEL:	0.0%	COARSE SAND:	0.0%
SAND:	5.7%	MEDIUM SAND:	0.0%
MUD:	94.3%	FINE SAND:	1.3%
		V FINE SAND:	4.4%
V COARSE GRAVEL:	0.0%	V COARSE SILT:	9.4%
COARSE GRAVEL:	0.0%	COARSE SILT:	15.3%
MEDIUM GRAVEL:	0.0%	MEDIUM SILT:	22.2%
FINE GRAVEL:	0.0%	FINE SILT:	22.1%
V FINE GRAVEL:	0.0%	V FINE SILT:	19.9%
V COARSE SAND:	0.0%	CLAY:	5.4%

	METHOD OF MOMENTS			FOLK & WARD METHOD		
	Arithmetic μm	Geometric μm	Logarithmic φ	Geometric μm	Logarithmic φ	Description
MEAN ($\bar{x}$):	17.57	9.236	6.758	9.004	6.795	Medium Silt
SORTING (σ):	25.31	2.973	1.572	3.067	1.617	Poorly Sorted
SKEWNESS (Sk):	3.315	0.418	-0.418	0.123	-0.123	Coarse Skewed
KURTOSIS (K):	16.63	2.538	2.538	0.921	0.921	Mesokurtic

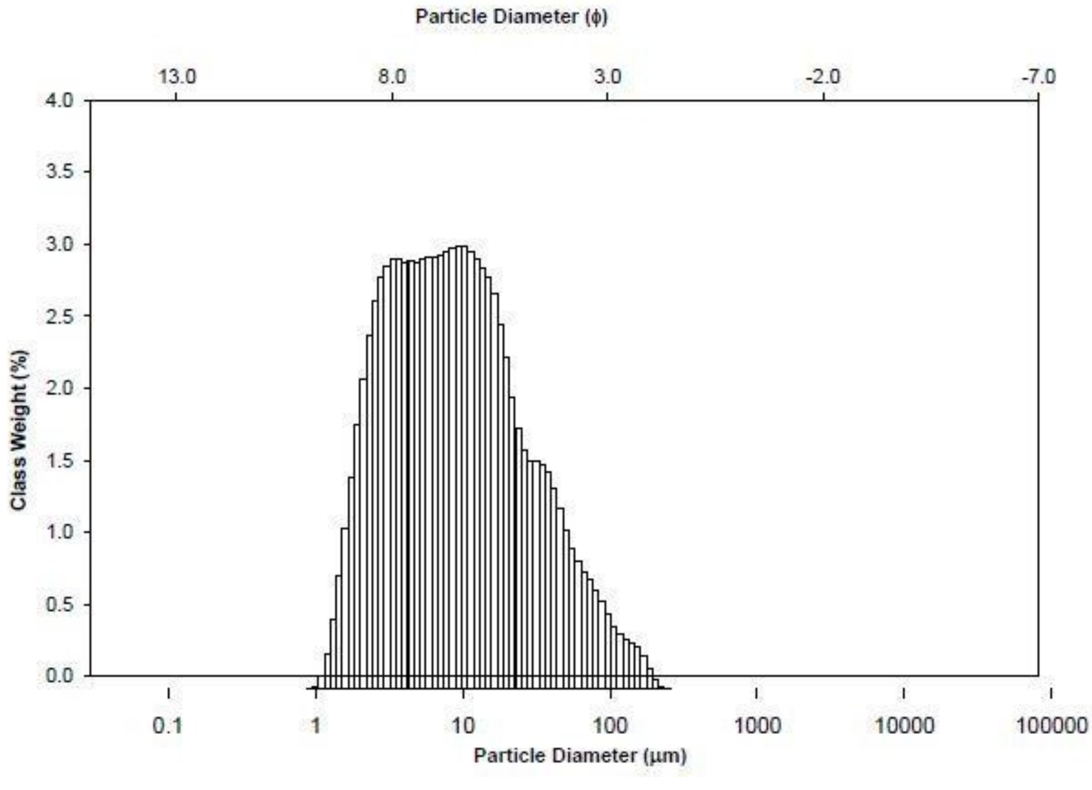

SAMPLE STATISTICS

SAMPLE IDENTITY: **MM205A** | ANALYST & DATE: ,

SAMPLE TYPE: Trimodal, Poorly Sorted | TEXTURAL GROUP: Mud

SEDIMENT NAME: Very Fine Silt

	μm	φ
MODE 1:	3.063	8.352
MODE 2:	10.30	6.603
MODE 3:	31.54	4.988
D_{10}:	2.152	5.021
MEDIAN or D_{50}:	7.218	7.114
D_{90}:	30.81	8.860
(D_{90} / D_{10}):	14.32	1.765
$(D_{90} - D_{10})$:	28.65	3.840
(D_{75} / D_{25}):	4.692	1.373
$(D_{75} - D_{25})$:	12.44	2.230

GRAIN SIZE DISTRIBUTION			
GRAVEL:	0.0%	COARSE SAND:	0.0%
SAND:	1.6%	MEDIUM SAND:	0.0%
MUD:	98.4%	FINE SAND:	0.0%
		V FINE SAND:	1.6%
V COARSE GRAVEL:	0.0%	V COARSE SILT:	8.1%
COARSE GRAVEL:	0.0%	COARSE SILT:	15.6%
MEDIUM GRAVEL:	0.0%	MEDIUM SILT:	22.1%
FINE GRAVEL:	0.0%	FINE SILT:	22.4%
V FINE GRAVEL:	0.0%	V FINE SILT:	22.7%
V COARSE SAND:	0.0%	CLAY:	7.4%

	METHOD OF MOMENTS			FOLK & WARD METHOD		
	Arithmetic μm	Geometric μm	Logarithmic φ	Geometric μm	Logarithmic φ	Description
MEAN ($\bar{x}$):	12.54	7.615	7.037	7.490	7.061	Fine Silt
SORTING (σ):	14.21	2.693	1.429	2.768	1.469	Poorly Sorted
SKEWNESS (Sk):	2.424	0.251	-0.251	0.079	-0.079	Symmetrical
KURTOSIS (K):	10.25	2.242	2.242	0.841	0.841	Platykurtic

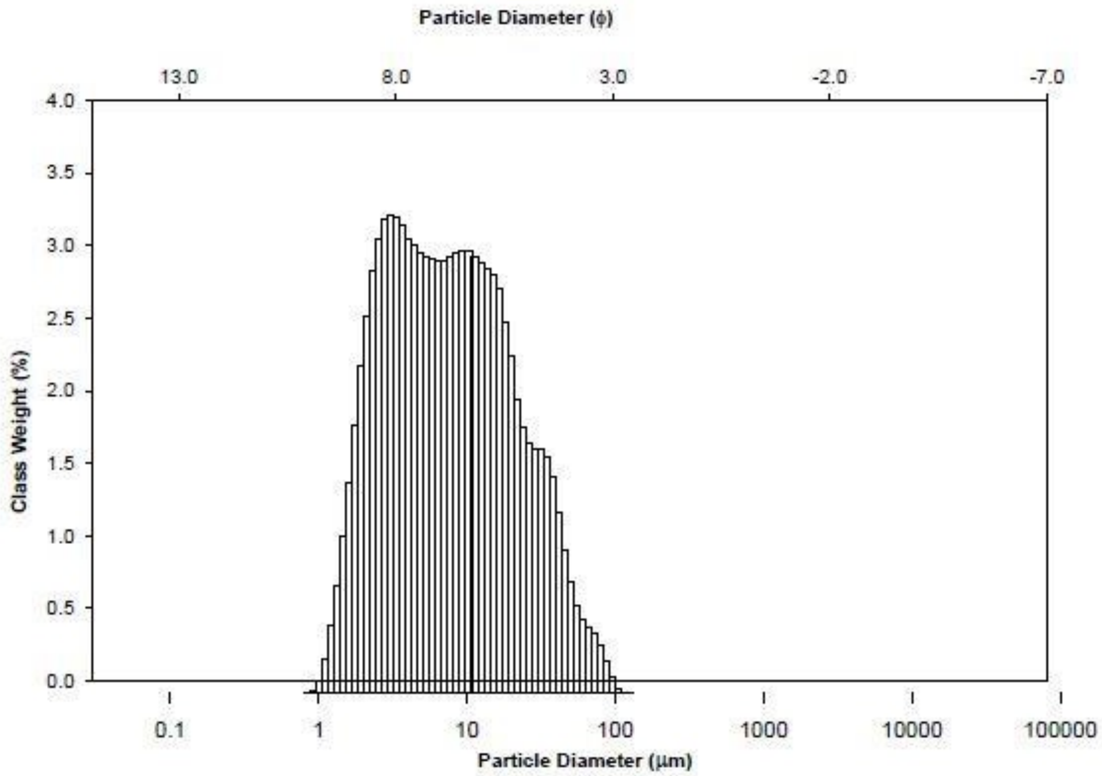

SAMPLE STATISTICS

SAMPLE IDENTITY: **MM206A** ANALYST & DATE: ,

SAMPLE TYPE: Bimodal, Poorly Sorted TEXTURAL GROUP: Mud

SEDIMENT NAME: Medium Silt

	μm	φ
MODE 1:	10.30	6.603
MODE 2:	3.363	8.218
MODE 3:		
D_{10}:	2.256	5.318
MEDIAN or D_{50}:	7.385	7.081
D_{90}:	25.08	8.792
(D_{90} / D_{10}):	11.11	1.653
$(D_{90} - D_{10})$:	22.82	3.474
(D_{75} / D_{25}):	4.178	1.339
$(D_{75} - D_{25})$:	11.24	2.063

GRAIN SIZE DISTRIBUTION

GRAVEL:	0.0%	COARSE SAND:	0.0%
SAND:	0.0%	MEDIUM SAND:	0.0%
MUD:	100.0%	FINE SAND:	0.0%
		V FINE SAND:	0.0%
V COARSE GRAVEL:	0.0%	V COARSE SILT:	5.7%
COARSE GRAVEL:	0.0%	COARSE SILT:	17.3%
MEDIUM GRAVEL:	0.0%	MEDIUM SILT:	25.0%
FINE GRAVEL:	0.0%	FINE SILT:	23.6%
V FINE GRAVEL:	0.0%	V FINE SILT:	22.2%
V COARSE SAND:	0.0%	CLAY:	6.2%

	METHOD OF MOMENTS			FOLK & WARD METHOD		
	Arithmetic μm	Geometric μm	Logarithmic φ	Geometric μm	Logarithmic φ	Description
MEAN ($\bar{x}$):	10.82	7.385	7.081	7.322	7.094	Fine Silt
SORTING (σ):	9.751	2.433	1.283	2.525	1.337	Poorly Sorted
SKEWNESS (Sk):	1.557	0.066	-0.066	0.011	-0.011	Symmetrical
KURTOSIS (K):	5.167	2.069	2.069	0.822	0.822	Platykurtic

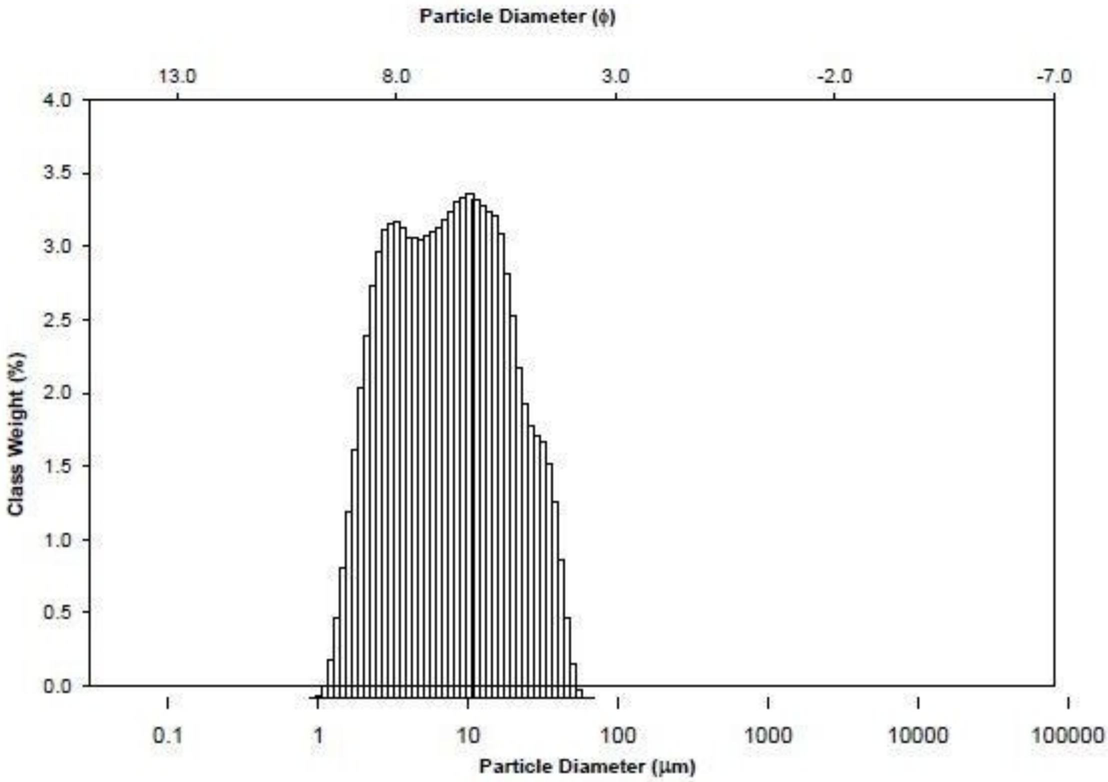

SAMPLE STATISTICS

SAMPLE IDENTITY: **MM207A**

ANALYST & DATE: ,

SAMPLE TYPE: Trimodal, Poorly Sorted

TEXTURAL GROUP: Mud

SEDIMENT NAME: Medium Silt

	μm	φ
MODE 1:	14.96	6.065
MODE 2:	3.063	8.352
MODE 3:	31.54	4.988
D_{10}:	2.351	5.168
MEDIAN or D_{50}:	7.952	6.975
D_{90}:	27.81	8.733
(D_{90} / D_{10}):	11.83	1.690
$(D_{90} - D_{10})$:	25.46	3.565
(D_{75} / D_{25}):	4.275	1.351
$(D_{75} - D_{25})$:	12.18	2.096

GRAIN SIZE DISTRIBUTION

GRAVEL:	0.0%	COARSE SAND:	0.0%
SAND:	0.0%	MEDIUM SAND:	0.0%
MUD:	100.0%	FINE SAND:	0.0%
		V FINE SAND:	0.0%
V COARSE GRAVEL:	0.0%	V COARSE SILT:	7.5%
COARSE GRAVEL:	0.0%	COARSE SILT:	18.1%
MEDIUM GRAVEL:	0.0%	MEDIUM SILT:	25.0%
FINE GRAVEL:	0.0%	FINE SILT:	22.8%
V FINE GRAVEL:	0.0%	V FINE SILT:	21.4%
V COARSE SAND:	0.0%	CLAY:	5.2%

	METHOD OF MOMENTS			FOLK & WARD METHOD		
	Arithmetic μm	Geometric μm	Logarithmic φ	Geometric μm	Logarithmic φ	Description
MEAN ($\bar{x}$):	11.62	7.888	6.986	7.824	6.998	Medium Silt
SORTING (σ):	10.41	2.460	1.299	2.563	1.358	Poorly Sorted
SKEWNESS (Sk):	1.448	0.044	-0.044	-0.001	0.001	Symmetrical
KURTOSIS (K):	4.593	2.027	2.027	0.817	0.817	Platykurtic

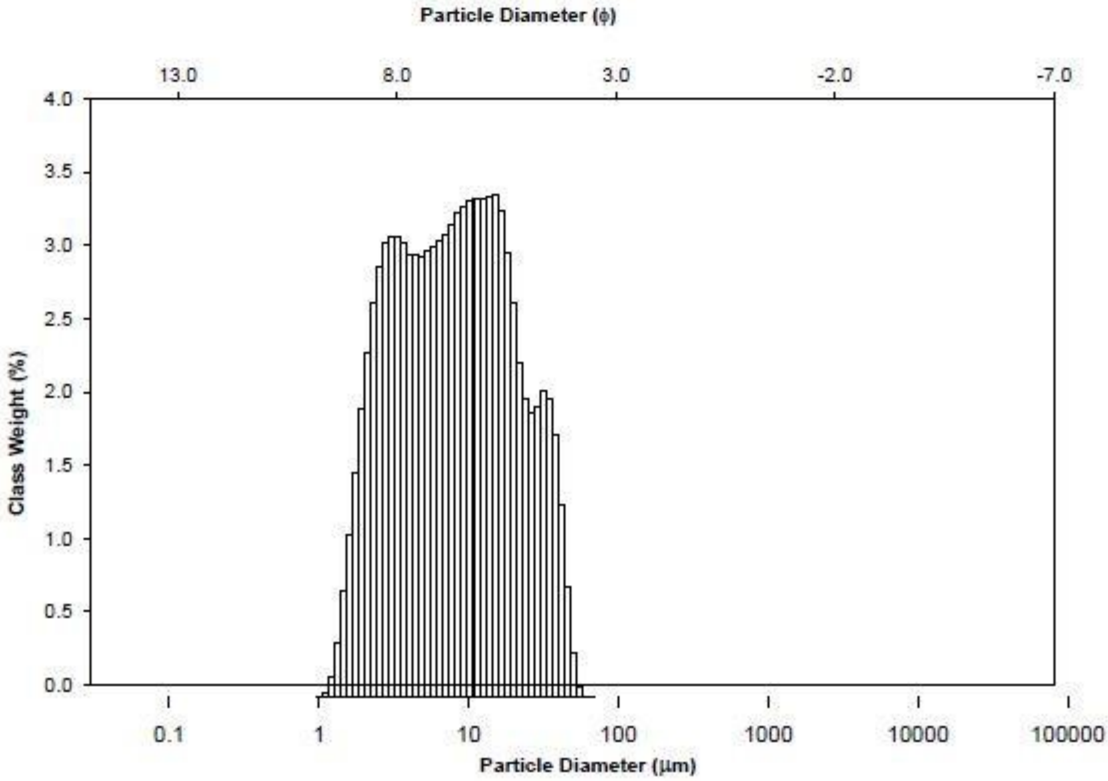

SAMPLE STATISTICS

SAMPLE IDENTITY: **MM208A** ANALYST & DATE: ,

SAMPLE TYPE: Polymodal, Poorly Sorted TEXTURAL GROUP: Mud

SEDIMENT NAME: Very Fine Silt

	μm	φ
MODE 1:	2.790	8.487
MODE 2:	14.96	6.065
MODE 3:	7.091	7.141
D_{10}:	2.494	4.782
MEDIAN or D_{50}:	10.66	6.552
D_{90}:	36.34	8.647
(D_{90} / D_{10}):	14.57	1.808
$(D_{90} - D_{10})$:	33.85	3.865
(D_{75} / D_{25}):	6.465	1.478
$(D_{75} - D_{25})$:	17.07	2.693

GRAIN SIZE DISTRIBUTION

GRAVEL:	0.0%	COARSE SAND:	0.0%
SAND:	2.7%	MEDIUM SAND:	0.0%
MUD:	97.3%	FINE SAND:	0.0%
		V FINE SAND:	2.7%
V COARSE GRAVEL:	0.0%	V COARSE SILT:	12.3%
COARSE GRAVEL:	0.0%	COARSE SILT:	18.9%
MEDIUM GRAVEL:	0.0%	MEDIUM SILT:	24.5%
FINE GRAVEL:	0.0%	FINE SILT:	12.1%
V FINE GRAVEL:	0.0%	V FINE SILT:	28.8%
V COARSE SAND:	0.0%	CLAY:	0.7%

	METHOD OF MOMENTS			FOLK & WARD METHOD		
	Arithmetic μm	Geometric μm	Logarithmic φ	Geometric μm	Logarithmic φ	Description
MEAN ($\bar{x}$):	15.61	9.608	6.702	9.575	6.706	Medium Silt
SORTING (σ):	15.85	2.758	1.463	2.904	1.538	Poorly Sorted
SKEWNESS (Sk):	1.820	0.061	-0.061	-0.071	0.071	Symmetrical
KURTOSIS (K):	6.537	1.898	1.898	0.671	0.671	Platykurtic

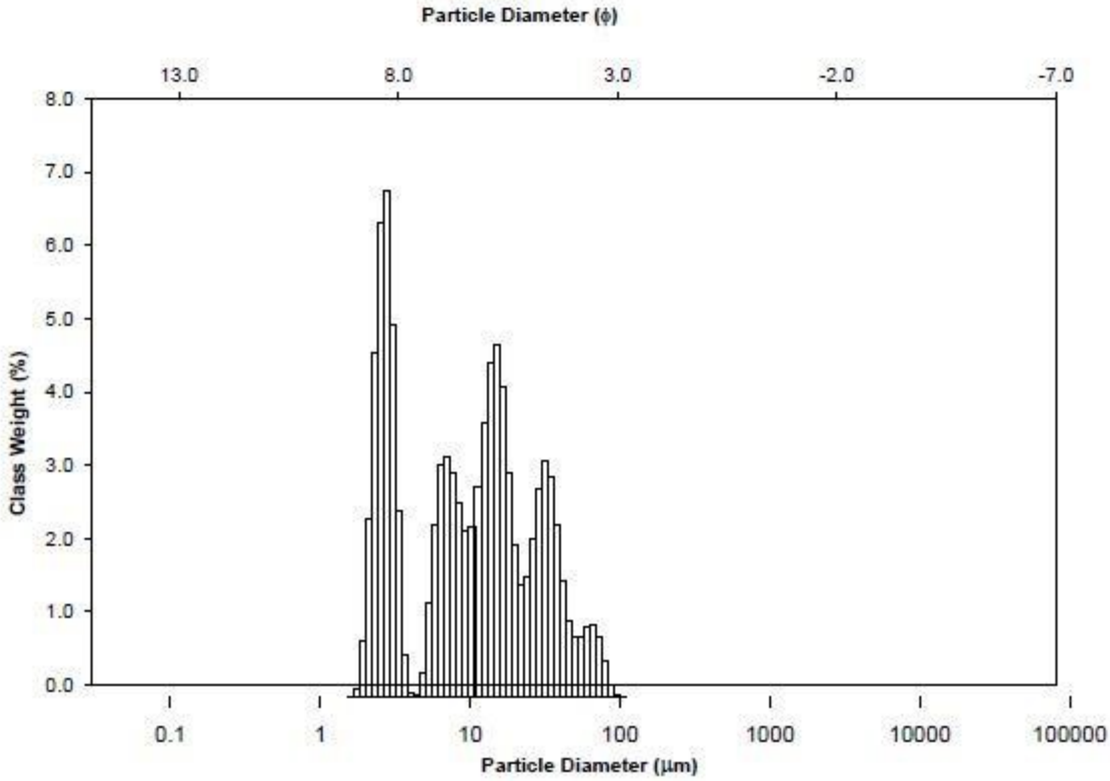

SAMPLE STATISTICS

SAMPLE IDENTITY: **MM209A**

ANALYST & DATE: ,

SAMPLE TYPE: Bimodal, Poorly Sorted

TEXTURAL GROUP: Mud

SEDIMENT NAME: Medium Silt

	μm	φ
MODE 1:	10.30	6.603
MODE 2:	3.363	8.218
MODE 3:		
D_{10}:	2.284	5.005
MEDIAN or D_{50}:	7.866	6.990
D_{90}:	31.13	8.774
(D_{90} / D_{10}):	13.63	1.753
(D_{90} - D_{10}):	28.85	3.769
(D_{75} / D_{25}):	4.560	1.370
(D_{75} - D_{25}):	12.96	2.189

GRAIN SIZE DISTRIBUTION

GRAVEL:	0.0%	COARSE SAND:	0.0%
SAND:	1.8%	MEDIUM SAND:	0.0%
MUD:	98.2%	FINE SAND:	0.0%
		V FINE SAND:	1.8%
V COARSE GRAVEL:	0.0%	V COARSE SILT:	8.1%
COARSE GRAVEL:	0.0%	COARSE SILT:	17.0%
MEDIUM GRAVEL:	0.0%	MEDIUM SILT:	23.3%
FINE GRAVEL:	0.0%	FINE SILT:	22.5%
V FINE GRAVEL:	0.0%	V FINE SILT:	21.3%
V COARSE SAND:	0.0%	CLAY:	6.0%

	METHOD OF MOMENTS			FOLK & WARD METHOD		
	Arithmetic μm	Geometric μm	Logarithmic φ	Geometric μm	Logarithmic φ	Description
MEAN ($\bar{x}$):	13.05	8.105	6.947	7.965	6.972	Medium Silt
SORTING (σ):	14.31	2.646	1.404	2.728	1.448	Poorly Sorted
SKEWNESS (Sk):	2.357	0.208	-0.208	0.048	-0.048	Symmetrical
KURTOSIS (K):	9.771	2.236	2.236	0.843	0.843	Platykurtic

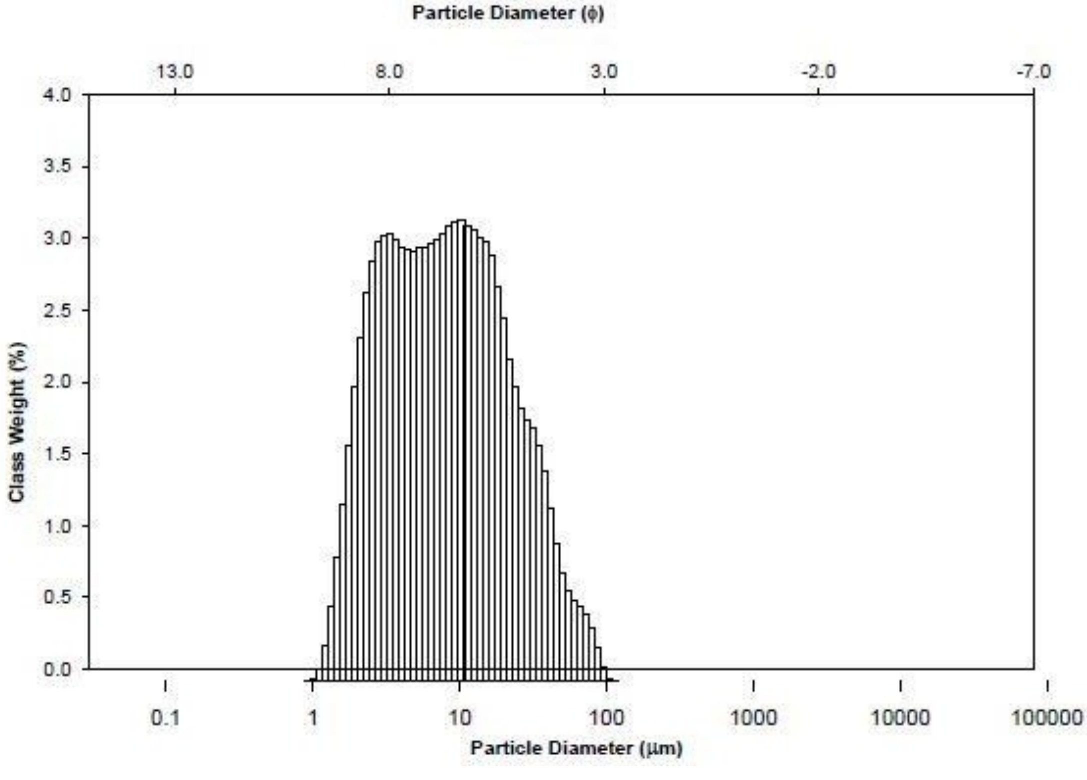

SAMPLE STATISTICS

SAMPLE IDENTITY: **MM210A** ANALYST & DATE: ,

SAMPLE TYPE: Polymodal, Poorly Sorted TEXTURAL GROUP: Mud

SEDIMENT NAME: Medium Silt

	μm	φ
MODE 1:	14.96	6.065
MODE 2:	3.063	8.352
MODE 3:	4.449	7.814
D_{10}:	2.443	4.211
MEDIAN or D_{50}:	10.17	6.620
D_{90}:	54.01	8.677
(D_{90} / D_{10}):	22.11	2.061
$(D_{90} - D_{10})$:	51.56	4.466
(D_{75} / D_{25}):	5.618	1.462
$(D_{75} - D_{25})$:	19.56	2.490

GRAIN SIZE DISTRIBUTION

GRAVEL:	0.0%	COARSE SAND:	0.0%
SAND:	8.5%	MEDIUM SAND:	0.2%
MUD:	91.5%	FINE SAND:	3.2%
		V FINE SAND:	5.1%
V COARSE GRAVEL:	0.0%	V COARSE SILT:	10.7%
COARSE GRAVEL:	0.0%	COARSE SILT:	17.2%
MEDIUM GRAVEL:	0.0%	MEDIUM SILT:	21.6%
FINE GRAVEL:	0.0%	FINE SILT:	19.1%
V FINE GRAVEL:	0.0%	V FINE SILT:	17.8%
V COARSE SAND:	0.0%	CLAY:	5.0%

	METHOD OF MOMENTS			FOLK & WARD METHOD		
	Arithmetic μm	Geometric μm	Logarithmic φ	Geometric μm	Logarithmic φ	Description
MEAN ($\bar{x}$):	23.06	10.88	6.523	10.41	6.586	Medium Silt
SORTING (σ):	37.01	3.245	1.698	3.332	1.736	Poorly Sorted
SKEWNESS (Sk):	3.479	0.406	-0.406	0.086	-0.086	Symmetrical
KURTOSIS (K):	16.85	2.585	2.585	0.914	0.914	Mesokurtic

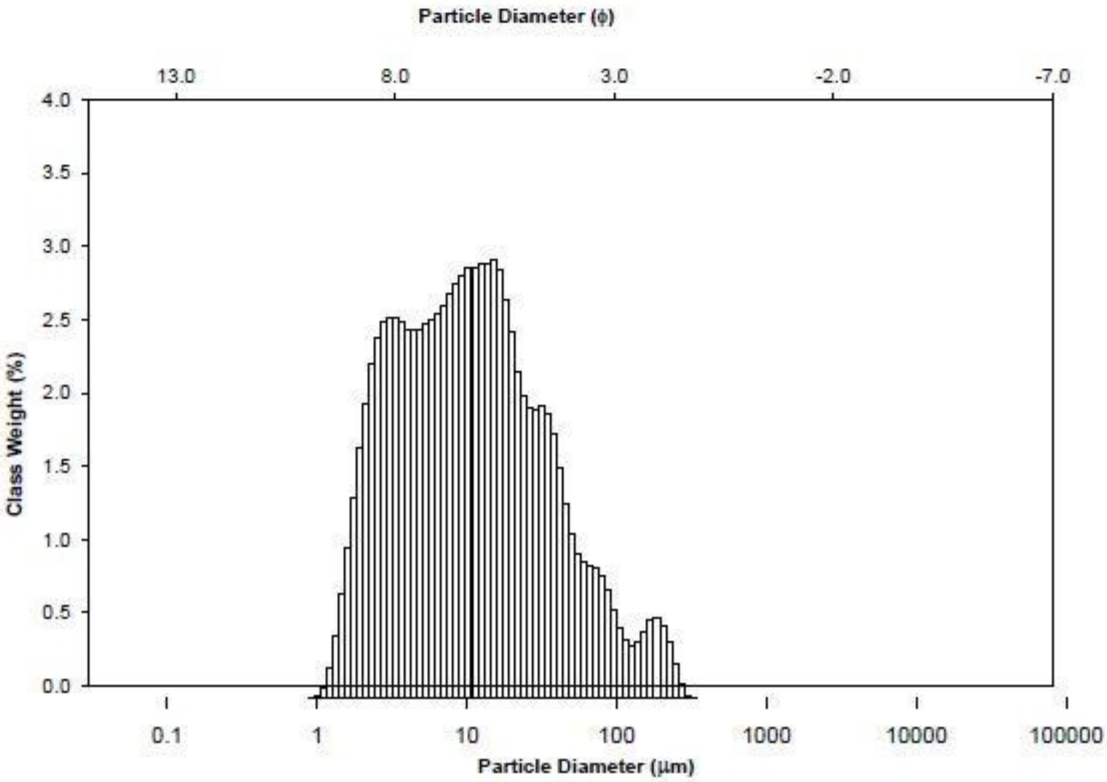

SAMPLE STATISTICS

SAMPLE IDENTITY: **MM211A**　　　ANALYST & DATE: ,

SAMPLE TYPE: Bimodal, Poorly Sorted　　　TEXTURAL GROUP: Mud

SEDIMENT NAME: Medium Silt

	μm	ϕ
MODE 1:	10.30	6.603
MODE 2:	3.363	8.218
MODE 3:		
D_{10}:	2.271	5.046
MEDIAN or D_{50}:	7.983	6.969
D_{90}:	30.26	8.783
(D_{90} / D_{10}):	13.33	1.740
$(D_{90} - D_{10})$:	27.99	3.736
(D_{75} / D_{25}):	4.523	1.368
$(D_{75} - D_{25})$:	12.90	2.177

GRAIN SIZE DISTRIBUTION

GRAVEL:	0.0%	COARSE SAND:	0.0%
SAND:	1.3%	MEDIUM SAND:	0.0%
MUD:	98.7%	FINE SAND:	0.0%
		V FINE SAND:	1.3%
V COARSE GRAVEL:	0.0%	V COARSE SILT:	8.1%
COARSE GRAVEL:	0.0%	COARSE SILT:	17.5%
MEDIUM GRAVEL:	0.0%	MEDIUM SILT:	23.8%
FINE GRAVEL:	0.0%	FINE SILT:	22.2%
V FINE GRAVEL:	0.0%	V FINE SILT:	20.9%
V COARSE SAND:	0.0%	CLAY:	6.2%

	METHOD OF MOMENTS			FOLK & WARD METHOD		
	Arithmetic μm	Geometric μm	Logarithmic ϕ	Geometric μm	Logarithmic ϕ	Description
MEAN ($\bar{x}$):	12.76	8.074	6.953	7.961	6.973	Medium Silt
SORTING (σ):	13.41	2.616	1.387	2.701	1.434	Poorly Sorted
SKEWNESS (Sk):	2.242	0.149	-0.149	0.023	-0.023	Symmetrical
KURTOSIS (K):	9.351	2.195	2.195	0.836	0.836	Platykurtic

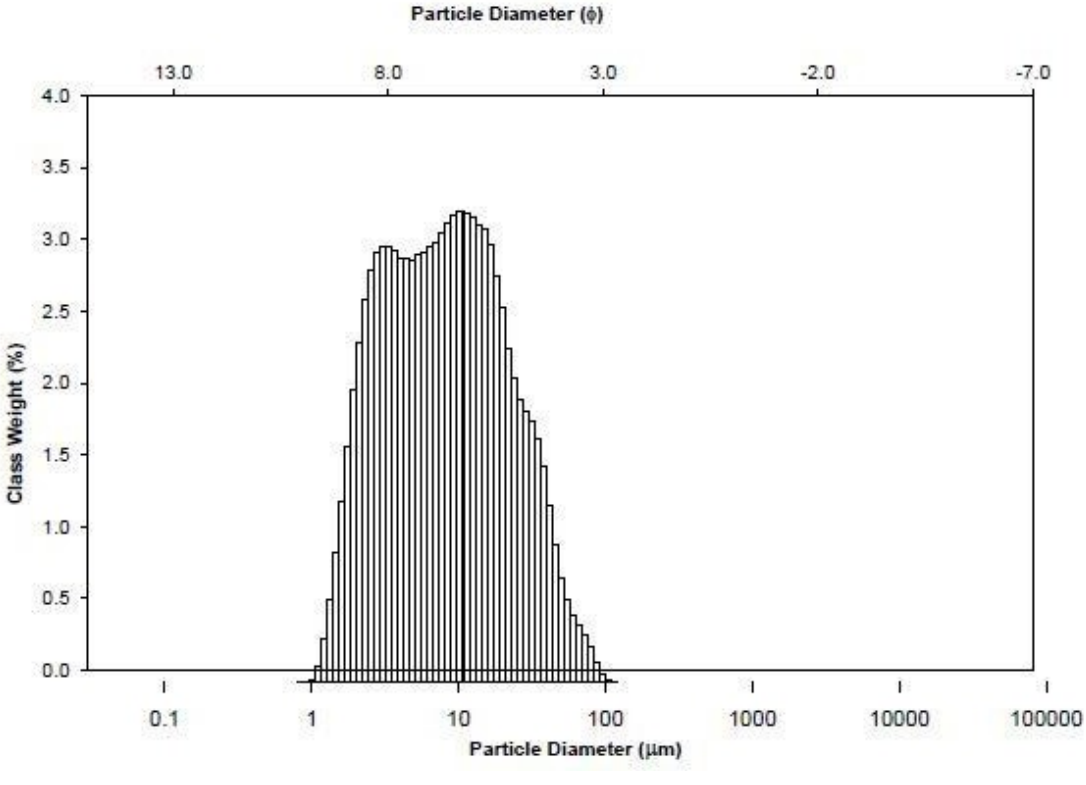

SAMPLE STATISTICS

SAMPLE IDENTITY: **MM212A** ANALYST & DATE: ,

SAMPLE TYPE: Bimodal, Poorly Sorted TEXTURAL GROUP: Mud

SEDIMENT NAME: Medium Silt

	μm	ϕ
MODE 1:	10.30	6.603
MODE 2:	3.363	8.218
MODE 3:		
D_{10}:	2.299	5.097
MEDIAN or D_{50}:	7.819	6.999
D_{90}:	29.22	8.765
(D_{90} / D_{10}):	12.71	1.720
$(D_{90} - D_{10})$:	26.92	3.668
(D_{75} / D_{25}):	4.313	1.353
$(D_{75} - D_{25})$:	12.22	2.109

GRAIN SIZE DISTRIBUTION

GRAVEL:	0.0%	COARSE SAND:	0.0%
SAND:	2.5%	MEDIUM SAND:	0.0%
MUD:	97.5%	FINE SAND:	1.0%
		V FINE SAND:	1.5%
V COARSE GRAVEL:	0.0%	V COARSE SILT:	6.3%
COARSE GRAVEL:	0.0%	COARSE SILT:	16.8%
MEDIUM GRAVEL:	0.0%	MEDIUM SILT:	24.4%
FINE GRAVEL:	0.0%	FINE SILT:	23.1%
V FINE GRAVEL:	0.0%	V FINE SILT:	21.0%
V COARSE SAND:	0.0%	CLAY:	5.9%

	METHOD OF MOMENTS			FOLK & WARD METHOD		
	Arithmetic μm	Geometric μm	Logarithmic ϕ	Geometric μm	Logarithmic ϕ	Description
MEAN ($\bar{x}$):	13.83	8.081	6.951	7.816	6.999	Medium Silt
SORTING (σ):	20.60	2.671	1.417	2.663	1.413	Poorly Sorted
SKEWNESS (Sk):	5.081	0.388	-0.388	0.035	-0.035	Symmetrical
KURTOSIS (K):	36.99	2.831	2.831	0.863	0.863	Platykurtic

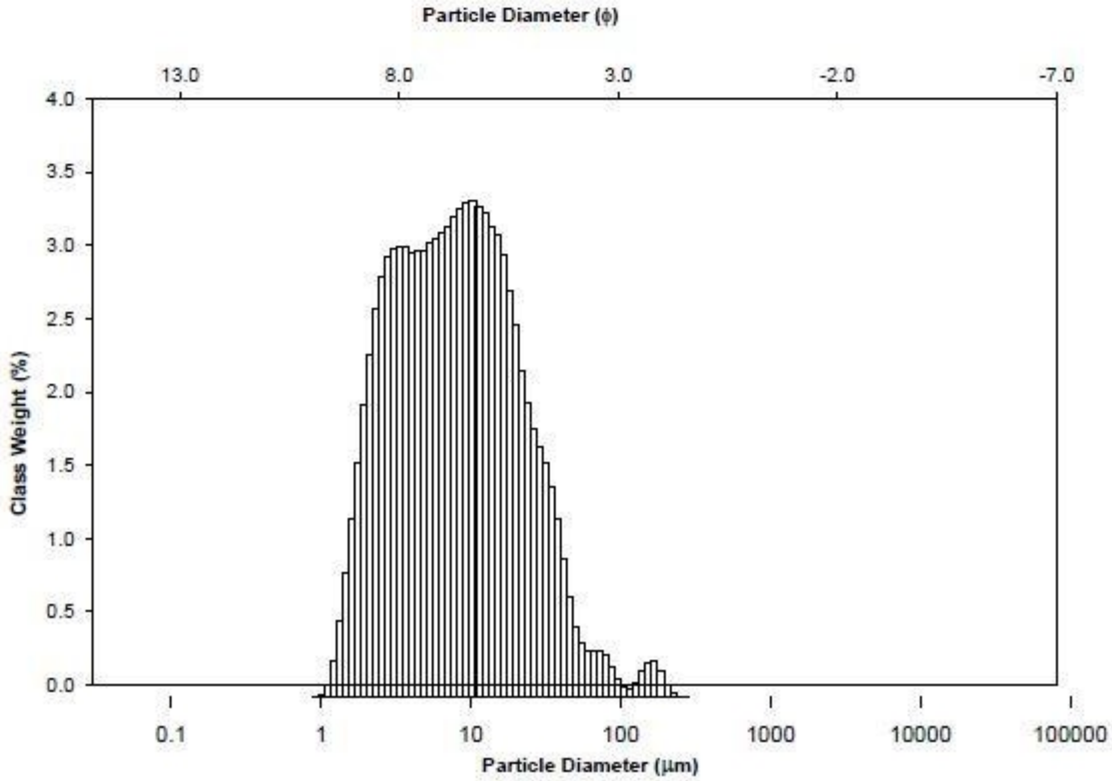

SAMPLE STATISTICS

SAMPLE IDENTITY: **MM213A** ANALYST & DATE: ,

SAMPLE TYPE: Bimodal, Poorly Sorted TEXTURAL GROUP: Mud

SEDIMENT NAME: Medium Silt

	μm	φ
MODE 1:	11.31	6.468
MODE 2:	3.691	8.084
MODE 3:		
D_{10}:	2.321	5.090
MEDIAN or D_{50}:	8.237	6.924
D_{90}:	29.37	8.751
(D_{90} / D_{10}):	12.66	1.719
$(D_{90} - D_{10})$:	27.05	3.662
(D_{75} / D_{25}):	4.366	1.360
$(D_{75} - D_{25})$:	12.82	2.126

GRAIN SIZE DISTRIBUTION

GRAVEL:	0.0%	COARSE SAND:	0.0%
SAND:	0.4%	MEDIUM SAND:	0.0%
MUD:	99.6%	FINE SAND:	0.0%
		V FINE SAND:	0.4%
V COARSE GRAVEL:	0.0%	V COARSE SILT:	8.3%
COARSE GRAVEL:	0.0%	COARSE SILT:	18.3%
MEDIUM GRAVEL:	0.0%	MEDIUM SILT:	24.7%
FINE GRAVEL:	0.0%	FINE SILT:	22.4%
V FINE GRAVEL:	0.0%	V FINE SILT:	20.0%
V COARSE SAND:	0.0%	CLAY:	5.9%

	METHOD OF MOMENTS			FOLK & WARD METHOD		
	Arithmetic μm	Geometric μm	Logarithmic φ	Geometric μm	Logarithmic φ	Description
MEAN ($\bar{x}$):	12.48	8.172	6.935	8.089	6.950	Medium Silt
SORTING (σ):	12.09	2.552	1.352	2.652	1.407	Poorly Sorted
SKEWNESS (Sk):	1.813	0.066	-0.066	-0.002	0.002	Symmetrical
KURTOSIS (K):	6.522	2.135	2.135	0.842	0.842	Platykurtic

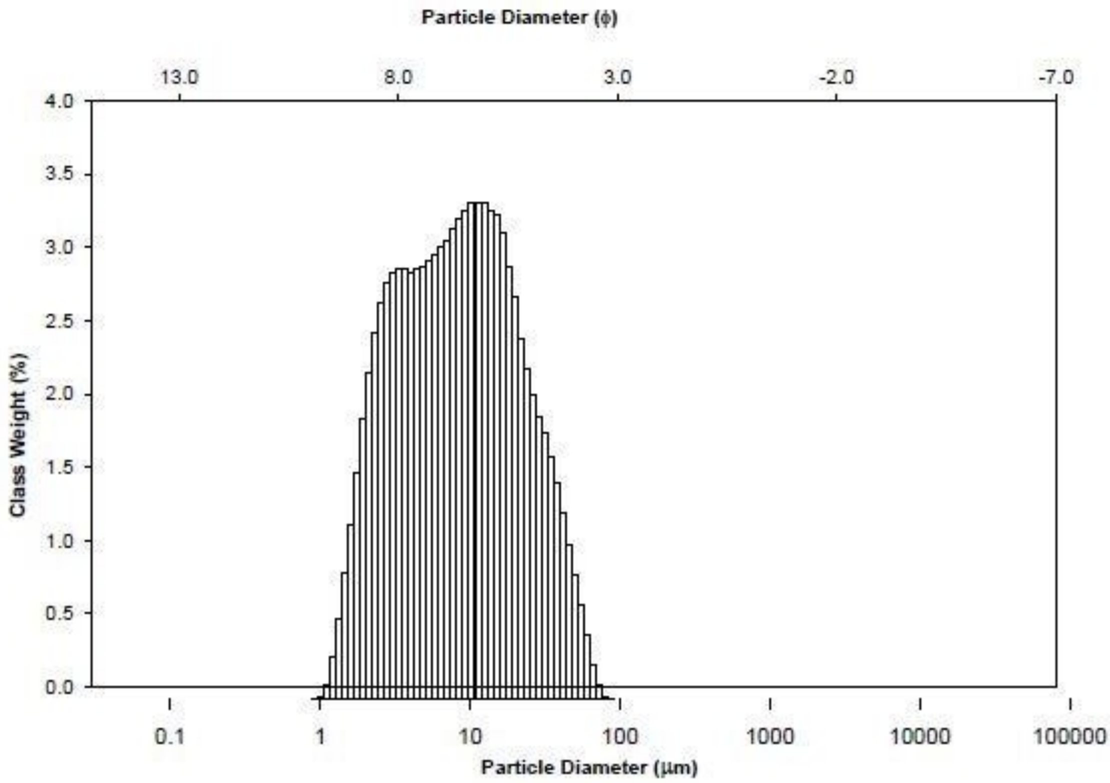

SAMPLE STATISTICS

SAMPLE IDENTITY: **MM214A**

ANALYST & DATE: ,

SAMPLE TYPE: Trimodal, Poorly Sorted

TEXTURAL GROUP: Mud

SEDIMENT NAME: Medium Silt

	μm	ϕ
MODE 1:	10.30	6.603
MODE 2:	3.363	8.218
MODE 3:	4.449	7.814
D_{10}:	2.185	5.261
MEDIAN or D_{50}:	7.392	7.080
D_{90}:	26.08	8.838
(D_{90} / D_{10}):	11.93	1.680
(D_{90} - D_{10}):	23.89	3.577
(D_{75} / D_{25}):	4.306	1.348
(D_{75} - D_{25}):	11.58	2.106

GRAIN SIZE DISTRIBUTION

GRAVEL:	0.0%	COARSE SAND:	0.0%
SAND:	0.3%	MEDIUM SAND:	0.0%
MUD:	99.7%	FINE SAND:	0.0%
		V FINE SAND:	0.3%
V COARSE GRAVEL:	0.0%	V COARSE SILT:	6.4%
COARSE GRAVEL:	0.0%	COARSE SILT:	17.1%
MEDIUM GRAVEL:	0.0%	MEDIUM SILT:	24.3%
FINE GRAVEL:	0.0%	FINE SILT:	23.3%
V FINE GRAVEL:	0.0%	V FINE SILT:	21.5%
V COARSE SAND:	0.0%	CLAY:	7.2%

	METHOD OF MOMENTS			FOLK & WARD METHOD		
	Arithmetic μm	Geometric μm	Logarithmic ϕ	Geometric μm	Logarithmic ϕ	Description
MEAN ($\bar{x}$):	11.30	7.440	7.071	7.355	7.087	Fine Silt
SORTING (σ):	11.03	2.521	1.334	2.605	1.381	Poorly Sorted
SKEWNESS (Sk):	1.941	0.100	-0.100	0.016	-0.016	Symmetrical
KURTOSIS (K):	7.393	2.163	2.163	0.837	0.837	Platykurtic

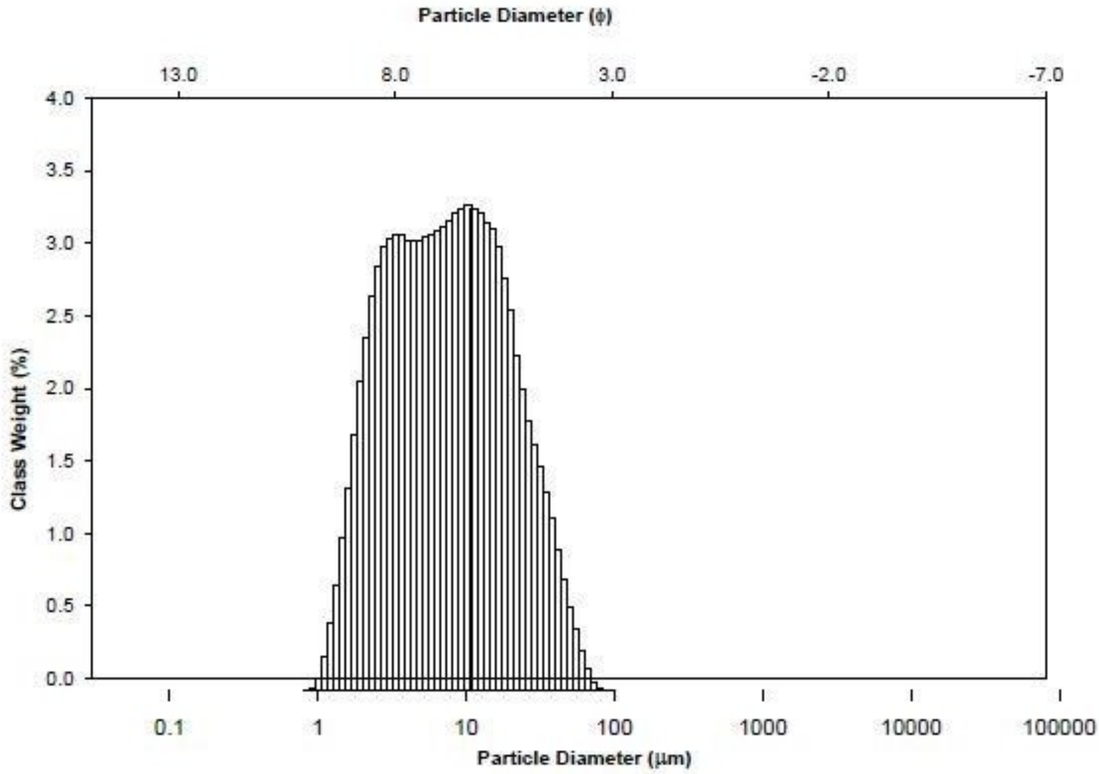

SAMPLE STATISTICS

SAMPLE IDENTITY: **MM215A** ANALYST & DATE: ,

SAMPLE TYPE: Trimodal, Poorly Sorted TEXTURAL GROUP: Mud

SEDIMENT NAME: Medium Silt

	μm	φ
MODE 1:	12.41	6.334
MODE 2:	14.96	6.065
MODE 3:	3.691	8.084
D_{10}:	2.382	5.022
MEDIAN or D_{50}:	8.829	6.824
D_{90}:	30.78	8.713
(D_{90} / D_{10}):	12.92	1.735
$(D_{90} - D_{10})$:	28.40	3.692
(D_{75} / D_{25}):	4.358	1.364
$(D_{75} - D_{25})$:	13.54	2.124

GRAIN SIZE DISTRIBUTION

GRAVEL:	0.0%	COARSE SAND:	0.0%
SAND:	1.4%	MEDIUM SAND:	0.0%
MUD:	98.6%	FINE SAND:	0.0%
		V FINE SAND:	1.4%
V COARSE GRAVEL:	0.0%	V COARSE SILT:	8.2%
COARSE GRAVEL:	0.0%	COARSE SILT:	19.5%
MEDIUM GRAVEL:	0.0%	MEDIUM SILT:	25.1%
FINE GRAVEL:	0.0%	FINE SILT:	21.7%
V FINE GRAVEL:	0.0%	V FINE SILT:	18.5%
V COARSE SAND:	0.0%	CLAY:	5.5%

	METHOD OF MOMENTS			FOLK & WARD METHOD		
	Arithmetic μm	Geometric μm	Logarithmic φ	Geometric μm	Logarithmic φ	Description
MEAN ($\bar{x}$):	13.41	8.646	6.854	8.544	6.871	Medium Silt
SORTING (σ):	13.67	2.590	1.373	2.671	1.418	Poorly Sorted
SKEWNESS (Sk):	2.280	0.057	-0.057	-0.028	0.028	Symmetrical
KURTOSIS (K):	9.913	2.234	2.234	0.849	0.849	Platykurtic

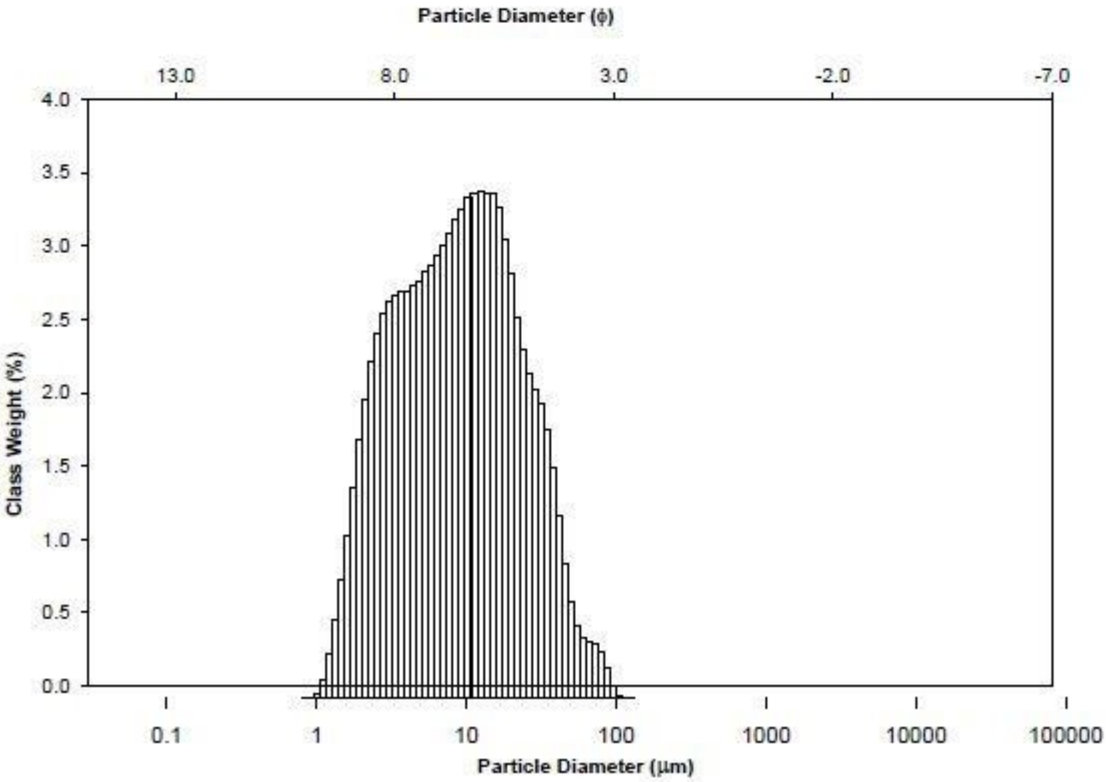

SAMPLE STATISTICS

SAMPLE IDENTITY: **MM216A** ANALYST & DATE: ,

SAMPLE TYPE: Trimodal, Poorly Sorted TEXTURAL GROUP: Mud

SEDIMENT NAME: Medium Silt

	μm	ϕ
MODE 1:	10.30	6.603
MODE 2:	3.063	8.352
MODE 3:	5.361	7.545
D_{10}:	2.091	5.282
MEDIAN or D_{50}:	7.003	7.158
D_{90}:	25.70	8.902
(D_{90} / D_{10}):	12.29	1.685
$(D_{90} - D_{10})$:	23.60	3.619
(D_{75} / D_{25}):	4.422	1.352
$(D_{75} - D_{25})$:	11.30	2.145

GRAIN SIZE DISTRIBUTION

GRAVEL:	0.0%	COARSE SAND:	0.0%
SAND:	1.4%	MEDIUM SAND:	0.0%
MUD:	98.6%	FINE SAND:	0.4%
		V FINE SAND:	1.0%
V COARSE GRAVEL:	0.0%	V COARSE SILT:	5.2%
COARSE GRAVEL:	0.0%	COARSE SILT:	16.1%
MEDIUM GRAVEL:	0.0%	MEDIUM SILT:	23.6%
FINE GRAVEL:	0.0%	FINE SILT:	22.9%
V FINE GRAVEL:	0.0%	V FINE SILT:	22.6%
V COARSE SAND:	0.0%	CLAY:	8.2%

	METHOD OF MOMENTS			FOLK & WARD METHOD		
	Arithmetic μm	Geometric μm	Logarithmic ϕ	Geometric μm	Logarithmic ϕ	Description
MEAN ($\bar{x}$):	11.78	7.204	7.117	7.046	7.149	Fine Silt
SORTING (σ):	15.69	2.617	1.388	2.640	1.400	Poorly Sorted
SKEWNESS (Sk):	5.292	0.280	-0.280	0.036	-0.036	Symmetrical
KURTOSIS (K):	46.88	2.566	2.566	0.835	0.835	Platykurtic

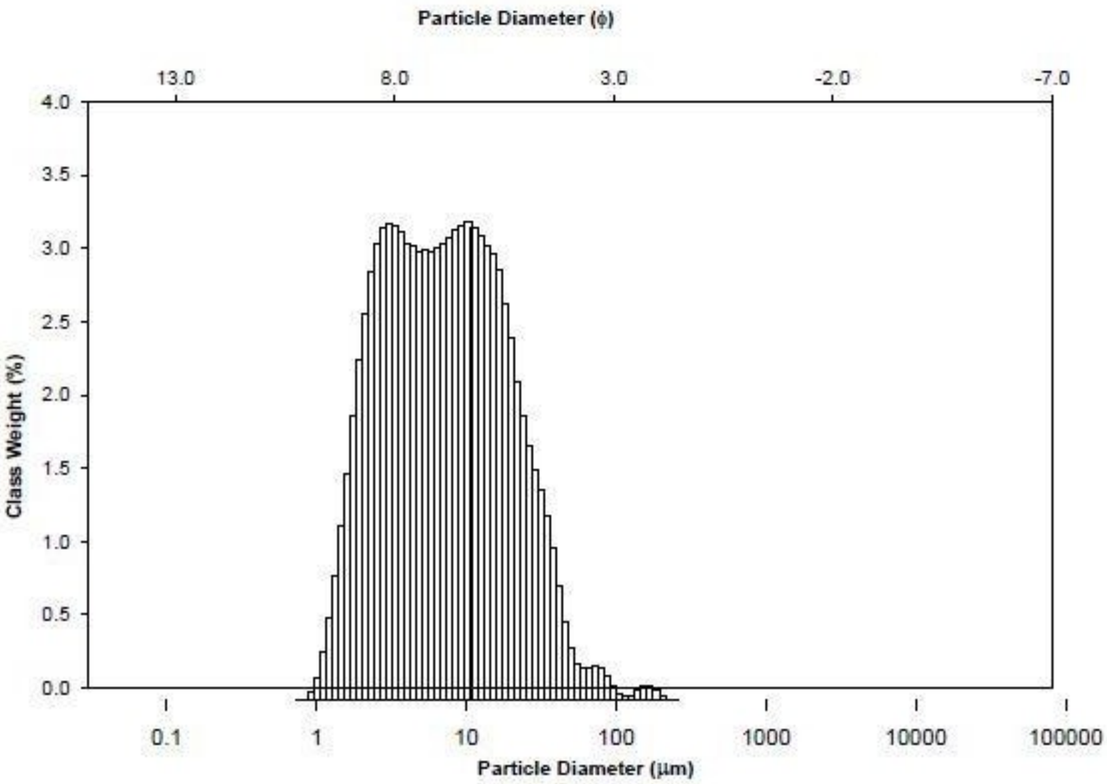

SAMPLE STATISTICS

SAMPLE IDENTITY: **MM217A**

ANALYST & DATE: ,

SAMPLE TYPE: Bimodal, Poorly Sorted

TEXTURAL GROUP: Mud

SEDIMENT NAME: Medium Silt

	μm	ϕ
MODE 1:	10.30	6.603
MODE 2:	3.063	8.352
MODE 3:		
D_{10}:	2.164	5.163
MEDIAN or D_{50}:	7.499	7.059
D_{90}:	27.90	8.852
(D_{90} / D_{10}):	12.89	1.714
$(D_{90} - D_{10})$:	25.74	3.688
(D_{75} / D_{25}):	4.483	1.360
$(D_{75} - D_{25})$:	12.03	2.165

GRAIN SIZE DISTRIBUTION

GRAVEL:	0.0%	COARSE SAND:	0.0%
SAND:	3.0%	MEDIUM SAND:	0.0%
MUD:	97.0%	FINE SAND:	1.9%
		V FINE SAND:	1.1%
V COARSE GRAVEL:	0.0%	V COARSE SILT:	5.1%
COARSE GRAVEL:	0.0%	COARSE SILT:	16.6%
MEDIUM GRAVEL:	0.0%	MEDIUM SILT:	23.9%
FINE GRAVEL:	0.0%	FINE SILT:	22.3%
V FINE GRAVEL:	0.0%	V FINE SILT:	21.7%
V COARSE SAND:	0.0%	CLAY:	7.3%

	METHOD OF MOMENTS			FOLK & WARD METHOD		
	Arithmetic μm	Geometric μm	Logarithmic ϕ	Geometric μm	Logarithmic ϕ	Description
MEAN ($\bar{x}$):	14.43	7.792	7.004	7.456	7.067	Fine Silt
SORTING (σ):	25.05	2.778	1.474	2.698	1.432	Poorly Sorted
SKEWNESS (Sk):	5.104	0.505	-0.505	0.032	-0.032	Symmetrical
KURTOSIS (K):	33.13	3.154	3.154	0.854	0.854	Platykurtic

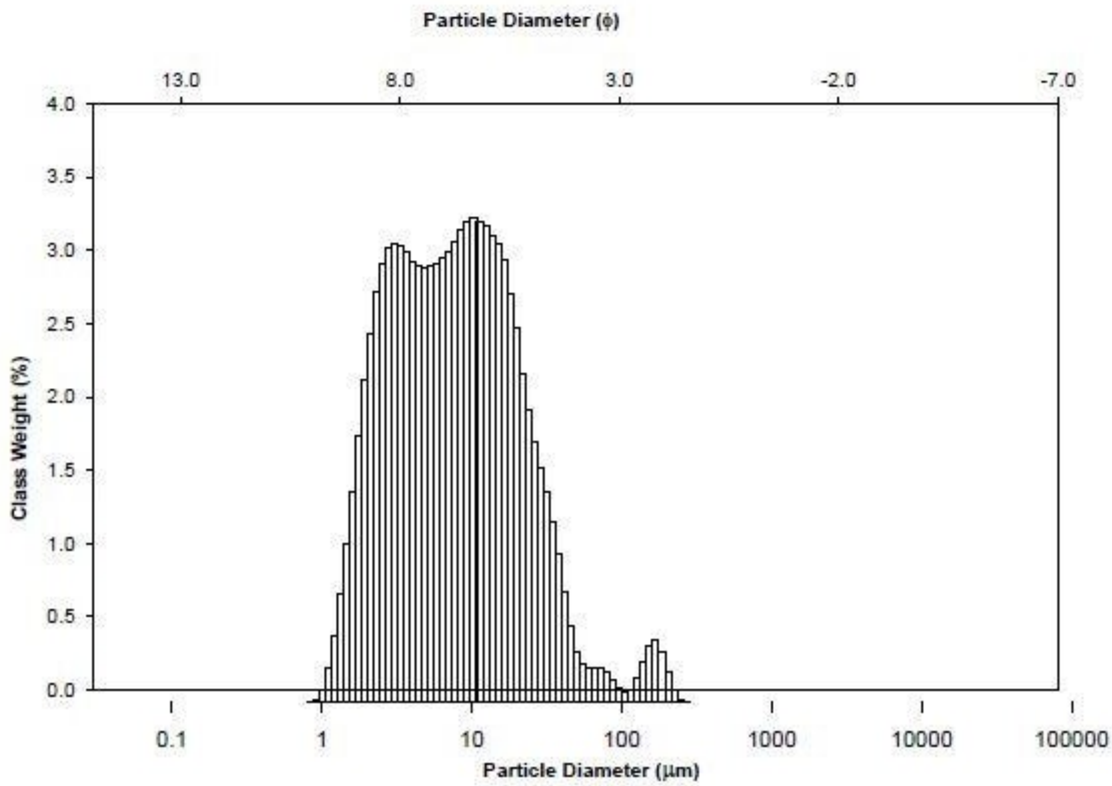

SAMPLE STATISTICS

SAMPLE IDENTITY: **MM218A** ANALYST & DATE: ,

SAMPLE TYPE: Trimodal, Poorly Sorted TEXTURAL GROUP: Mud

SEDIMENT NAME: Medium Silt

	µm	φ
MODE 1:	14.96	6.065
MODE 2:	3.063	8.352
MODE 3:	31.54	4.988
D_{10}:	2.115	4.795
MEDIAN or D_{50}:	8.466	6.884
D_{90}:	36.03	8.885
(D_{90} / D_{10}):	17.03	1.853
$(D_{90} - D_{10})$:	33.91	4.090
(D_{75} / D_{25}):	5.469	1.430
$(D_{75} - D_{25})$:	15.67	2.451

GRAIN SIZE DISTRIBUTION

GRAVEL:	0.0%	COARSE SAND:	0.0%
SAND:	2.8%	MEDIUM SAND:	0.0%
MUD:	97.2%	FINE SAND:	0.7%
		V FINE SAND:	2.1%
V COARSE GRAVEL:	0.0%	V COARSE SILT:	10.4%
COARSE GRAVEL:	0.0%	COARSE SILT:	18.0%
MEDIUM GRAVEL:	0.0%	MEDIUM SILT:	21.1%
FINE GRAVEL:	0.0%	FINE SILT:	19.5%
V FINE GRAVEL:	0.0%	V FINE SILT:	20.2%
V COARSE SAND:	0.0%	CLAY:	8.0%

	METHOD OF MOMENTS			FOLK & WARD METHOD		
	Arithmetic µm	Geometric µm	Logarithmic φ	Geometric µm	Logarithmic φ	Description
MEAN ($\bar{x}$):	15.32	8.574	6.866	8.493	6.880	Medium Silt
SORTING (σ):	20.16	2.929	1.551	2.999	1.584	Poorly Sorted
SKEWNESS (Sk):	3.849	0.188	-0.188	0.021	-0.021	Symmetrical
KURTOSIS (K):	25.09	2.294	2.294	0.809	0.809	Platykurtic

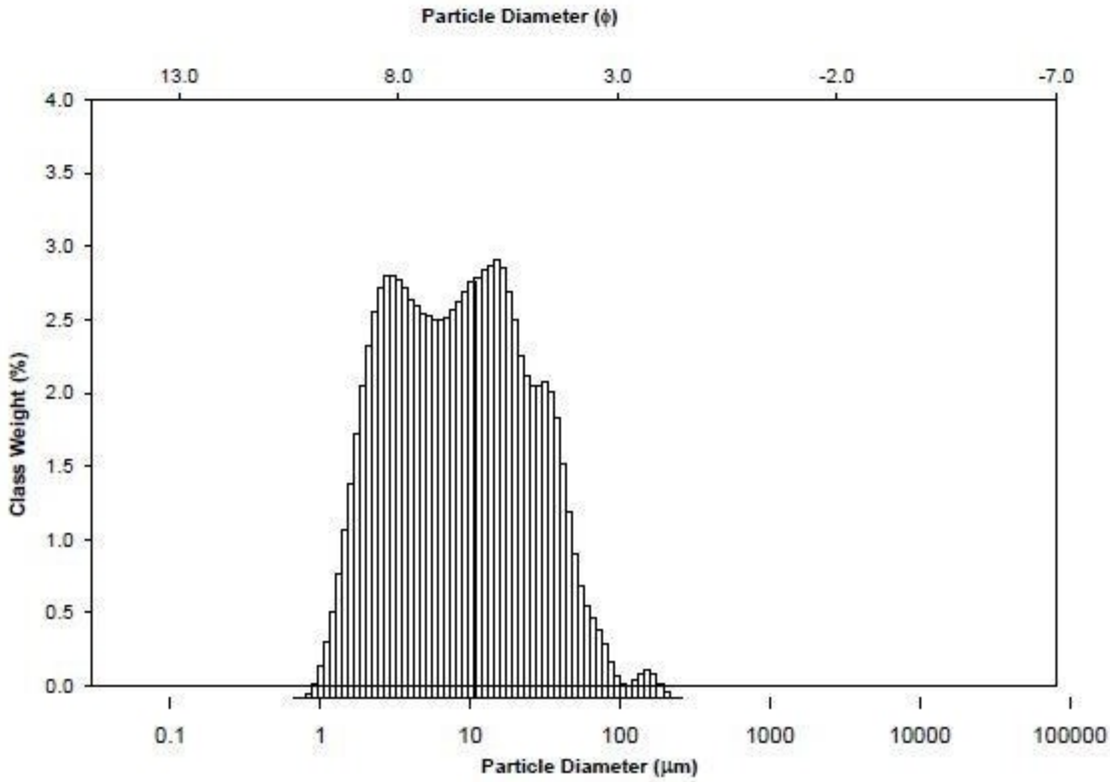

SAMPLE STATISTICS

SAMPLE IDENTITY: **MM219A** ANALYST & DATE: ,

SAMPLE TYPE: Polymodal, Poorly Sorted TEXTURAL GROUP: Mud

SEDIMENT NAME: Very Coarse Silt

	μm	φ
MODE 1:	38.01	4.719
MODE 2:	16.41	5.931
MODE 3:	3.363	8.218
D_{10}:	2.871	4.048
MEDIAN or D_{50}:	17.06	5.873
D_{90}:	60.46	8.444
(D_{90} / D_{10}):	21.06	2.086
$(D_{90} - D_{10})$:	57.59	4.396
(D_{75} / D_{25}):	5.761	1.531
$(D_{75} - D_{25})$:	30.51	2.526

GRAIN SIZE DISTRIBUTION

GRAVEL:	0.0%	COARSE SAND:	0.0%
SAND:	9.3%	MEDIUM SAND:	0.6%
MUD:	90.7%	FINE SAND:	2.8%
		V FINE SAND:	6.0%
V COARSE GRAVEL:	0.0%	V COARSE SILT:	22.0%
COARSE GRAVEL:	0.0%	COARSE SILT:	21.6%
MEDIUM GRAVEL:	0.0%	MEDIUM SILT:	18.2%
FINE GRAVEL:	0.0%	FINE SILT:	13.2%
V FINE GRAVEL:	0.0%	V FINE SILT:	12.1%
V COARSE SAND:	0.0%	CLAY:	3.7%

	METHOD OF MOMENTS			FOLK & WARD METHOD		
	Arithmetic μm	Geometric μm	Logarithmic φ	Geometric μm	Logarithmic φ	Description
MEAN ($\bar{x}$):	29.28	15.48	6.013	14.75	6.083	Medium Silt
SORTING (σ):	40.05	3.213	1.684	3.250	1.700	Poorly Sorted
SKEWNESS (Sk):	3.700	-0.079	0.079	-0.152	0.152	Fine Skewed
KURTOSIS (K):	20.59	2.439	2.439	0.860	0.860	Platykurtic

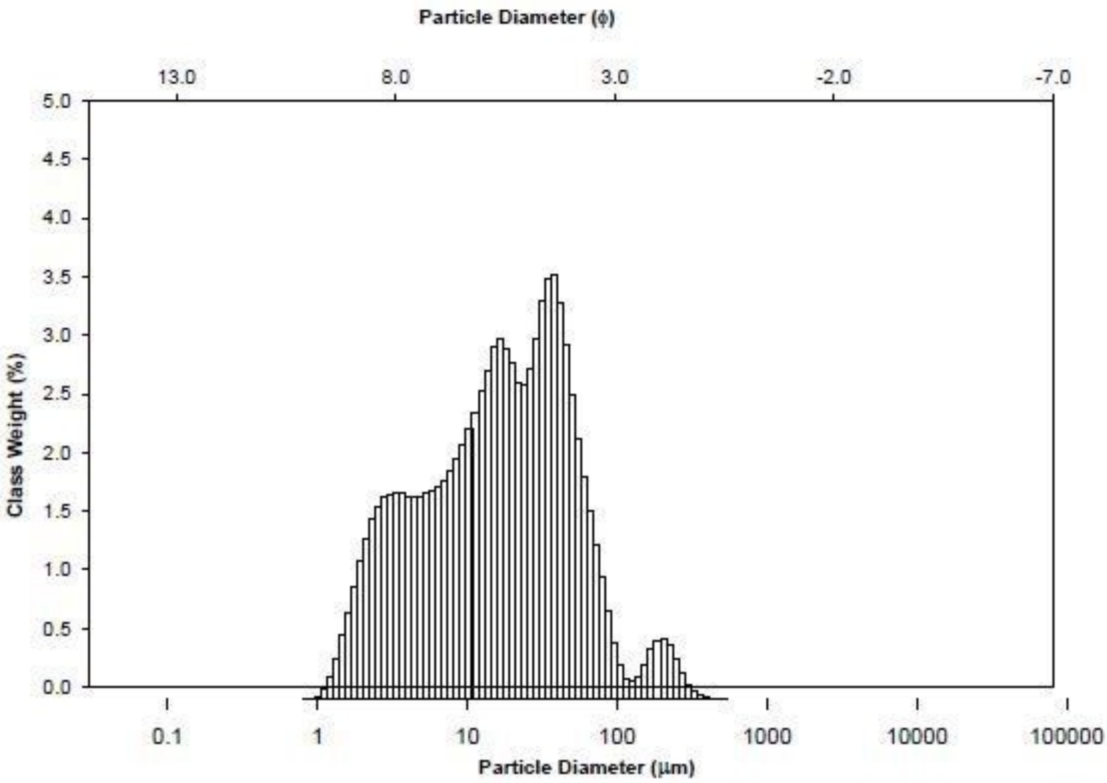

SAMPLE STATISTICS

SAMPLE IDENTITY: **MM220A**

ANALYST & DATE: ,

SAMPLE TYPE: Polymodal, Poorly Sorted

TEXTURAL GROUP: Mud

SEDIMENT NAME: Coarse Silt

	μm	φ
MODE 1:	34.62	4.854
MODE 2:	16.41	5.931
MODE 3:	3.063	8.352
D_{10}:	2.496	4.237
MEDIAN or D_{50}:	13.74	6.186
D_{90}:	53.05	8.646
(D_{90} / D_{10}):	21.26	2.041
$(D_{90} - D_{10})$:	50.55	4.410
(D_{75} / D_{25}):	6.589	1.549
$(D_{75} - D_{25})$:	27.32	2.720

GRAIN SIZE DISTRIBUTION

GRAVEL:	0.0%	COARSE SAND:	0.0%
SAND:	6.7%	MEDIUM SAND:	0.0%
MUD:	93.3%	FINE SAND:	0.7%
		V FINE SAND:	6.0%
V COARSE GRAVEL:	0.0%	V COARSE SILT:	19.3%
COARSE GRAVEL:	0.0%	COARSE SILT:	20.0%
MEDIUM GRAVEL:	0.0%	MEDIUM SILT:	18.7%
FINE GRAVEL:	0.0%	FINE SILT:	15.2%
V FINE GRAVEL:	0.0%	V FINE SILT:	14.8%
V COARSE SAND:	0.0%	CLAY:	5.3%

	METHOD OF MOMENTS			FOLK & WARD METHOD		
	Arithmetic μm	Geometric μm	Logarithmic φ	Geometric μm	Logarithmic φ	Description
MEAN ($\bar{x}$):	22.26	12.53	6.318	12.38	6.336	Medium Silt
SORTING (σ):	24.19	3.129	1.646	3.267	1.708	Poorly Sorted
SKEWNESS (Sk):	2.259	-0.131	0.131	-0.111	0.111	Fine Skewed
KURTOSIS (K):	10.81	2.060	2.060	0.779	0.779	Platykurtic

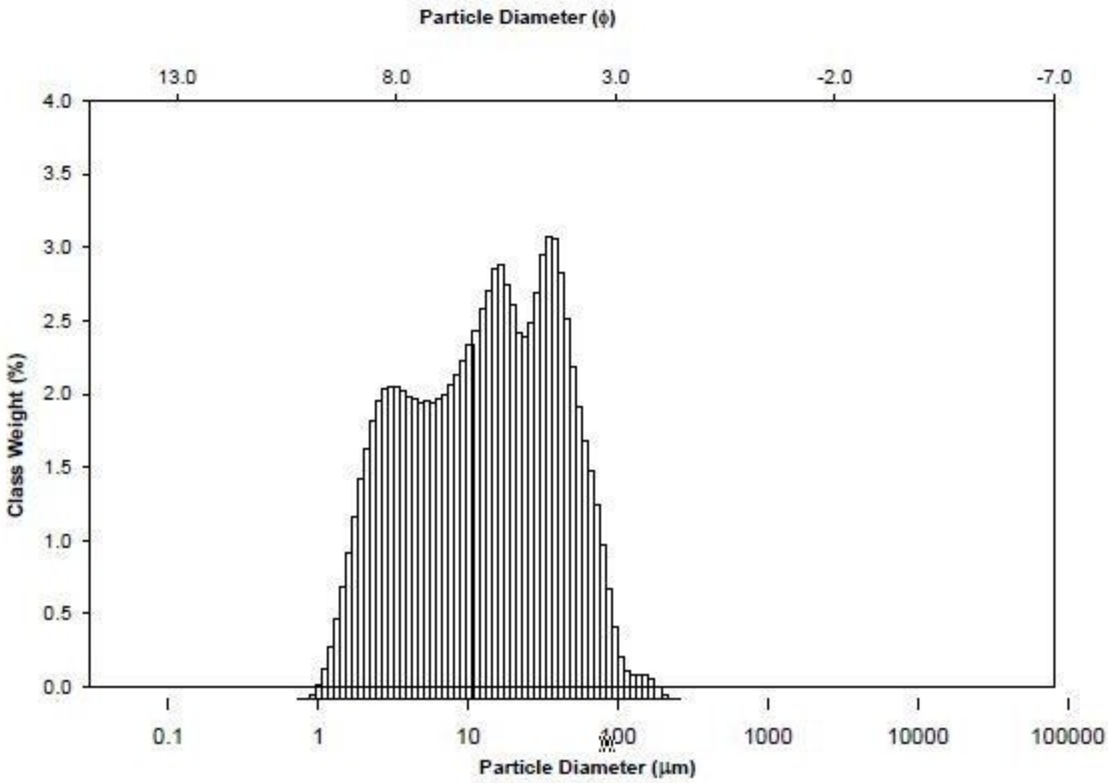

SAMPLE STATISTICS

SAMPLE IDENTITY: **MM221A** ANALYST & DATE: ,

SAMPLE TYPE: Trimodal, Poorly Sorted TEXTURAL GROUP: Sandy Mud

SEDIMENT NAME: Very Fine Sandy Very Coarse Silt

	μm	φ
MODE 1:	38.01	4.719
MODE 2:	16.41	5.931
MODE 3:	3.363	8.218
D_{10}:	3.063	3.770
MEDIAN or D_{50}:	20.02	5.643
D_{90}:	73.29	8.351
(D_{90} / D_{10}):	23.92	2.215
$(D_{90} - D_{10})$:	70.22	4.580
(D_{75} / D_{25}):	5.900	1.567
$(D_{75} - D_{25})$:	36.29	2.561

GRAIN SIZE DISTRIBUTION

GRAVEL:	0.0%	COARSE SAND:	0.0%
SAND:	14.1%	MEDIUM SAND:	0.0%
MUD:	85.9%	FINE SAND:	1.5%
		V FINE SAND:	12.6%
V COARSE GRAVEL:	0.0%	V COARSE SILT:	23.1%
COARSE GRAVEL:	0.0%	COARSE SILT:	20.0%
MEDIUM GRAVEL:	0.0%	MEDIUM SILT:	16.7%
FINE GRAVEL:	0.0%	FINE SILT:	11.9%
V FINE GRAVEL:	0.0%	V FINE SILT:	10.7%
V COARSE SAND:	0.0%	CLAY:	3.3%

	METHOD OF MOMENTS			FOLK & WARD METHOD		
	Arithmetic μm	Geometric μm	Logarithmic φ	Geometric μm	Logarithmic φ	Description
MEAN ($\bar{x}$):	30.58	17.50	5.837	17.25	5.858	Coarse Silt
SORTING (σ):	30.48	3.195	1.676	3.359	1.748	Poorly Sorted
SKEWNESS (Sk):	1.634	-0.331	0.331	-0.175	0.175	Fine Skewed
KURTOSIS (K):	6.090	2.186	2.186	0.860	0.860	Platykurtic

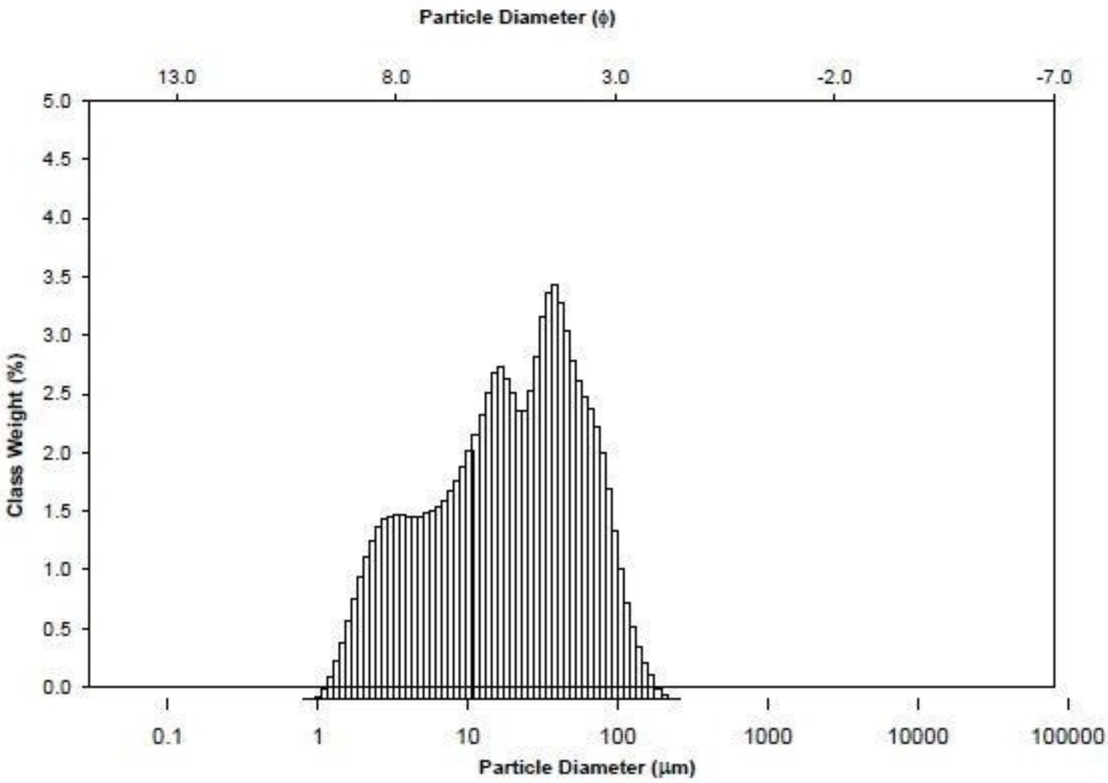

SAMPLE STATISTICS

SAMPLE IDENTITY: **MM222A** ANALYST & DATE: ,

SAMPLE TYPE: Trimodal, Poorly Sorted TEXTURAL GROUP: Sandy Mud

SEDIMENT NAME: Very Fine Sandy Very Coarse Silt

	μm	φ
MODE 1:	38.01	4.719
MODE 2:	16.41	5.931
MODE 3:	3.691	8.084
D_{10}:	3.017	3.994
MEDIAN or D_{50}:	17.93	5.801
D_{90}:	62.75	8.373
(D_{90} / D_{10}):	20.80	2.096
$(D_{90} - D_{10})$:	59.74	4.379
(D_{75} / D_{25}):	5.528	1.525
$(D_{75} - D_{25})$:	31.48	2.467

GRAIN SIZE DISTRIBUTION

GRAVEL:	0.0%	COARSE SAND:	0.0%
SAND:	10.1%	MEDIUM SAND:	0.0%
MUD:	89.9%	FINE SAND:	1.2%
		V FINE SAND:	8.9%
V COARSE GRAVEL:	0.0%	V COARSE SILT:	22.7%
COARSE GRAVEL:	0.0%	COARSE SILT:	21.7%
MEDIUM GRAVEL:	0.0%	MEDIUM SILT:	18.2%
FINE GRAVEL:	0.0%	FINE SILT:	12.8%
V FINE GRAVEL:	0.0%	V FINE SILT:	11.2%
V COARSE SAND:	0.0%	CLAY:	3.3%

	METHOD OF MOMENTS			FOLK & WARD METHOD		
	Arithmetic μm	Geometric μm	Logarithmic φ	Geometric μm	Logarithmic φ	Description
MEAN ($\bar{x}$):	27.20	15.94	5.971	15.61	6.001	Medium Silt
SORTING (σ):	27.89	3.062	1.615	3.191	1.674	Poorly Sorted
SKEWNESS (Sk):	2.122	-0.286	0.286	-0.166	0.166	Fine Skewed
KURTOSIS (K):	9.667	2.234	2.234	0.860	0.860	Platykurtic

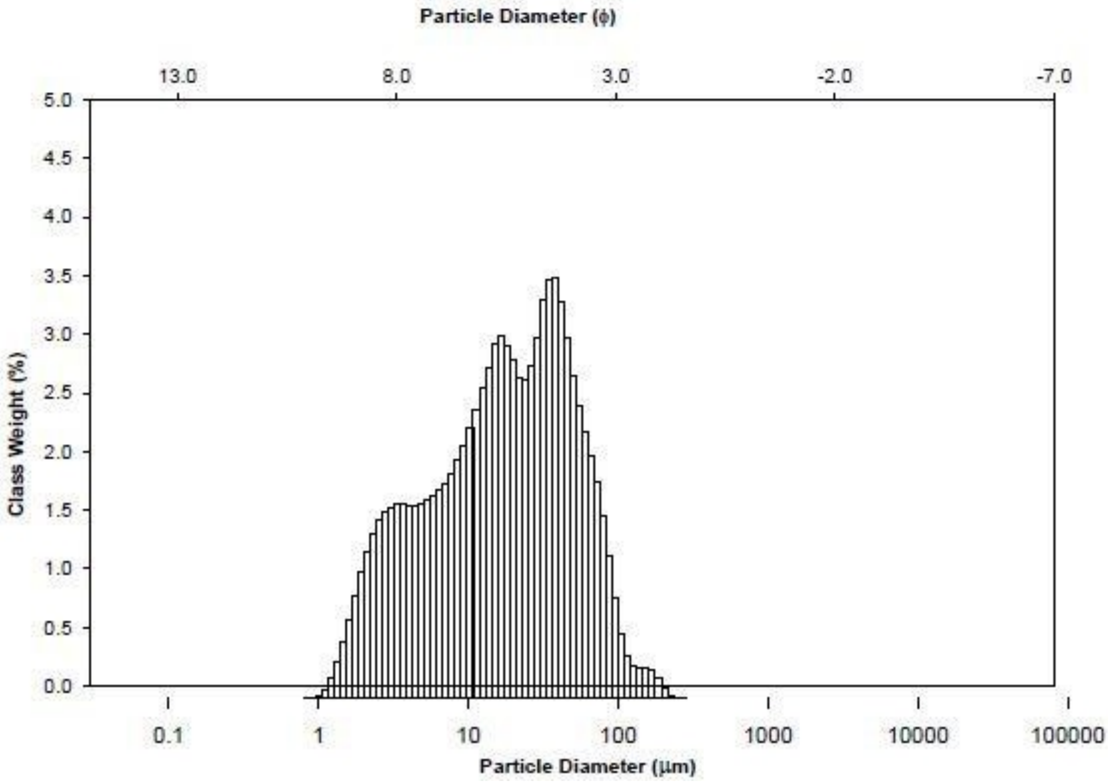

SAMPLE STATISTICS

SAMPLE IDENTITY: **MM223A**

ANALYST & DATE: ,

SAMPLE TYPE: Polymodal, Poorly Sorted

TEXTURAL GROUP: Sandy Mud

SEDIMENT NAME: Very Fine Sandy Very Coarse Silt

	μm	ϕ
MODE 1:	38.01	4.719
MODE 2:	16.41	5.931
MODE 3:	3.363	8.218
D_{10}:	2.666	3.961
MEDIAN or D_{50}:	15.29	6.032
D_{90}:	64.20	8.551
(D_{90} / D_{10}):	24.08	2.159
$(D_{90} - D_{10})$:	61.53	4.590
(D_{75} / D_{25}):	6.673	1.576
$(D_{75} - D_{25})$:	31.49	2.738

GRAIN SIZE DISTRIBUTION

GRAVEL:	0.0%	COARSE SAND:	0.0%
SAND:	10.6%	MEDIUM SAND:	0.0%
MUD:	89.4%	FINE SAND:	0.1%
		V FINE SAND:	10.5%
V COARSE GRAVEL:	0.0%	V COARSE SILT:	19.7%
COARSE GRAVEL:	0.0%	COARSE SILT:	19.0%
MEDIUM GRAVEL:	0.0%	MEDIUM SILT:	18.4%
FINE GRAVEL:	0.0%	FINE SILT:	14.5%
V FINE GRAVEL:	0.0%	V FINE SILT:	13.3%
V COARSE SAND:	0.0%	CLAY:	4.6%

	METHOD OF MOMENTS			FOLK & WARD METHOD		
	Arithmetic μm	Geometric μm	Logarithmic ϕ	Geometric μm	Logarithmic ϕ	Description
MEAN ($\bar{x}$):	25.08	14.10	6.148	14.01	6.158	Medium Silt
SORTING (σ):	25.34	3.192	1.675	3.384	1.759	Poorly Sorted
SKEWNESS (Sk):	1.396	-0.193	0.193	-0.100	0.100	Symmetrical
KURTOSIS (K):	4.404	2.015	2.015	0.795	0.795	Platykurtic

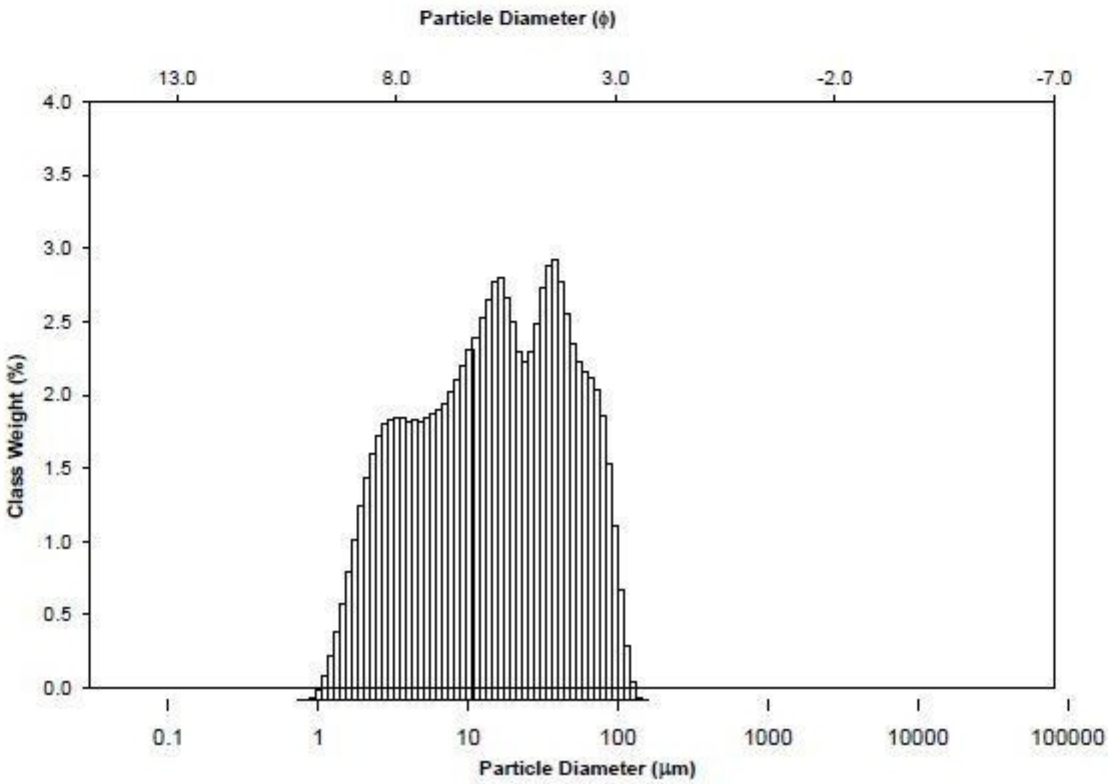

SAMPLE STATISTICS

SAMPLE IDENTITY: **MM224A**

ANALYST & DATE: ,

SAMPLE TYPE: Trimodal, Poorly Sorted

TEXTURAL GROUP: Sandy Mud

SEDIMENT NAME: Very Fine Sandy Coarse Silt

	μm	ϕ
MODE 1:	16.41	5.931
MODE 2:	34.62	4.854
MODE 3:	3.363	8.218
D_{10}:	2.730	3.933
MEDIAN or D_{50}:	14.76	6.082
D_{90}:	65.49	8.517
(D_{90} / D_{10}):	23.98	2.166
$(D_{90} - D_{10})$:	62.76	4.584
(D_{75} / D_{25}):	6.308	1.551
$(D_{75} - D_{25})$:	29.68	2.657

GRAIN SIZE DISTRIBUTION

GRAVEL:	0.0%	COARSE SAND:	0.0%
SAND:	11.0%	MEDIUM SAND:	0.0%
MUD:	89.0%	FINE SAND:	1.4%
		V FINE SAND:	9.6%
V COARSE GRAVEL:	0.0%	V COARSE SILT:	17.6%
COARSE GRAVEL:	0.0%	COARSE SILT:	19.6%
MEDIUM GRAVEL:	0.0%	MEDIUM SILT:	19.3%
FINE GRAVEL:	0.0%	FINE SILT:	15.0%
V FINE GRAVEL:	0.0%	V FINE SILT:	13.5%
V COARSE SAND:	0.0%	CLAY:	4.0%

	METHOD OF MOMENTS			FOLK & WARD METHOD		
	Arithmetic μm	Geometric μm	Logarithmic ϕ	Geometric μm	Logarithmic ϕ	Description
MEAN ($\bar{x}$):	25.72	14.05	6.154	13.84	6.175	Medium Silt
SORTING (σ):	28.98	3.193	1.675	3.370	1.753	Poorly Sorted
SKEWNESS (Sk):	2.069	-0.075	0.075	-0.064	0.064	Symmetrical
KURTOSIS (K):	8.233	2.103	2.103	0.827	0.827	Platykurtic

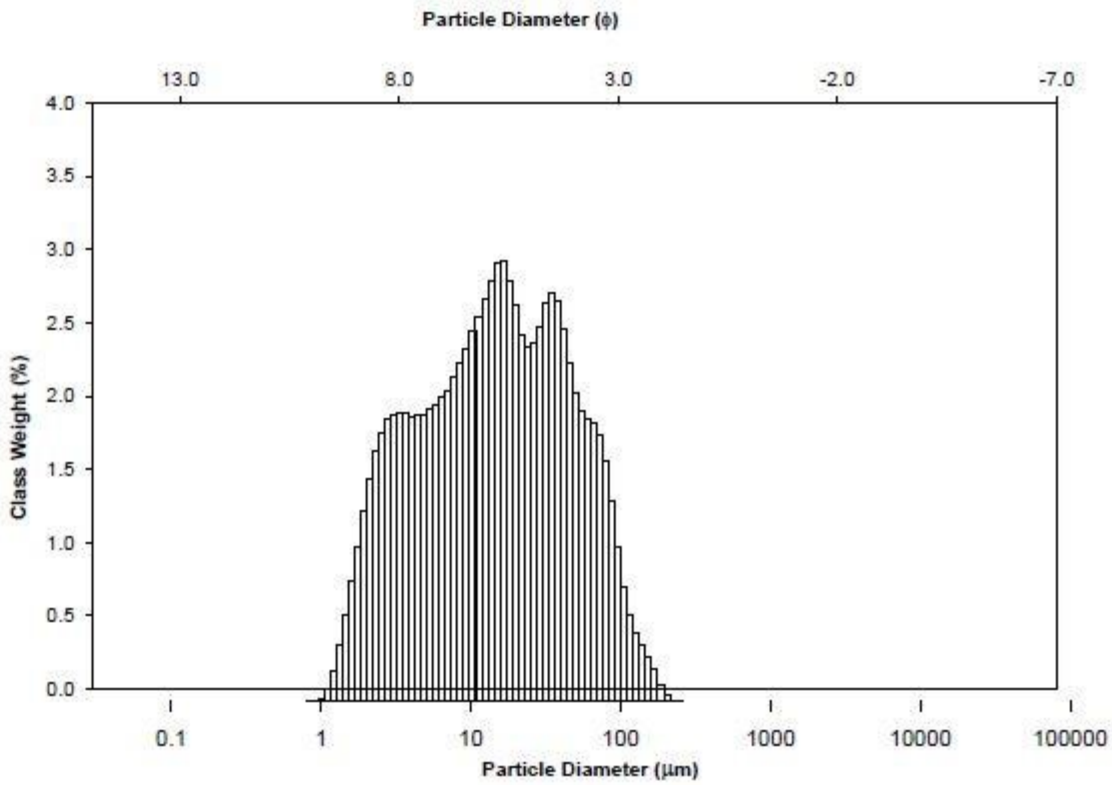

SAMPLE STATISTICS

SAMPLE IDENTITY: **MM225A**

ANALYST & DATE: ,

SAMPLE TYPE: Polymodal, Poorly Sorted

TEXTURAL GROUP: Sandy Mud

SEDIMENT NAME: Very Fine Sandy Very Coarse Silt

	µm	φ
MODE 1:	38.01	4.719
MODE 2:	16.41	5.931
MODE 3:	3.363	8.218
D_{10}:	3.001	3.654
MEDIAN or D_{50}:	20.12	5.635
D_{90}:	79.42	8.380
(D_{90} / D_{10}):	26.46	2.293
$(D_{90} - D_{10})$:	76.42	4.726
(D_{75} / D_{25}):	6.570	1.616
$(D_{75} - D_{25})$:	39.82	2.716

GRAIN SIZE DISTRIBUTION

GRAVEL:	0.0%	COARSE SAND:	0.0%
SAND:	16.5%	MEDIUM SAND:	0.2%
MUD:	83.5%	FINE SAND:	3.3%
		V FINE SAND:	13.0%
V COARSE GRAVEL:	0.0%	V COARSE SILT:	22.1%
COARSE GRAVEL:	0.0%	COARSE SILT:	18.3%
MEDIUM GRAVEL:	0.0%	MEDIUM SILT:	16.4%
FINE GRAVEL:	0.0%	FINE SILT:	12.1%
V FINE GRAVEL:	0.0%	V FINE SILT:	11.2%
V COARSE SAND:	0.0%	CLAY:	3.4%

	METHOD OF MOMENTS			FOLK & WARD METHOD		
	Arithmetic µm	Geometric µm	Logarithmic φ	Geometric µm	Logarithmic φ	Description
MEAN ($\bar{x}$):	34.05	18.05	5.792	17.60	5.828	Coarse Silt
SORTING (σ):	39.14	3.381	1.757	3.524	1.817	Poorly Sorted
SKEWNESS (Sk):	2.381	-0.220	0.220	-0.148	0.148	Fine Skewed
KURTOSIS (K):	10.43	2.181	2.181	0.839	0.839	Platykurtic

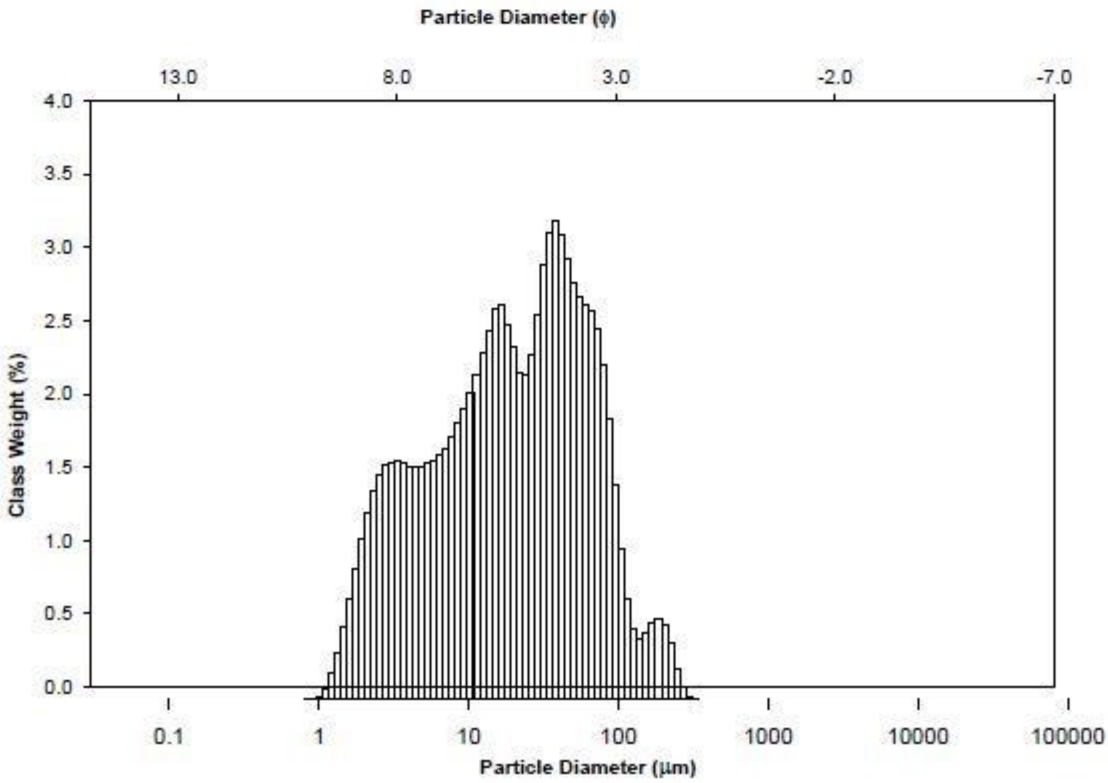

SAMPLE STATISTICS

SAMPLE IDENTITY: **MM226A** ANALYST & DATE: ,

SAMPLE TYPE: Trimodal, Poorly Sorted TEXTURAL GROUP: Sandy Mud

SEDIMENT NAME: Very Fine Sandy Very Coarse Silt

	μm	ϕ
MODE 1:	38.01	4.719
MODE 2:	16.41	5.931
MODE 3:	3.363	8.218
D_{10}:	2.968	3.929
MEDIAN or D_{50}:	17.15	5.865
D_{90}:	65.65	8.396
(D_{90} / D_{10}):	22.12	2.137
$(D_{90} - D_{10})$:	62.68	4.467
(D_{75} / D_{25}):	5.873	1.545
$(D_{75} - D_{25})$:	32.30	2.554

GRAIN SIZE DISTRIBUTION

GRAVEL:	0.0%	COARSE SAND:	0.0%
SAND:	11.2%	MEDIUM SAND:	0.0%
MUD:	88.8%	FINE SAND:	1.7%
		V FINE SAND:	9.5%
V COARSE GRAVEL:	0.0%	V COARSE SILT:	21.5%
COARSE GRAVEL:	0.0%	COARSE SILT:	20.4%
MEDIUM GRAVEL:	0.0%	MEDIUM SILT:	18.6%
FINE GRAVEL:	0.0%	FINE SILT:	13.4%
V FINE GRAVEL:	0.0%	V FINE SILT:	11.7%
V COARSE SAND:	0.0%	CLAY:	3.3%

	METHOD OF MOMENTS			FOLK & WARD METHOD		
	Arithmetic μm	Geometric μm	Logarithmic ϕ	Geometric μm	Logarithmic ϕ	Description
MEAN ($\bar{x}$):	27.81	15.76	5.987	15.42	6.019	Medium Silt
SORTING (σ):	30.20	3.132	1.647	3.266	1.708	Poorly Sorted
SKEWNESS (Sk):	2.300	-0.203	0.203	-0.127	0.127	Fine Skewed
KURTOSIS (K):	10.55	2.187	2.187	0.841	0.841	Platykurtic

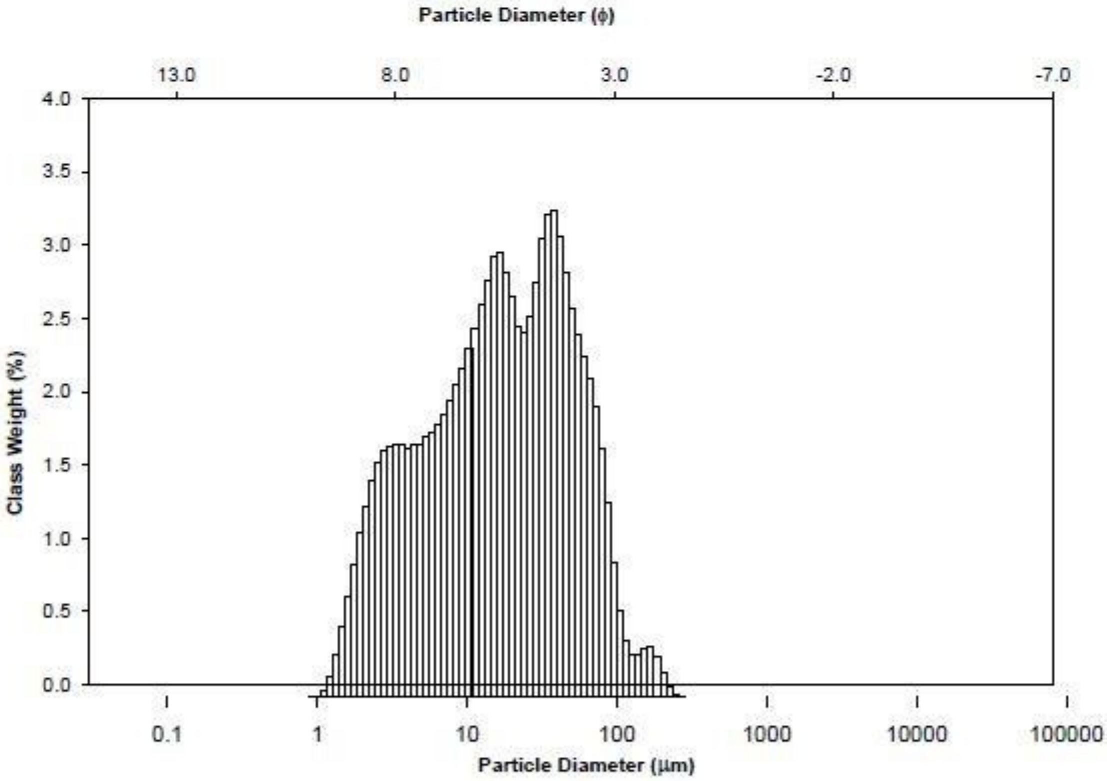

SAMPLE STATISTICS

SAMPLE IDENTITY: **MM227A**

ANALYST & DATE: ,

SAMPLE TYPE: Trimodal, Poorly Sorted

TEXTURAL GROUP: Sandy Mud

SEDIMENT NAME: Very Fine Sandy Very Coarse Silt

	μm	φ
MODE 1:	38.01	4.719
MODE 2:	16.41	5.931
MODE 3:	3.363	8.218
D_{10}:	3.225	3.851
MEDIAN or D_{50}:	20.59	5.602
D_{90}:	69.31	8.277
(D_{90} / D_{10}):	21.49	2.149
$(D_{90} - D_{10})$:	66.08	4.426
(D_{75} / D_{25}):	5.551	1.547
$(D_{75} - D_{25})$:	35.67	2.473

GRAIN SIZE DISTRIBUTION

GRAVEL:	0.0%	COARSE SAND:	0.0%
SAND:	12.9%	MEDIUM SAND:	0.0%
MUD:	87.1%	FINE SAND:	1.2%
		V FINE SAND:	11.7%
V COARSE GRAVEL:	0.0%	V COARSE SILT:	25.0%
COARSE GRAVEL:	0.0%	COARSE SILT:	20.2%
MEDIUM GRAVEL:	0.0%	MEDIUM SILT:	16.9%
FINE GRAVEL:	0.0%	FINE SILT:	11.8%
V FINE GRAVEL:	0.0%	V FINE SILT:	10.4%
V COARSE SAND:	0.0%	CLAY:	2.8%

	METHOD OF MOMENTS			FOLK & WARD METHOD		
	Arithmetic μm	Geometric μm	Logarithmic φ	Geometric μm	Logarithmic φ	Description
MEAN ($\bar{x}$):	30.03	17.80	5.812	17.57	5.830	Coarse Silt
SORTING (σ):	28.79	3.086	1.626	3.222	1.688	Poorly Sorted
SKEWNESS (Sk):	1.637	-0.371	0.371	-0.198	0.198	Fine Skewed
KURTOSIS (K):	6.540	2.218	2.218	0.863	0.863	Platykurtic

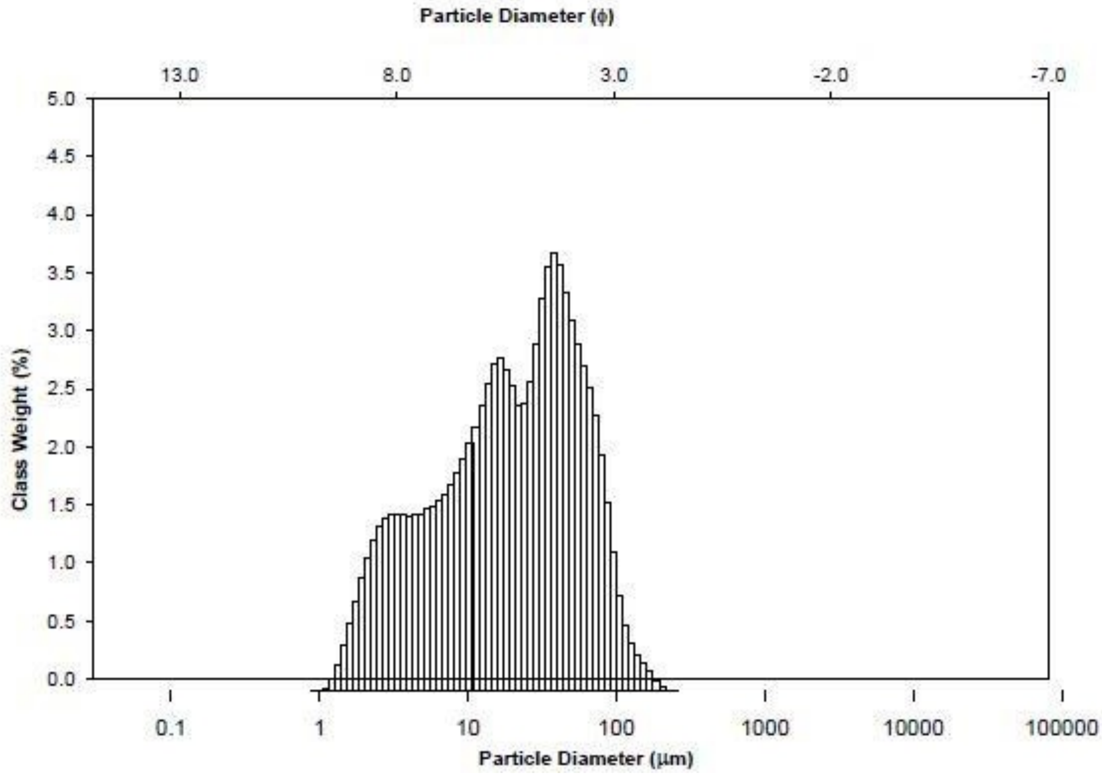

SAMPLE STATISTICS

SAMPLE IDENTITY: **MM228A** ANALYST & DATE: ,

SAMPLE TYPE: Trimodal, Poorly Sorted TEXTURAL GROUP: Mud

SEDIMENT NAME: Coarse Silt

	μm	φ
MODE 1:	16.41	5.931
MODE 2:	34.62	4.854
MODE 3:	3.363	8.218
D_{10}:	2.777	4.078
MEDIAN or D_{50}:	14.57	6.101
D_{90}:	59.19	8.492
(D_{90} / D_{10}):	21.31	2.082
(D_{90} - D_{10}):	56.42	4.414
(D_{75} / D_{25}):	5.819	1.518
(D_{75} - D_{25}):	27.58	2.541

GRAIN SIZE DISTRIBUTION

GRAVEL:	0.0%	COARSE SAND:	0.0%
SAND:	9.0%	MEDIUM SAND:	0.0%
MUD:	91.0%	FINE SAND:	1.1%
		V FINE SAND:	7.9%
V COARSE GRAVEL:	0.0%	V COARSE SILT:	18.0%
COARSE GRAVEL:	0.0%	COARSE SILT:	20.7%
MEDIUM GRAVEL:	0.0%	MEDIUM SILT:	20.3%
FINE GRAVEL:	0.0%	FINE SILT:	15.0%
V FINE GRAVEL:	0.0%	V FINE SILT:	13.3%
V COARSE SAND:	0.0%	CLAY:	3.8%

	METHOD OF MOMENTS			FOLK & WARD METHOD		
	Arithmetic μm	Geometric μm	Logarithmic φ	Geometric μm	Logarithmic φ	Description
MEAN ($\bar{x}$):	24.22	13.73	6.187	13.48	6.213	Medium Silt
SORTING (σ):	26.74	3.072	1.619	3.232	1.692	Poorly Sorted
SKEWNESS (Sk):	2.190	-0.096	0.096	-0.080	0.080	Symmetrical
KURTOSIS (K):	9.340	2.154	2.154	0.842	0.842	Platykurtic

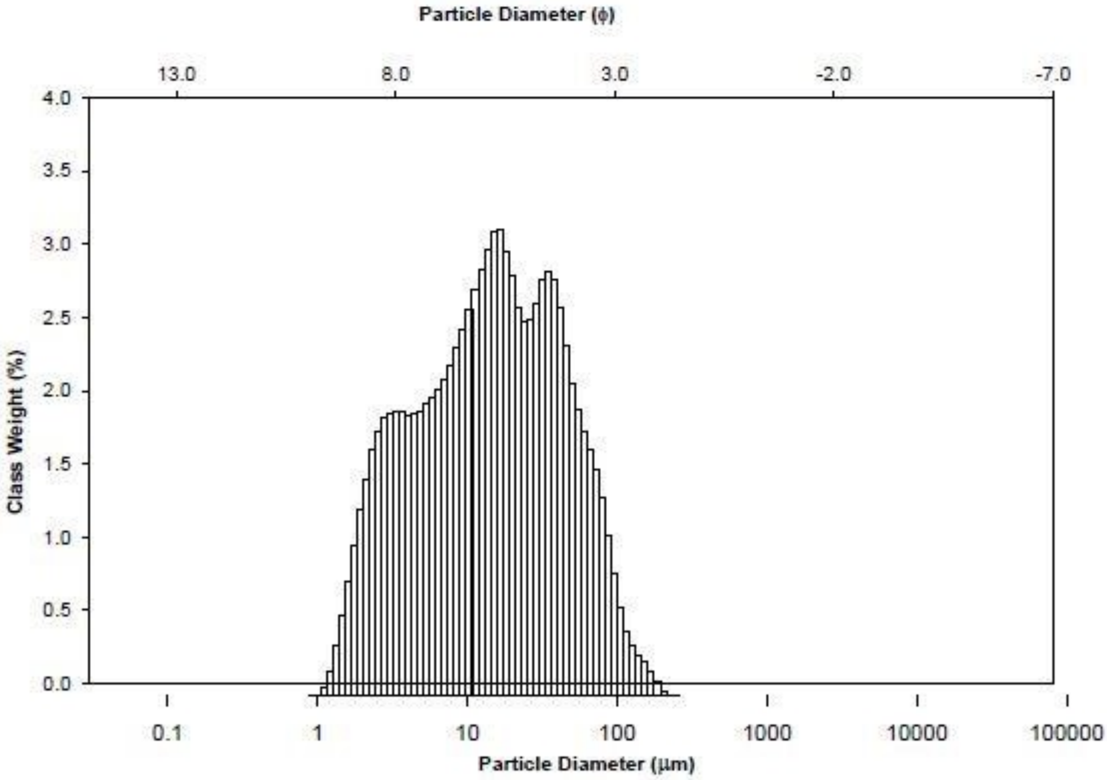

SAMPLE STATISTICS

SAMPLE IDENTITY: **MM229A** ANALYST & DATE: ,

SAMPLE TYPE: Trimodal, Poorly Sorted TEXTURAL GROUP: Sandy Mud

SEDIMENT NAME: Very Fine Sandy Coarse Silt

	μm	φ
MODE 1:	34.62	4.854
MODE 2:	16.41	5.931
MODE 3:	3.691	8.084
D_{10}:	2.880	3.964
MEDIAN or D_{50}:	16.19	5.949
D_{90}:	64.09	8.440
(D_{90} / D_{10}):	22.25	2.129
$(D_{90} - D_{10})$:	61.21	4.476
(D_{75} / D_{25}):	5.939	1.540
$(D_{75} - D_{25})$:	30.70	2.570

GRAIN SIZE DISTRIBUTION

GRAVEL:	0.0%	COARSE SAND:	0.0%
SAND:	10.5%	MEDIUM SAND:	0.0%
MUD:	89.5%	FINE SAND:	1.3%
		V FINE SAND:	9.2%
V COARSE GRAVEL:	0.0%	V COARSE SILT:	20.0%
COARSE GRAVEL:	0.0%	COARSE SILT:	20.6%
MEDIUM GRAVEL:	0.0%	MEDIUM SILT:	19.0%
FINE GRAVEL:	0.0%	FINE SILT:	14.0%
V FINE GRAVEL:	0.0%	V FINE SILT:	12.3%
V COARSE SAND:	0.0%	CLAY:	3.6%

	METHOD OF MOMENTS			FOLK & WARD METHOD		
	Arithmetic μm	Geometric μm	Logarithmic φ	Geometric μm	Logarithmic φ	Description
MEAN ($\bar{x}$):	26.43	14.96	6.063	14.67	6.091	Medium Silt
SORTING (σ):	28.45	3.123	1.643	3.278	1.713	Poorly Sorted
SKEWNESS (Sk):	2.074	-0.170	0.170	-0.109	0.109	Fine Skewed
KURTOSIS (K):	8.701	2.152	2.152	0.841	0.841	Platykurtic

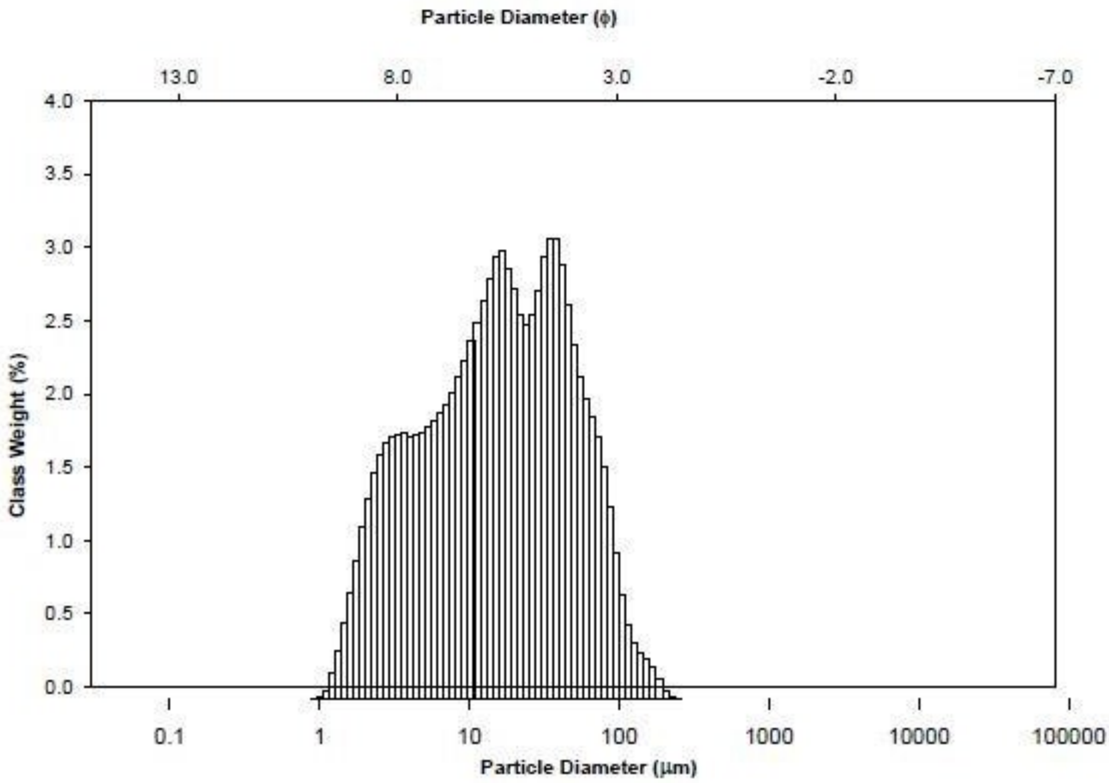

SAMPLE STATISTICS

SAMPLE IDENTITY: **MM230A** ANALYST & DATE: ,

SAMPLE TYPE: Trimodal, Poorly Sorted TEXTURAL GROUP: Mud

SEDIMENT NAME: Coarse Silt

	μm	φ
MODE 1:	34.62	4.854
MODE 2:	16.41	5.931
MODE 3:	3.691	8.084
D_{10}:	2.968	4.049
MEDIAN or D_{50}:	16.47	5.924
D_{90}:	60.39	8.396
(D_{90} / D_{10}):	20.35	2.073
$(D_{90} - D_{10})$:	57.43	4.347
(D_{75} / D_{25}):	5.381	1.504
$(D_{75} - D_{25})$:	28.92	2.428

GRAIN SIZE DISTRIBUTION

GRAVEL:	0.0%	COARSE SAND:	0.0%
SAND:	9.3%	MEDIUM SAND:	0.0%
MUD:	90.7%	FINE SAND:	1.0%
		V FINE SAND:	8.3%
V COARSE GRAVEL:	0.0%	V COARSE SILT:	20.2%
COARSE GRAVEL:	0.0%	COARSE SILT:	22.4%
MEDIUM GRAVEL:	0.0%	MEDIUM SILT:	19.6%
FINE GRAVEL:	0.0%	FINE SILT:	13.6%
V FINE GRAVEL:	0.0%	V FINE SILT:	11.6%
V COARSE SAND:	0.0%	CLAY:	3.4%

	METHOD OF MOMENTS			FOLK & WARD METHOD		
	Arithmetic μm	Geometric μm	Logarithmic φ	Geometric μm	Logarithmic φ	Description
MEAN ($\bar{x}$):	25.60	15.00	6.058	14.72	6.086	Medium Silt
SORTING (σ):	26.72	3.022	1.595	3.164	1.662	Poorly Sorted
SKEWNESS (Sk):	2.083	-0.219	0.219	-0.130	0.130	Fine Skewed
KURTOSIS (K):	8.926	2.235	2.235	0.874	0.874	Platykurtic

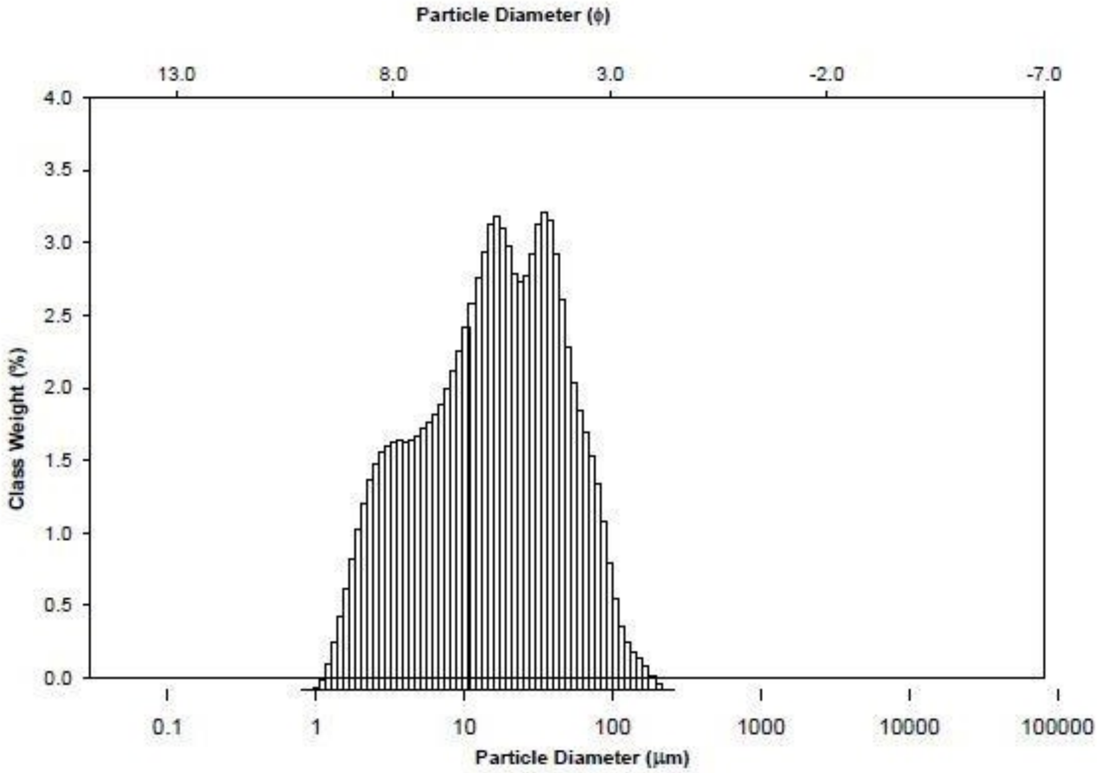

SAMPLE STATISTICS

SAMPLE IDENTITY: **MM231A** ANALYST & DATE: ,

SAMPLE TYPE: Trimodal, Poorly Sorted TEXTURAL GROUP: Sandy Mud

SEDIMENT NAME: Very Fine Sandy Very Coarse Silt

	μm	φ
MODE 1:	38.01	4.719
MODE 2:	16.41	5.931
MODE 3:	3.691	8.084
D_{10}:	3.264	3.832
MEDIAN or D_{50}:	21.50	5.539
D_{90}:	70.20	8.259
(D_{90} / D_{10}):	21.50	2.155
$(D_{90} - D_{10})$:	66.93	4.427
(D_{75} / D_{25}):	5.462	1.545
$(D_{75} - D_{25})$:	36.29	2.449

GRAIN SIZE DISTRIBUTION

GRAVEL:	0.0%	COARSE SAND:	0.0%
SAND:	13.4%	MEDIUM SAND:	0.0%
MUD:	86.6%	FINE SAND:	1.5%
		V FINE SAND:	11.9%
V COARSE GRAVEL:	0.0%	V COARSE SILT:	25.3%
COARSE GRAVEL:	0.0%	COARSE SILT:	20.7%
MEDIUM GRAVEL:	0.0%	MEDIUM SILT:	16.4%
FINE GRAVEL:	0.0%	FINE SILT:	11.5%
V FINE GRAVEL:	0.0%	V FINE SILT:	9.8%
V COARSE SAND:	0.0%	CLAY:	3.0%

	METHOD OF MOMENTS			FOLK & WARD METHOD		
	Arithmetic μm	Geometric μm	Logarithmic φ	Geometric μm	Logarithmic φ	Description
MEAN ($\bar{x}$):	30.85	18.23	5.777	18.08	5.789	Coarse Silt
SORTING (σ):	29.95	3.105	1.635	3.226	1.690	Poorly Sorted
SKEWNESS (Sk):	1.808	-0.402	0.402	-0.218	0.218	Fine Skewed
KURTOSIS (K):	7.726	2.291	2.291	0.877	0.877	Platykurtic

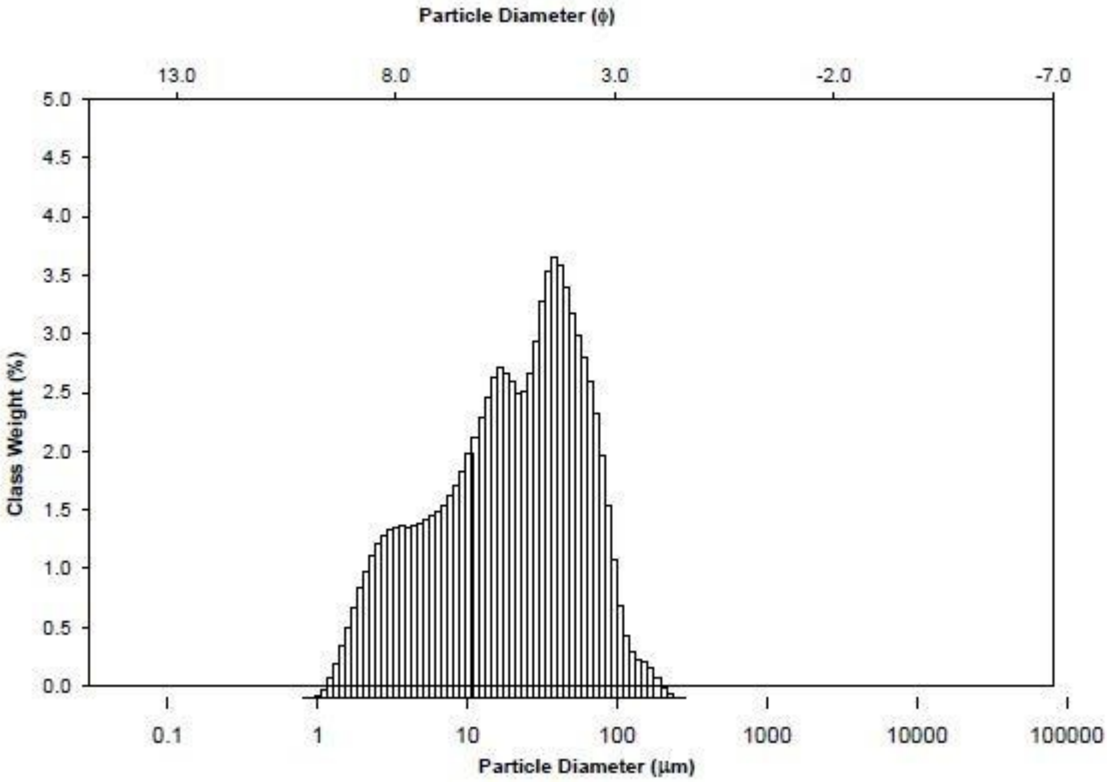

SAMPLE STATISTICS

SAMPLE IDENTITY: **MM232A** ANALYST & DATE: ,

SAMPLE TYPE: Trimodal, Poorly Sorted TEXTURAL GROUP: Sandy Mud

SEDIMENT NAME: Very Fine Sandy Very Coarse Silt

	μm	φ
MODE 1:	38.01	4.719
MODE 2:	16.41	5.931
MODE 3:	3.691	8.084
D_{10}:	3.351	3.911
MEDIAN or D_{50}:	20.71	5.593
D_{90}:	66.46	8.221
(D_{90} / D_{10}):	19.83	2.102
$(D_{90} - D_{10})$:	63.11	4.310
(D_{75} / D_{25}):	5.104	1.515
$(D_{75} - D_{25})$:	33.88	2.352

GRAIN SIZE DISTRIBUTION

GRAVEL:	0.0%	COARSE SAND:	0.0%
SAND:	11.6%	MEDIUM SAND:	0.0%
MUD:	88.4%	FINE SAND:	1.3%
		V FINE SAND:	10.3%
V COARSE GRAVEL:	0.0%	V COARSE SILT:	25.4%
COARSE GRAVEL:	0.0%	COARSE SILT:	21.8%
MEDIUM GRAVEL:	0.0%	MEDIUM SILT:	17.2%
FINE GRAVEL:	0.0%	FINE SILT:	11.6%
V FINE GRAVEL:	0.0%	V FINE SILT:	9.6%
V COARSE SAND:	0.0%	CLAY:	2.7%

	METHOD OF MOMENTS			FOLK & WARD METHOD		
	Arithmetic μm	Geometric μm	Logarithmic φ	Geometric μm	Logarithmic φ	Description
MEAN ($\bar{x}$):	29.61	17.87	5.807	17.66	5.823	Coarse Silt
SORTING (σ):	28.76	3.013	1.591	3.120	1.641	Poorly Sorted
SKEWNESS (Sk):	1.967	-0.391	0.391	-0.209	0.209	Fine Skewed
KURTOSIS (K):	8.890	2.335	2.335	0.894	0.894	Platykurtic

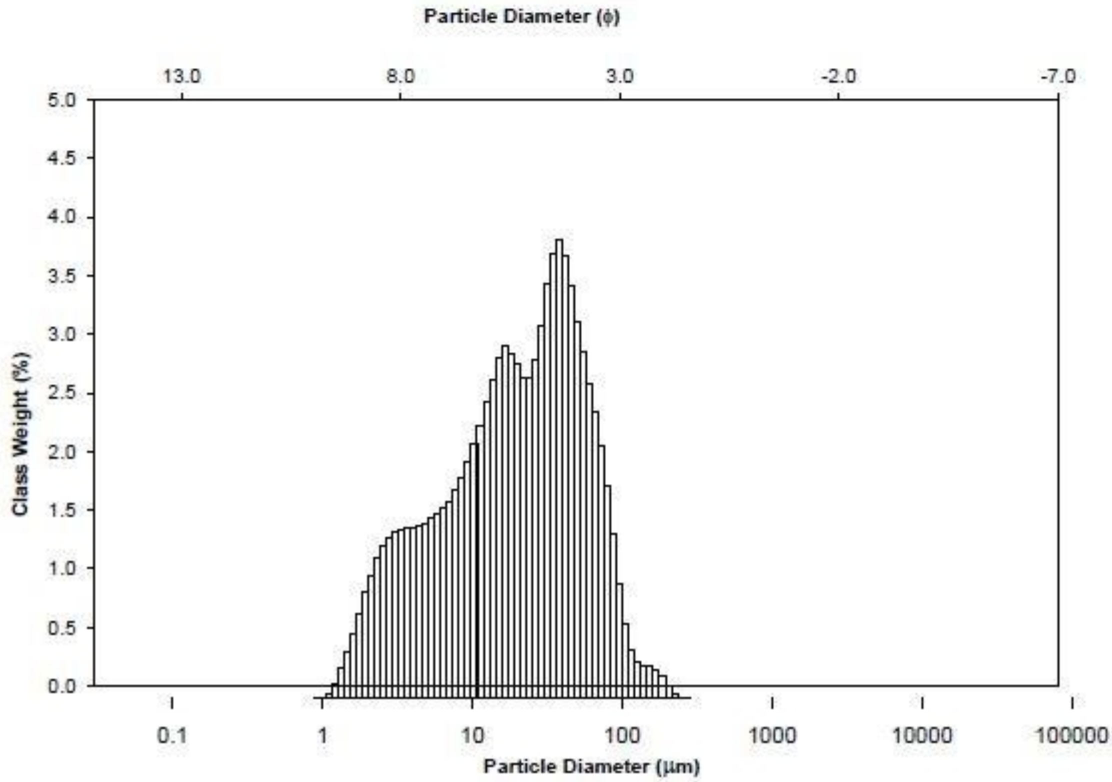

SAMPLE STATISTICS

SAMPLE IDENTITY: **MM233A** ANALYST & DATE: ,

SAMPLE TYPE: Trimodal, Poorly Sorted TEXTURAL GROUP: Mud

SEDIMENT NAME: Coarse Silt

	μm	φ
MODE 1:	34.62	4.854
MODE 2:	16.41	5.931
MODE 3:	3.691	8.084
D_{10}:	3.096	4.144
MEDIAN or D_{50}:	16.92	5.885
D_{90}:	56.57	8.335
(D_{90} / D_{10}):	18.27	2.012
$(D_{90} - D_{10})$:	53.47	4.192
(D_{75} / D_{25}):	5.026	1.483
$(D_{75} - D_{25})$:	28.33	2.330

GRAIN SIZE DISTRIBUTION

GRAVEL:	0.0%	COARSE SAND:	0.0%
SAND:	7.9%	MEDIUM SAND:	0.0%
MUD:	92.1%	FINE SAND:	1.0%
		V FINE SAND:	6.9%
V COARSE GRAVEL:	0.0%	V COARSE SILT:	21.8%
COARSE GRAVEL:	0.0%	COARSE SILT:	23.3%
MEDIUM GRAVEL:	0.0%	MEDIUM SILT:	19.9%
FINE GRAVEL:	0.0%	FINE SILT:	13.2%
V FINE GRAVEL:	0.0%	V FINE SILT:	10.9%
V COARSE SAND:	0.0%	CLAY:	3.1%

	METHOD OF MOMENTS			FOLK & WARD METHOD		
	Arithmetic μm	Geometric μm	Logarithmic φ	Geometric μm	Logarithmic φ	Description
MEAN ($\bar{x}$):	25.17	15.25	6.035	14.98	6.061	Medium Silt
SORTING (σ):	25.59	2.928	1.550	3.042	1.605	Poorly Sorted
SKEWNESS (Sk):	2.286	-0.273	0.273	-0.156	0.156	Fine Skewed
KURTOSIS (K):	11.10	2.306	2.306	0.884	0.884	Platykurtic

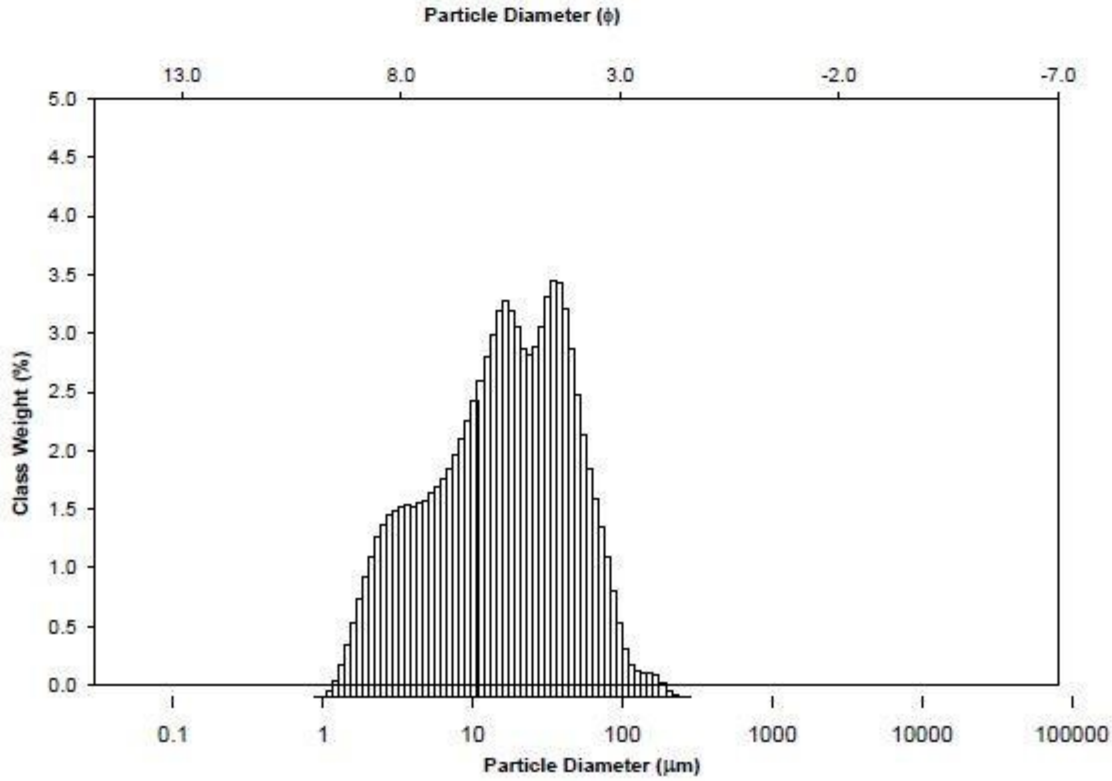

SAMPLE STATISTICS

SAMPLE IDENTITY: **MM234A** ANALYST & DATE: ,

SAMPLE TYPE: Trimodal, Poorly Sorted TEXTURAL GROUP: Sandy Mud

SEDIMENT NAME: Very Fine Sandy Very Coarse Silt

	μm	φ
MODE 1:	38.01	4.719
MODE 2:	16.41	5.931
MODE 3:	3.363	8.218
D_{10}:	3.080	3.900
MEDIAN or D_{50}:	18.35	5.768
D_{90}:	67.00	8.343
(D_{90} / D_{10}):	21.75	2.139
(D_{90} - D_{10}):	63.92	4.443
(D_{75} / D_{25}):	5.469	1.527
(D_{75} - D_{25}):	32.47	2.451

GRAIN SIZE DISTRIBUTION

GRAVEL:	0.0%	COARSE SAND:	0.0%
SAND:	11.6%	MEDIUM SAND:	0.0%
MUD:	88.4%	FINE SAND:	1.4%
		V FINE SAND:	10.2%
V COARSE GRAVEL:	0.0%	V COARSE SILT:	22.2%
COARSE GRAVEL:	0.0%	COARSE SILT:	21.5%
MEDIUM GRAVEL:	0.0%	MEDIUM SILT:	18.3%
FINE GRAVEL:	0.0%	FINE SILT:	12.4%
V FINE GRAVEL:	0.0%	V FINE SILT:	10.8%
V COARSE SAND:	0.0%	CLAY:	3.2%

	METHOD OF MOMENTS			FOLK & WARD METHOD		
	Arithmetic μm	Geometric μm	Logarithmic φ	Geometric μm	Logarithmic φ	Description
MEAN ($\bar{x}$):	28.38	16.51	5.921	16.19	5.949	Coarse Silt
SORTING (σ):	29.04	3.088	1.626	3.233	1.693	Poorly Sorted
SKEWNESS (Sk):	1.923	-0.280	0.280	-0.151	0.151	Fine Skewed
KURTOSIS (K):	7.847	2.235	2.235	0.880	0.880	Platykurtic

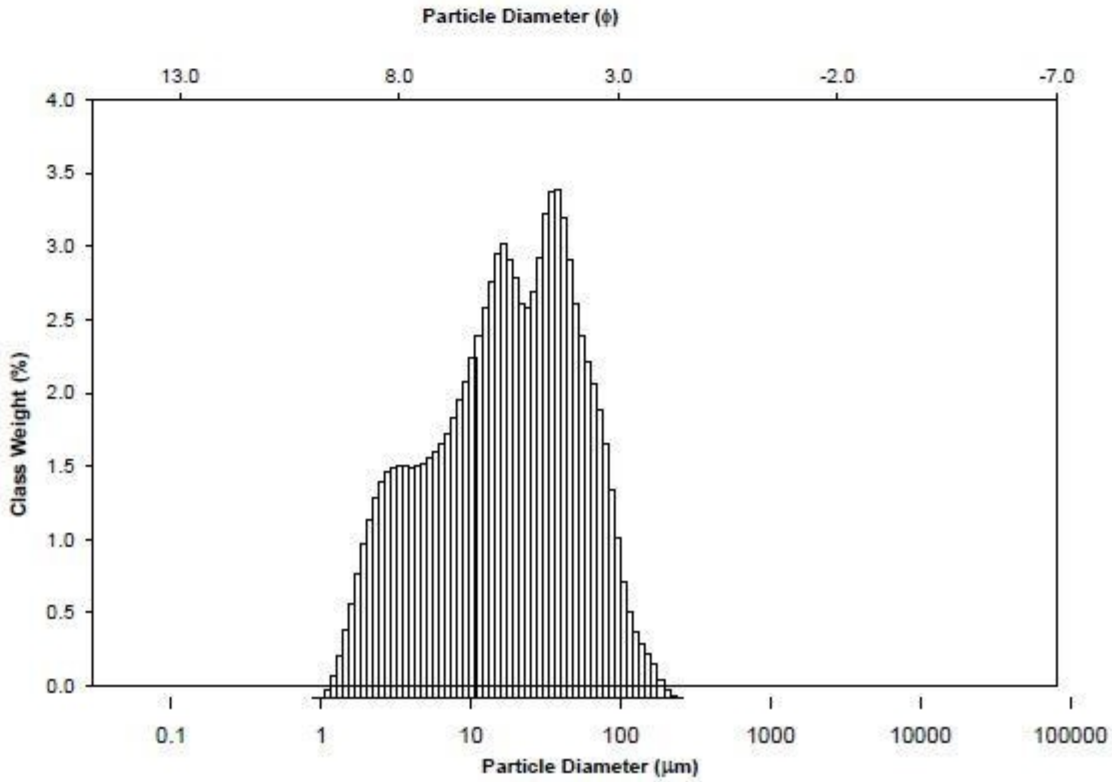

SAMPLE STATISTICS

SAMPLE IDENTITY: **MM235A**

ANALYST & DATE: ,

SAMPLE TYPE: Trimodal, Poorly Sorted

TEXTURAL GROUP: Sandy Mud

SEDIMENT NAME: Very Fine Sandy Very Coarse Silt

	µm	φ
MODE 1:	38.01	4.719
MODE 2:	16.41	5.931
MODE 3:	3.691	8.084
D_{10}:	3.495	3.664
MEDIAN or D_{50}:	24.23	5.367
D_{90}:	78.87	8.160
(D_{90} / D_{10}):	22.56	2.227
$(D_{90} - D_{10})$:	75.37	4.496
(D_{75} / D_{25}):	5.317	1.555
$(D_{75} - D_{25})$:	39.94	2.411

GRAIN SIZE DISTRIBUTION

GRAVEL:	0.0%	COARSE SAND:	0.0%
SAND:	17.0%	MEDIUM SAND:	0.0%
MUD:	83.0%	FINE SAND:	2.2%
		V FINE SAND:	14.9%
V COARSE GRAVEL:	0.0%	V COARSE SILT:	25.1%
COARSE GRAVEL:	0.0%	COARSE SILT:	20.1%
MEDIUM GRAVEL:	0.0%	MEDIUM SILT:	15.8%
FINE GRAVEL:	0.0%	FINE SILT:	10.4%
V FINE GRAVEL:	0.0%	V FINE SILT:	8.9%
V COARSE SAND:	0.0%	CLAY:	2.7%

	METHOD OF MOMENTS			FOLK & WARD METHOD		
	Arithmetic µm	Geometric µm	Logarithmic φ	Geometric µm	Logarithmic φ	Description
MEAN ($\bar{x}$):	34.29	20.19	5.630	20.30	5.623	Coarse Silt
SORTING (σ):	32.98	3.140	1.651	3.269	1.709	Poorly Sorted
SKEWNESS (Sk):	1.657	-0.439	0.439	-0.228	0.228	Fine Skewed
KURTOSIS (K):	6.526	2.353	2.353	0.909	0.909	Mesokurtic

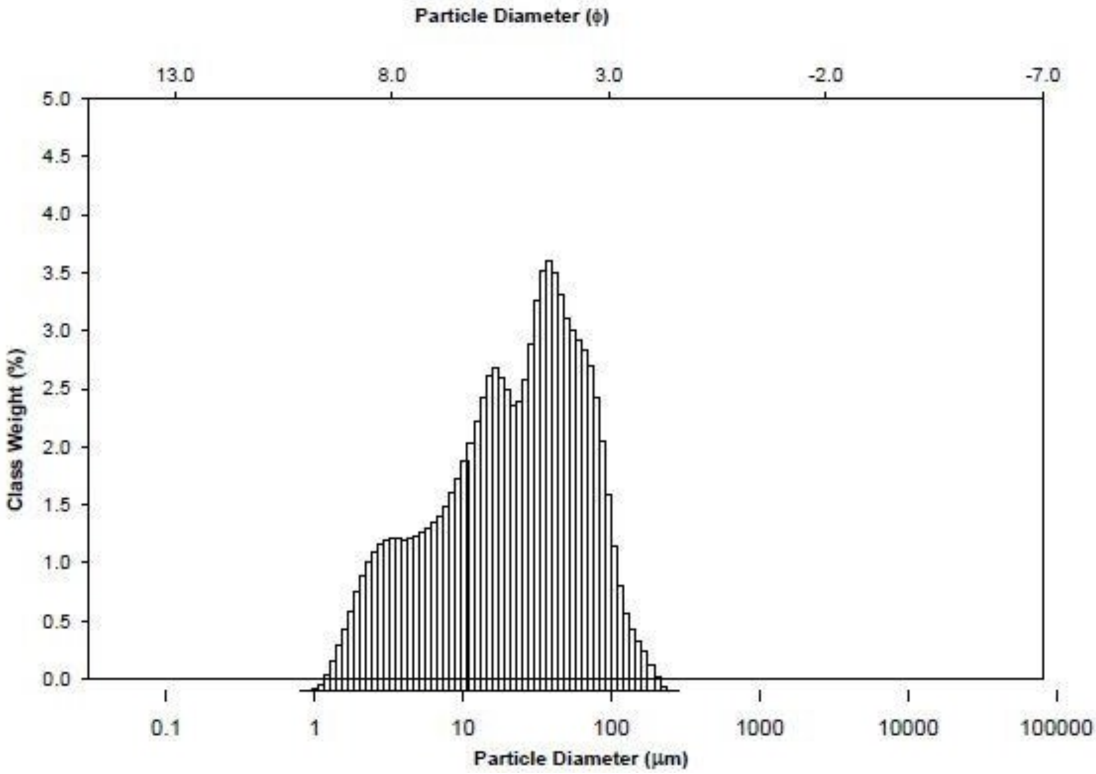

12.5 Stratigraphic Height Calculations

Sample Numbers	Elevation (m)	Latitude	Longitude	Distance (mm)	Distance (m)
235	108.64	-41.323743	175.476841	0.00	0.00
228	107.28	-41.32372	175.476917	1.60	5.21
234	105.33	-41.323635	175.477175	29.46	95.92
227	104.67	-41.323441	175.477322	30.30	98.65
225	104.61	-41.323359	175.477055	31.50	102.56
230	103.81	-41.322977	175.476734	34.87	113.53
226	104.7	-41.323031	175.476397	38.40	125.02
233	103.64	-41.32298	175.476491	41.30	134.47
232	107.47	-41.32293	175.476476	58.10	189.16
231	107.69	-41.322896	175.476398	60.10	195.67
229	108.01	-41.322789	175.476366	62.36	203.03
224	102.08	-41.322716	175.476739	74.07	241.16
223	101.74	-41.322311	175.477141	70.83	230.61
222	100.71	-41.321955	175.477004	123.50	402.09
221	99.63	-41.321979	175.476671	124.20	404.37
220	98.74	-41.321924	175.476614	156.19	508.53
219	98.38	-41.321879	175.476591	156.60	509.86
218	98.27	-41.321453	175.476887	166.74	542.87
217	97.66	-41.321398	175.476797	168.65	549.09
216	102.74	-41.321279	175.476938	176.49	574.62
214	103.24	-41.321254	175.476911	177.85	579.05
215	102.93	-41.320658	175.475775	178.67	581.72
213	116.53	-41.320325	175.475508	182.66	594.71
212	105.55	-41.320287	175.475627	189.87	618.18
211	121.83	-41.320148	175.475708	179.02	582.86
210	134.25	-41.320127	175.475662	175.75	572.21
209	107.65	-41.319806	175.47442	175.66	571.92
208	108.43	-41.319995	175.474366	187.81	611.47
207	99.59	-41.319859	175.473992	189.00	615.35
206	100.24	-41.319856	175.473995	190.72	620.95
205	96.79	-41.319723	175.474343	197.73	643.77
204	96.08	-41.317989	175.47317	204.27	665.07
203	95.3	-41.317989	175.47317	215.00	700.00

12.6 Foraminiferal Plates

Plate 1

1. *Haeuslerella pliocenia*. Juvenile cf.

2. *Haeuslerella pliocenia*. Juvenile cf.

3. Bolivinita pliozea

4. *Bulimina cf. aculeate*. No spines

5. *Cibicides deliquatus*. Umbilical side

6. *Cibicides deliquatus*. Spiral side

7. Cibicides deliquatus

8. *Cibicides deliquatus.* Juvenille

9. *Cibicides cf. finlayi.* Spiral side

10. *Cibicides cf. finlayi.* Spiral side

11. Astrononion parki

12. Astrononion parki

13. Nonionella flemingi

14. Evolvocassidulina orientalis

15. *Evolvocassidulina carinata.* Juvenille

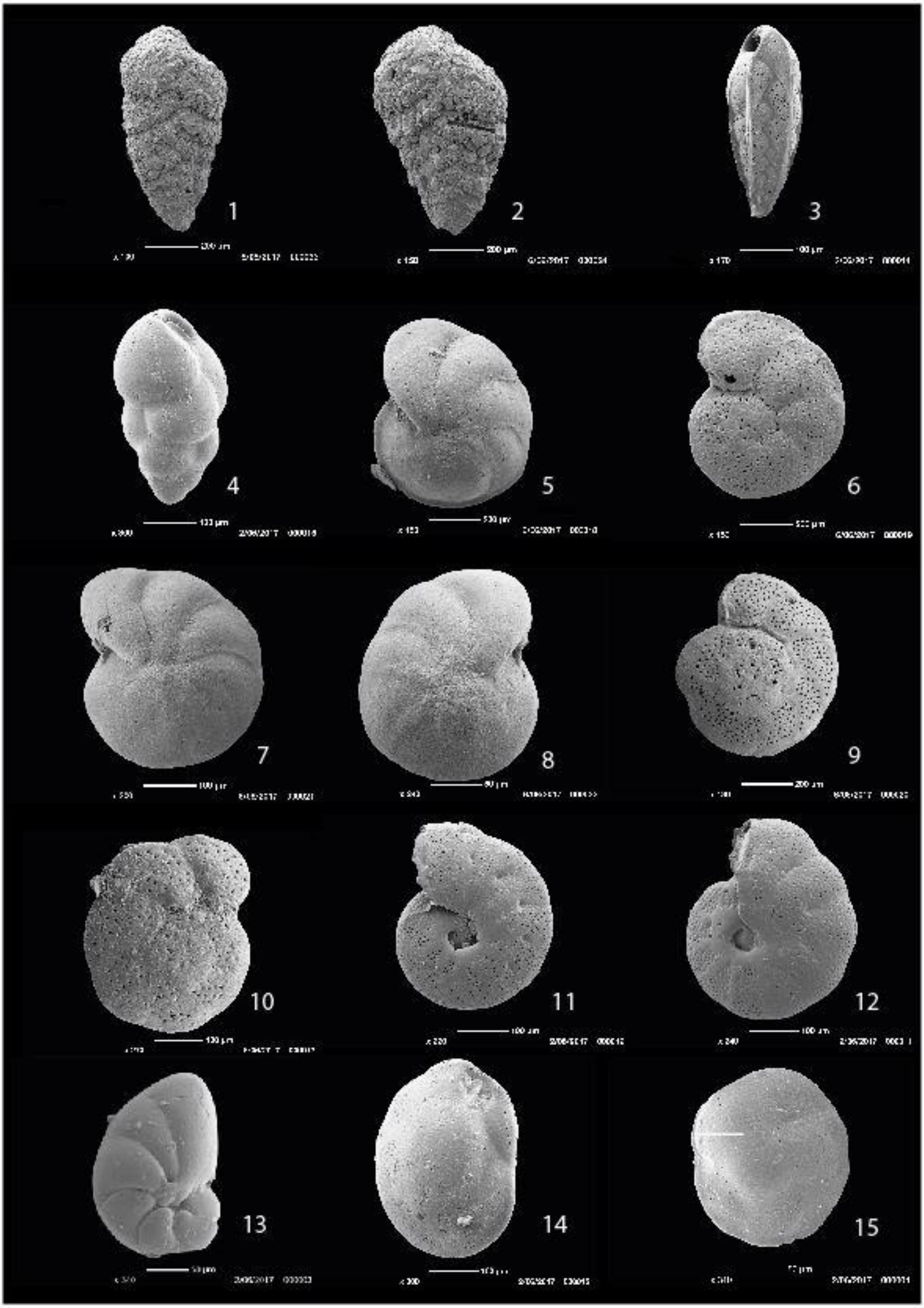
1
2
3
4
5
6
7
8
9
10
11
12
13
14
15

Plate 2

1. Elphidium charlottense

2. Elphidium charlottense

3. Elphidium charlottense

4. *Notorotalia cf. pristina.* Spiral side. Juvenille

5. *Notorotalia cf. pristina.* Umbilical side

6. *Notorotalia hurupiensis.* Spiral side

7. *Notorotalia cf. pristina*. Spiral side

8. *Notorotalia cf. pristina.* Spiral side

9. *Globigerina glutinata*. Broken bulla

10. *Neogloboquadrina cf. pachyderma*. Umbilical side

11. *Turborotalia quinqueloba*. Spiral side

12. Turborotalia quinqueloba

13. Zeaglobigerina woodi

14. *Zeaglobigerina woodi*. Umbilical side

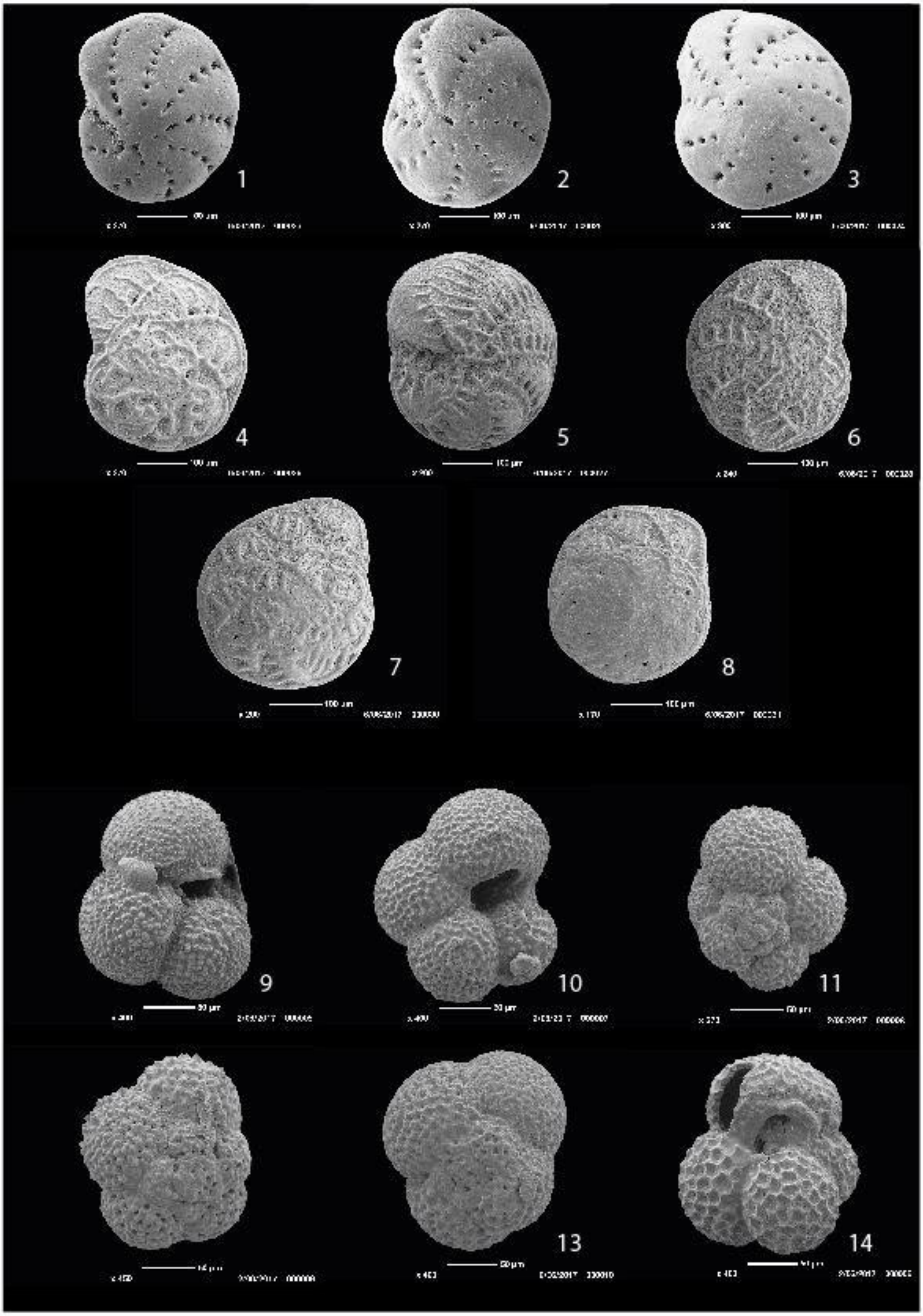
1
2
3
4
5
6
7
8
9
10
11
13
14